REPORT DOCUMENTATION PAGE

AFRL-SR-AR-TR-06-0048

1. REPORT DATE (DD-MM-YYYY)	2. REPORT TYPE	3. DATES COVERED (From - To)
21/02/2006	Final Technical	15/04/2000 - 30/09/2005

4. TITLE AND SUBTITLE
Cirrus Characterization for Laser Propagation and Global Modeling

5a. CONTRACT NUMBER

5b. GRANT NUMBER
F49620-00-1-0215

5c. PROGRAM ELEMENT NUMBER

6. AUTHOR(S)
John Hallett (PI)
Matt Bailey

5d. PROJECT NUMBER

5e. TASK NUMBER
3484/BS

5f. WORK UNIT NUMBER

7. PERFORMING ORGANIZATION NAME(S) AND ADDRESS(ES)
Desert Research Institute
Division of Atmospheric Sciences
2215 Raggio Parkway
Reno, NV 89512-1095

8. PERFORMING ORGANIZATION REPORT NUMBER

9. SPONSORING / MONITORING AGENCY NAME(S) AND ADDRESS(ES)
AFOSR/PK3
801 N. Randolph St., Room 732
Arlington, VA 22203-1977

10. SPONSOR/MONITOR'S ACRONYM(S)

11. SPONSOR/MONITOR'S REPORT NUMBER(S)

12. DISTRIBUTION / AVAILABILITY STATEMENT
unlimited

DISTRIBUTION STATEMENT A
Approved for Public Release
Distribution Unlimited

13. SUPPLEMENTARY NOTES
None

14. ABSTRACT

Laser beam propagation through the earth's atmosphere is influenced by absorption and scattering by ice crystals as occur in cirrus clouds. New instruments (cloudscopes) and laboratory chambers (thermal diffusion, fall tower) have been designed and built to characterize and simulate such crystals to measure absorption and scatter of laser beams. The cloudscope, deployed for aircraft or laboratory use, collects and video-records ice crystals to provide a measure of their size, habit, concentration and also density by evaporating the particles after collection. This procedure also reveals their inner structure and the presence of any impurity. These investigations provide protocols for aircraft sampling and analysis of cirrus particles to be analyzed in real-time. This provides input for regional scale models of ice crystal evolution in terms of temperature, supersaturation and fall velocity, resulting in prediction of habits following growth, melt and evaporation and their likely optical properties.

15. SUBJECT TERMS
Aircraft icing, Aircraft instrumentation, Cirrus, Ice habit, Ice particle density, Ice optical properties

16. SECURITY CLASSIFICATION OF:			17. LIMITATION OF ABSTRACT	18. NUMBER OF PAGES	19a. NAME OF RESPONSIBLE PERSON
a. REPORT	b. ABSTRACT	c. THIS PAGE			John Hallett
Unclassified	N/A	Unclassified		74	19b. TELEPHONE NUMBER (include area code) 775-674-7013

Final Technical Report
Department of the Air Force (AFOSR)
Contract #F49620-00-1-0215
Period: 4/15/00 – 9/30/05

Cirrus Characterization for Laser Propagation and Global Modeling
Dr. John Hallett

I. SUMMARY

The work undertaken during the period of this report extends earlier work (Final report March 16, 2000, F49620-96-1-0470) concerned with the optical properties of cirrus clouds from the viewpoint of laser energy propagation. New instruments have been designed, constructed, and both laboratory and aircraft flight tested from the viewpoint of characterizing cirrus clouds in sufficient detail to model the passage of a collimated laser beam, from the viewpoint of absorption and angle dependent scattering, integrated over the optical path of the beam.

The characterization of any cloud depends on the detail of the individual components of the cloud. In the case of cirrus, the composition is mostly water ice, as is used in the laboratory studies. Also, on occasion, trace impurity as sulfuric acid, nitrate hydrates and other materials may be present. Such impurities result from the composition of the initial nucleating particle, if any and from aerosol and gas scavenging and surface chemical reactions. Such impurities may be used in the laboratory. Such impurities are of importance in evaporating cirrus and are measurable within certain limits with the instruments developed. In the case of individual particles in the liquid phase, the shape is usually spherical and Raleigh/Mie modeling is applicable using known properties of water substance extrapolated to low temperature. In the case of significant impurity concentrations as may occur following evaporation, there is uncertainty both in the composition and also the concentration to be considered. The liquid phase readily occurs at low temperature by supercooling of pure water (to <-40°C) and the supersaturation and /or supercooling of solution droplets to the lowest temperatures likely to be encountered in tropical cirrus (<-90°C).

Once nucleation of ice has occurred, a different set of uncertainties arise because of the complex habit of ice crystals during growth from the vapor. Such habit has been explored in the laboratory under specific constraints: the temperature and mechanism of nucleation; the temperature of growth; the supersaturation of growth; the air pressure, and the fall velocity of the particle through the air. The presence of ambient electric field further influences to growth and the fall orientation of asymmetric crystals. Both laboratory and theoretical studies have investigated these uncertainties leading to specific criteria for different habits in any predicted cirrus transect.

A practical concern for a crystal of arbitrary shape is the crystal density as a mean and as a variability radially from an assigned center of mass. For many crystals the shape may approximate either a two (as a plate or dendrite or a snow flake) or three dimensional crystal array (as plates or dendrites radiating from a common center) depending on whether the initial nucleation event was as a single crystal or as a polycrystal. In the latter case a radial distribution function may be specified for particles growing under known or predicted conditions. Thus complete specifications of an individual particle will be through a circumscribing circle or sphere diameter, a density function from a center, together with environmental growth conditions and a

fall velocity from an estimate of drag coefficient and particle mass. Depending on fall Reynolds' number and electric field, crystals may fall in a stable orientation, oscillate or tumble, computable depending on conditions.

Since the local absolute air vertical velocity depends on larger scale phenomena, as the propagation of a gravity wave through a cirrus layer initiated by a convective disturbance long gone, only a general satellite measurement of stability and water vapor - height profile (possibly backed with an occasional radiosonde air truth) may be available for such prediction. This leaves a possible inverse approach using cirrus particle property measured and analyzed in situ by any penetrating aircraft to provide a temperature (direct measurement), supersaturation (inferred from the peripheral ice habit), ice particle size and concentration (measured in situ) and total ice mass content) measured *in situ* by T probe.

II. ACCOMPLISHMENTS

A. Instrumentation.

The cloudscope has been developed for laboratory, balloon and aircraft use to capture cloud particles, liquid or solid, on a forward facing (into the airflow) optical flat, imaged from behind and video-recorded and displayed at a standard speed of 1/30 second. In a modified version of the cloudscope, the optical flat can be heated to evaporate the particles and reveal the presence of impurities as soluble (the water evaporates to reveal crystallization of a soluble residue) or insoluble residue (it fails to dissolve on cooling or increasing relative humidity and is stable to heating to 30°C). The rate of evaporation can be varied to demonstrate how an individual ice crystal evaporates, to reveal its interior structure and to provide information on its density variation outside inwards as it evaporates without melting. The larger cloudscope, 3cm, has been used on C130, DC-8 for larger (several mm) particles; the standard cloudscope 3mm, for smaller (100μm) particles; and the high resolution cloudscope, mm for smaller particles (few μm). The smaller cloudscope has been used in the laboratory and in the cloudscope designed for balloon deployment.

B. Laboratory simulation.

Fall Column:

A double walled insulated refrigerated fall column (10m tall, 30cm diameter) has been designed, built and operated down to <-45°C to simulate crystals likely to be found in the atmosphere. Ultrasonic nebulizers provide a source of water cloud drops 10 -20μm diameter, these are cooled and nucleated by LN2 to produce ice crystals which fallout into a base refrigerated chamber to be collected and video recorded. Selected temperature and supersaturation grown crystals (plates, columns, rosettes) can be produced and examined for their optical properties in a polar nephelometer beneath the column.

Diffusion chamber:

A static thermal gradient diffusion chamber (3cm deep, 30cm diameter) covering a wide range of supersaturation (1% over ice to water saturation to 50% above water saturation) temperature (+10 to -70°C) grows ice crystals on a thin vertical glass filament to reveal their habit, linear area and volume (mass) growth rates. The supersaturation can also be changed by momentary near adiabatic expansion to provide a pulse of supersaturation as might occur in a

transient atmospheric gravity wave. The crystals can also be subject to evaporation by use of an infra red radiation source and transient under-saturation evaporation by slight adiabatic compression. The system can also be used for testing for nucleation of various atmospheric components (as volcanic dust and clay residues) as may enter the upper troposphere where cirrus clouds form.

C. Application to optical turbulence.

Even a cursory examination of cirrus clouds reveals a complexity resulting from nucleation and growth of ice crystals at specific levels and a fallout of larger crystals to lower unsaturated levels where they may evaporate almost completely or regrow should they enter supercooled clouds at lower levels. The process of evaporation must involve both a cooling of the crystal and the air through which it falls and a parallel enhancement of the water vapor content of that air. The overall result for the evaporation layers is an induced turbulent structure is equivalent to 0.few degrees C and 0.1 kg m^{-3} mixing ratio initially on the scale of the cirrus strands. This structure is not steady, but must decay with time constant until the virtual temperature is constant but the components of the virtual temperature are themselves vary over a limited range of air temperature and water vapor mixing ratio, to decay by long time scale molecular diffusion processes and radiative heat loss/gain. The optical effects of passage through such regions merit detailed investigation.

D. Application to subvisual cirrus.

Insight into the properties of subvisual cirrus can be inferred by extending the knowledge gained from laboratory and field studies in other systems. The phenomenon occurs at low temperatures, -60 ±10°C; there appears to be a lack of larger (>20μm diameter) particles; the lack of granularity and optical phenomena in their appearance suggests a lack of well defined facets. These attributes alone suggest an origin in evaporation of preexisting cirrus, together with the presence of soluble impurity sufficient to dissolve (melt) ice as evaporation of water substance progresses and the effective concentration increases. Sulfuric acid is a likely impurity under such conditions, with sea salt and ammonium sulfate as possible additional components. The presence of such particles under sufficient low relative humidity of a descending long wavelength gravity wave (100km) could therefore provide droplets of highly concentrated solutions in the complete absence of any crystalline material. At this point one of two things can happen. Should such particles be subsequently lifted in the ascending part of the wave, slow condensation occurs leading to a lower concentration soluble material and growing drops which are supercooled well below ambient temperature to remain as liquid spherical particles. These eventually nucleate ice homogeneously and freeze, the drop having a high degree of polycrystallinity, to grow from the vapor as a near spherical particle at a velocity of 0.01 to 0.05 μm/s having a high density interior and a lower density exterior. Otherwise, should the particle descend further and evaporate more, hydrate crystals may nucleate and grow. In either case the optical properties would be as a sphere, but containing irregular dispersed scattering centers. The resolution of the occurrence and nature of such particles requires in situ measurement using the high resolution cloudscope (as designed for the balloon experiment) but carried by an aircraft capable of penetration the appropriate altitudes.

Publications supported by or related to this program.

Bailey, M., and J. Hallett, 2004: Growth rates and habits of ice crystals between -20°C and -70°C. *J. Atmos. Sci.*, **61,** 514-544.

Bailey, M. and J. Hallett, 2002: Nucleation effects on the habit of vapour grown ice crystals from –18 to –42C. *Q.J.R. Meteorol. Soc.*, **128,** 1461-1483.

Bailey, M., J. Hallett, a. Korolev, and G. Isaac, 2002: Laboratory Growth, Sublimation and Regrowth of Ice Crystals. *AMS 11th Conference on Cloud Physics*, 3-7 June 2002, Ogden, UT. **(CD)** P1.4.

Bailey, M.P. and J. Hallett, 2002: Ice Crystal Habits and Growth Rates for Temperatures Below -20°C. *AFOSR-ABL Atmospheric Workshop,* Kirtland AFB, New Mexico, April 9-11, 2002.

Barkey, B., K.N. Liou, M. Bailey, J. Hallett, 2002: Experimentally measured scattering properties of plate and column ice crystals. *AMS 11th Conference on Cloud Physics*, 3-7 June 2002, Ogden, UT. **(CD)** JP3.5.

Barkey, B., M. Bailey, K.-N. Liou, and J. Hallett, 2002: Light-scattering properties of plate and column ice crystals generated in a laboratory cold chamber. *Applied Optics,* **41 (27),** 5792-5796.

Black, R.A., G.M. Heymsfield, and J. Hallett, 2003: Extra large particle images at 12 km in a hurricane eyewall: Evidence of high-altitude supercooled water? *Geophys. Res. Ltrs.,* **30(21),** 2124, doi:10.1029/2003GL017864, 2003.

Foster, T.C. and J. Hallett, 2002: The alignment of ice crystals in changing electric fields. *Atmos. Res.*, **62,** 149-169.

Foster, T.C. and J. Hallett, 2006: Complete alignment of plate ice crystals by non-uniformly divergent electric fields. In preparation.

Hallett, J., R. Purcell, M. Roberts, G. Vidaurre, and D. Wermers, 2005: Measurement for Characterization of Mixed Phase Clouds. Paper presented at the *43rd AIAA Aerospace Science Meeting.* Reno, NV, 10-13 January 2005. Paper No. 862.

Hallett, J. and G.A. Isaac, 2002: Aircraft icing in glaciated and mixed phase clouds. *40th AIAA Aerospace Sciences Meeting and Exhibit.* 14-17 January 2002, Reno, NV. AIAA 2002-0677.

Hallett, J., J.G. Hudson, D.H. Lowenthal, and R. Purcell, 2002: Real-time processing and characterization of atmospheric particulates. *AMS 11th Conference on Cloud Physics*, 3-7 June 2002, Ogden, UT. **(CD)** 10.1.

Hallett, J., W.P. Arnott, M.P. Bailey, and J.T. Hallett, 2002: Ice Crystals in Cirrus, in *Cirrus*, edited by K.D. Lynch, K. Sassen, D. O'C. Starr, G. Stephens, Chpt. 3, pp. 41-77, Oxford University Press, Inc., New York.

Korolev, A.V., M.P. Bailey, J. Hallett, and G.A. Isaac, 2004: Laboratory and in situ observation of deposition growth of frozen drops. *J. Applied Met.,* **43,** 612-622.

Korolev, A.V., G.A. Isaac, S.G. Cober, J.W. Strapp, and J. Hallett, 2003: Microphysical characterization of mixed phase clouds. *Q.J.R. Meteorol. Soc.,* **129,** 39-66.

Korolev, A., G.A. Isaac, and J. Hallett, 2000: Ice particle habits in stratiform clouds. *Q.J.R. Meteorol. Soc.,* **126,** 2873-2902.

Mo, Q., A.G. Detwiler, 2003: Horizontal structure of the electric field in the stratiform region of an Oklahoma mesoscale convective system. *J. Geophys. Res.,* **108(D7),** 4225, doi:10.1029/2001JD001140.

Oraltay, R.G., and Hallett, J., 2005: The Melting Layer: A Laboratory Investigation of Ice Particle Melt and Evaporation near 0°C. *J. Applied Met.*, **44(2),** 206-220.

APPENDIX A

Cirrus Characterization for Laser Propagation and Global Modeling

Dr. John Hallett; Matthew Bailey
Division of Atmospheric Sciences, Desert Research Institute

Work has continued on laboratory studies for characterization of ice crystals as occur in natural cirrus clouds in the laboratory. This has utilized two approaches: 1. A horizontal ice coated thermal diffusion chamber, where crystals are grown on a central, vertical, thin glass filament. This has mapped the ice crystal habit, area, volume and linear growth rates from -20C to -70C and a range of realistic ice saturation ratios. Further, crystals have been produced in free fall under controlled conditions in a 5m column at controlled temperature and supercooled cloud content and fed to optical systems produced by the UCLA group (Professor Liou, Dr. Barkey) to measure extinction and scattering phase relation and characterized by the cloudscope.

A field version of the cloudscope has been developed and is being deployed by balloon flight in natural cirrus to track the direct optical and growth properties of crystals by a semi -Lagrangian vertical flight profile in cirrus clouds from Holloman AFB in October 2003. Frost point and ambient conditions will be measured by separate instrumentation and telemetered to the ground, along with video the detailed measurements. Specific results are shown in the following figures.

- Figure 1. Map of ice crystal habit of crystals grown under cirrus conditions from -20C to -70C over a range of supersaturation typical of cirrus growth.
- Figure 2. Thermal water vapor diffusion chamber capable of producing a controlled temperature and supersaturation growth conditions selectable independently by choice of top and bottom temperatures. Crystals are grown near the chamber center on a thin vertical glass filament where the supersaturation has a broad maximum.
- Figure 3. Comparison of ice crystals grown in laboratory and crystals observed in the atmosphere under similar conditions by various authors.
- Figure 4. Contrail crystals grown near -60C. Note trigonal symmetry.
- Figs. 5,6,7,8. Crystals grown near the indicated temperature and supersaturation showing the probability of different habits grown under similar conditions, depending on the nucleation process.
- Figure 9. Derived growth rate data for dimension, area and volume related to temperature and normalized to supersaturation.
- For further details of above see Bailey & Hallett *QJRMS* 2002 and *J. Atmos. Sci.*, 2004, in press.
- Figure 10. Schematic of high resolution cloudscope and fall column for growing crystals at controlled temperature and near water saturation.
- Figs. 11, 12. Crystals collected by the cloudscope at the base of the fall column at -20 and -40C and simultaneously passed through the optical phase measuring system described by Barkey et al (this conference).
- Figs. 13, 14. Schematics of arrangements of cloudscope for the balloon cirrus experiment.

References:

Bailey, M., and J. Hallett, 2002: Nucleation effects on the habit of vapour grown ice crystals from -18 to -42°C. *Q.J.R. Meteorol. Soc.*, **128,** 1461-1483.

Bailey, M., and J. Hallett, 2002: Growth Rates and Habits of Ice Crystals Between -20°C and -70°C. *J. Atmos. Sci.*, In press.

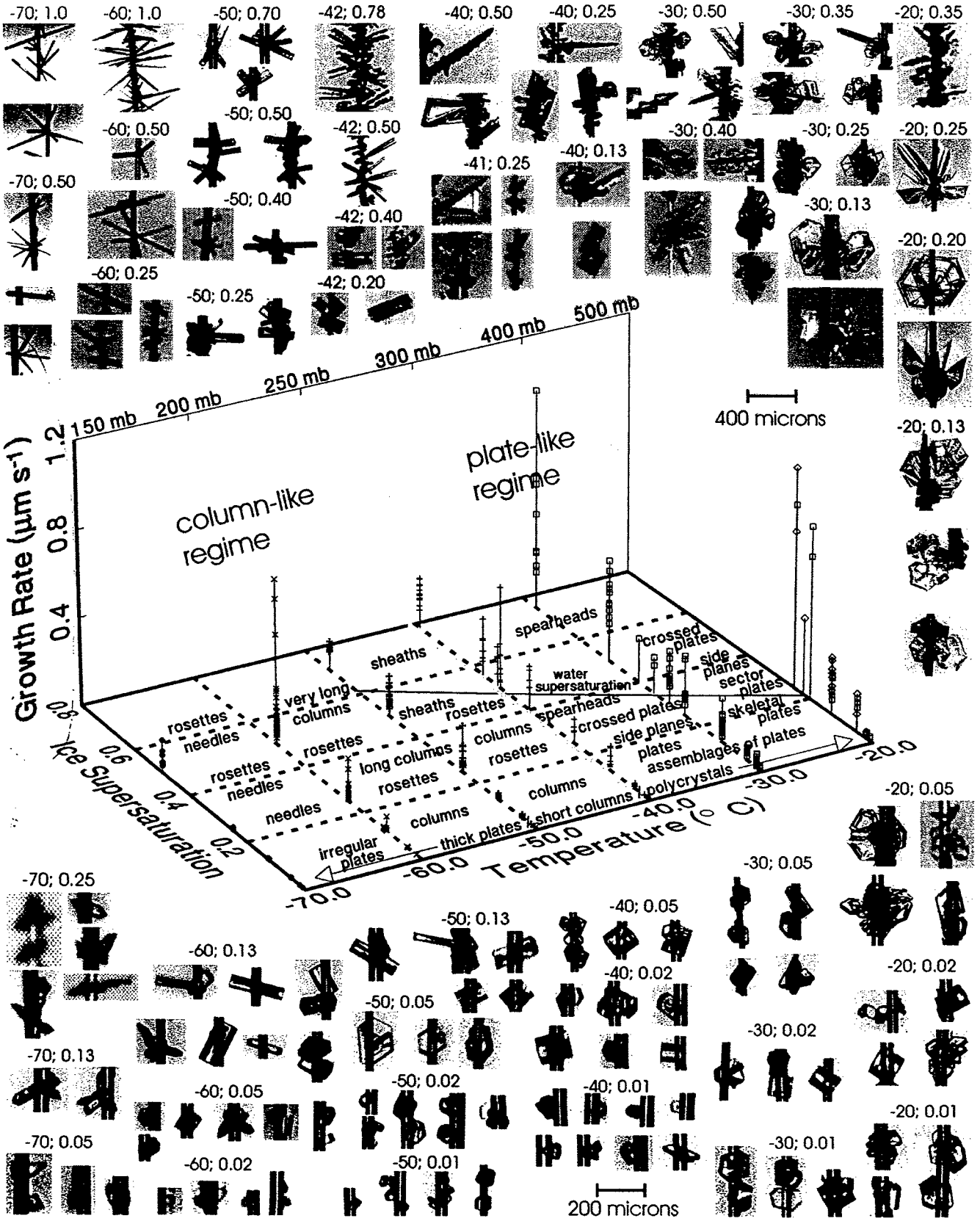

Figure 1. Map of ice crystal habit of crystals grown under cirrus conditions from -20C to -70C over a range of supersaturation typical of cirrus growth.

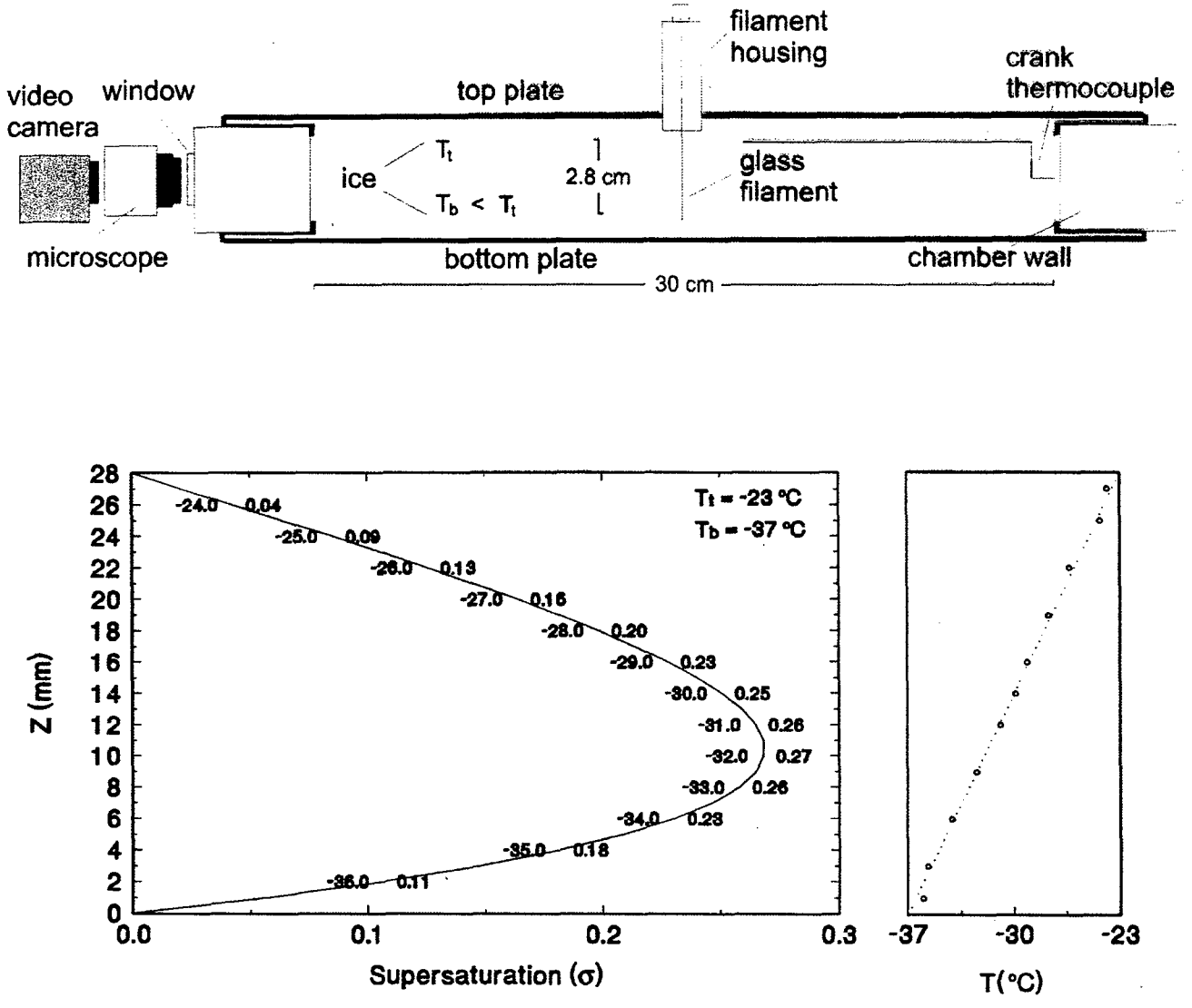

Figure 2. Thermal water vapor diffusion chamber capable of producing a controlled temperature and supersaturation growth conditions selectable independently by choice of top and bottom temperatures. Crystals are grown near the chamber center on a thin vertical glass filament where the supersaturation has a broad maximum.

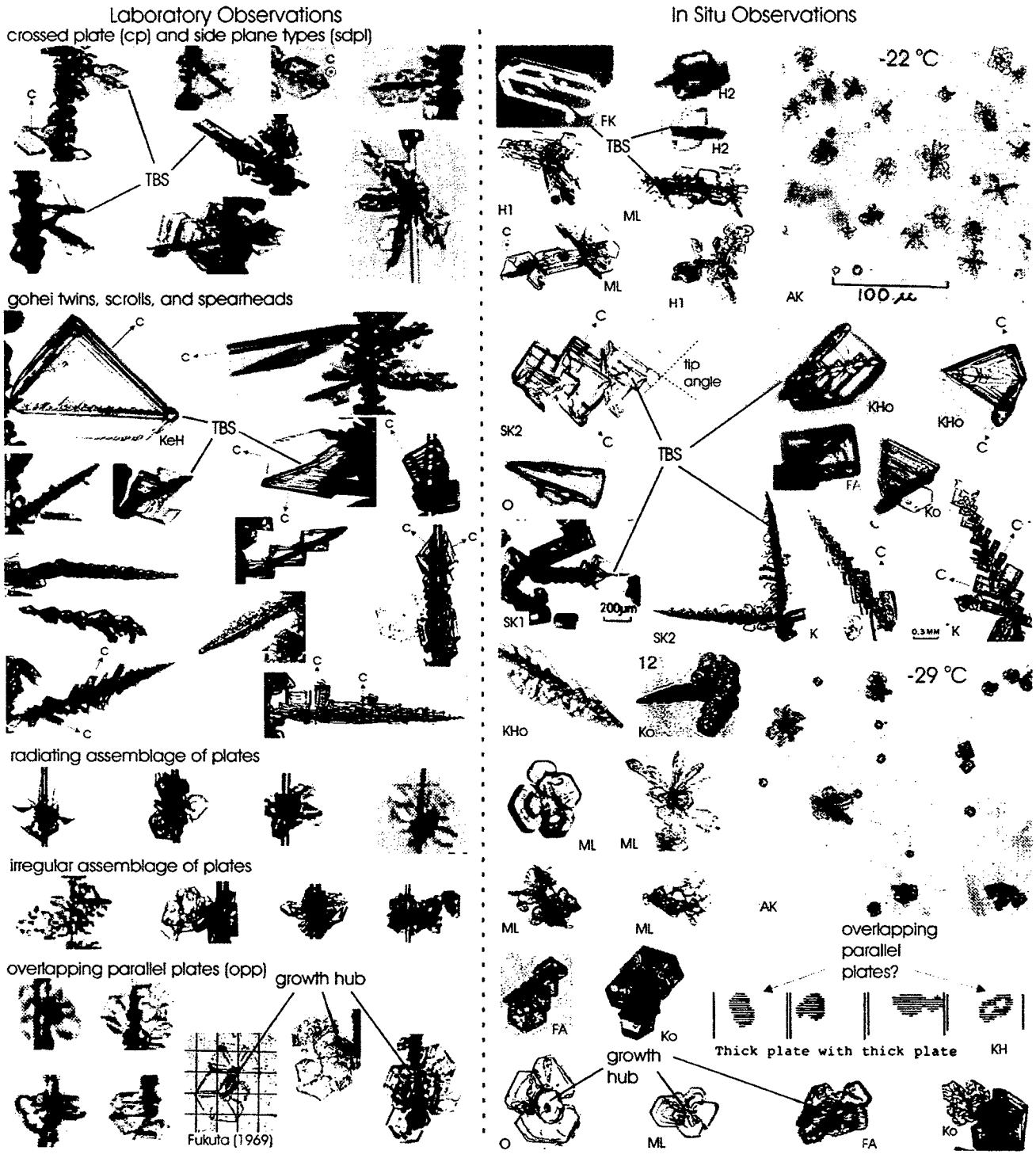

Figure 3. Comparison of ice crystals grown in laboratory and crystals observed in the atmosphere under similar conditions by various authors.

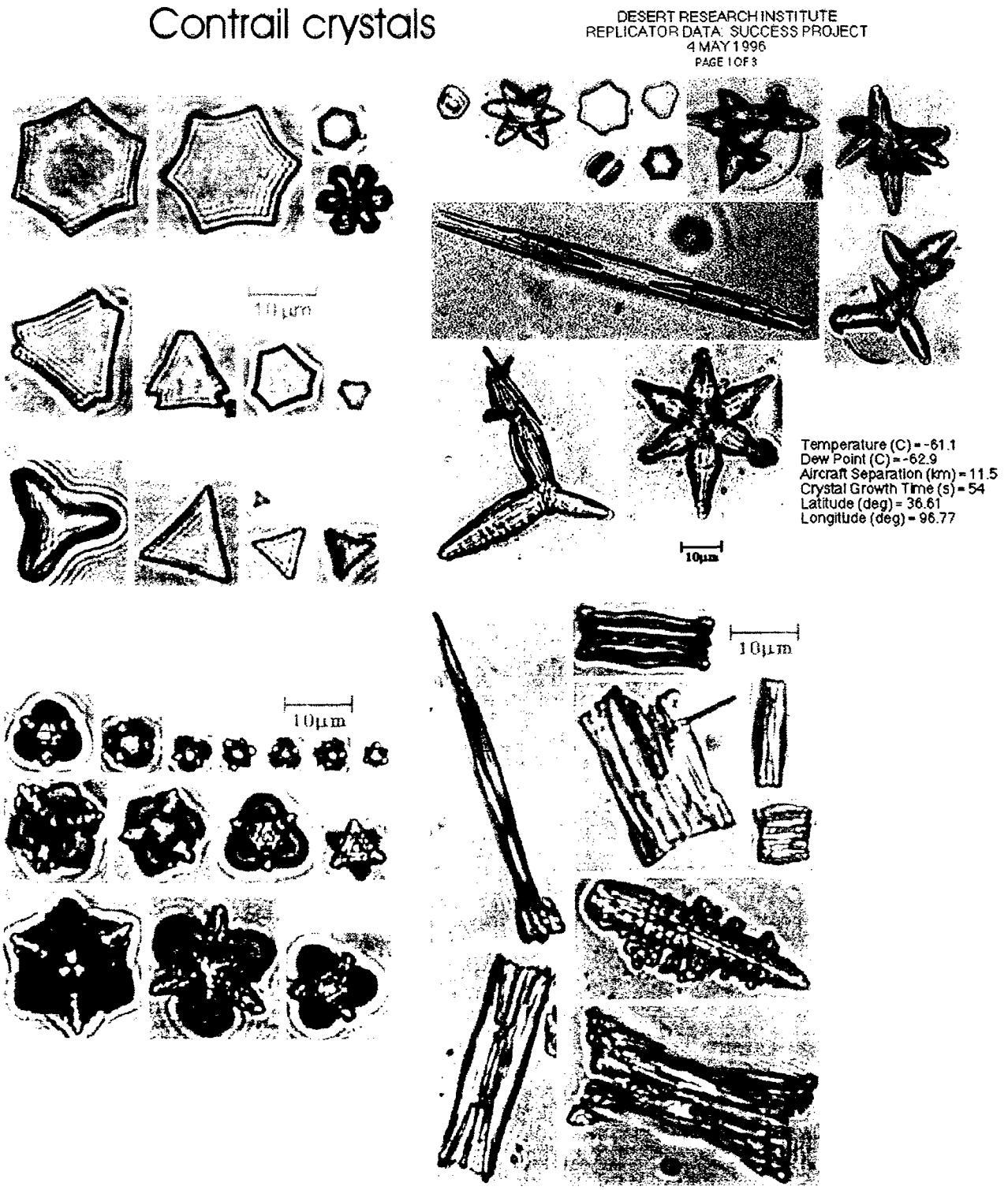

Figure 4. Contrail crystals grown near -60C. Note trigonal symmetry.

Figs. 5,6,7,8. Crystals grown near the indicated temperature and supersaturation showing the probability of different habits grown under similar conditions, depending on the nucleation process.

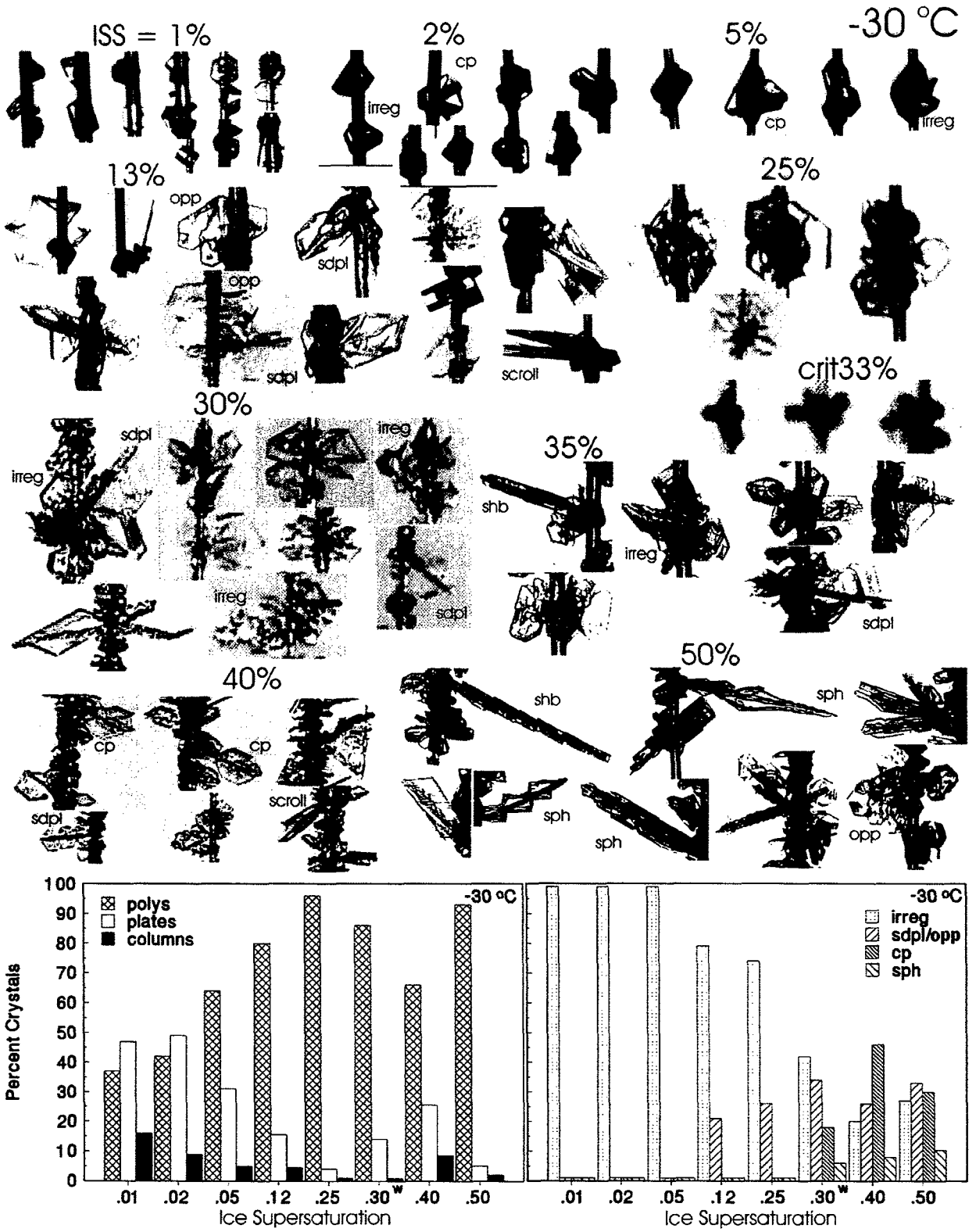

Figure 5

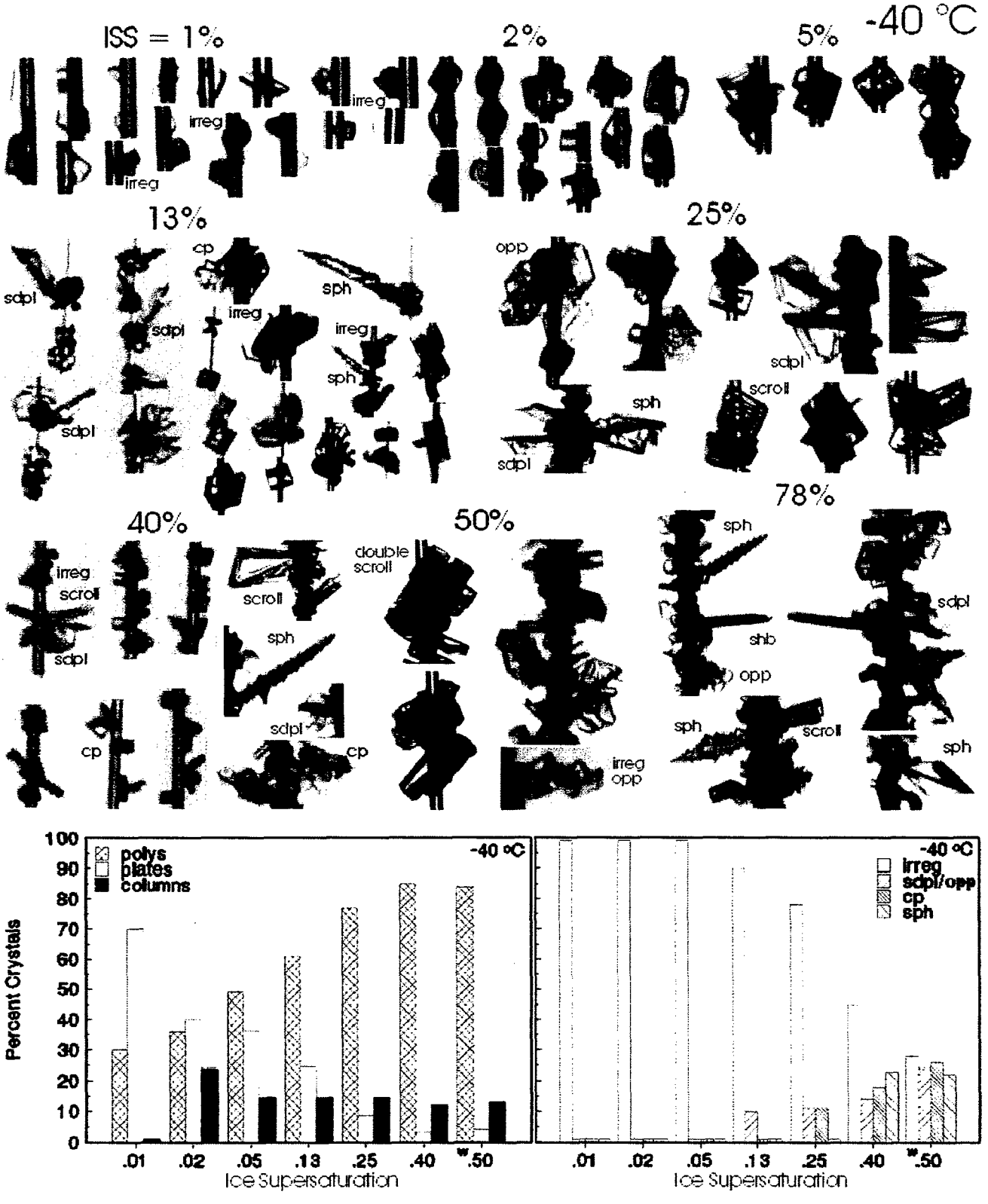
ISS = 1%
2%
5%
-40 °C
irreg
irreg
irreg
13%
cp
sdpl
sdpl
irreg
sph
irreg
sph
sdpl
25%
opp
sdpl
scroll
sph
sdpl
78%
40%
irreg
scroll
sdpl
scroll
sph
sdpl
cp
cp
50%
double scroll
sph
shb
opp
sph
scroll
sdpl
sph
irreg
opp
Percent Crystals
polys
plates
columns
-40 °C
irreg
sdpl/opp
cp
sph
-40 °C
.01
.02
.05
.13
.25
.40
.50
Ice Supersaturation
.01
.02
.05
.13
.25
.40
.50
Ice Supersaturation

Figure 6

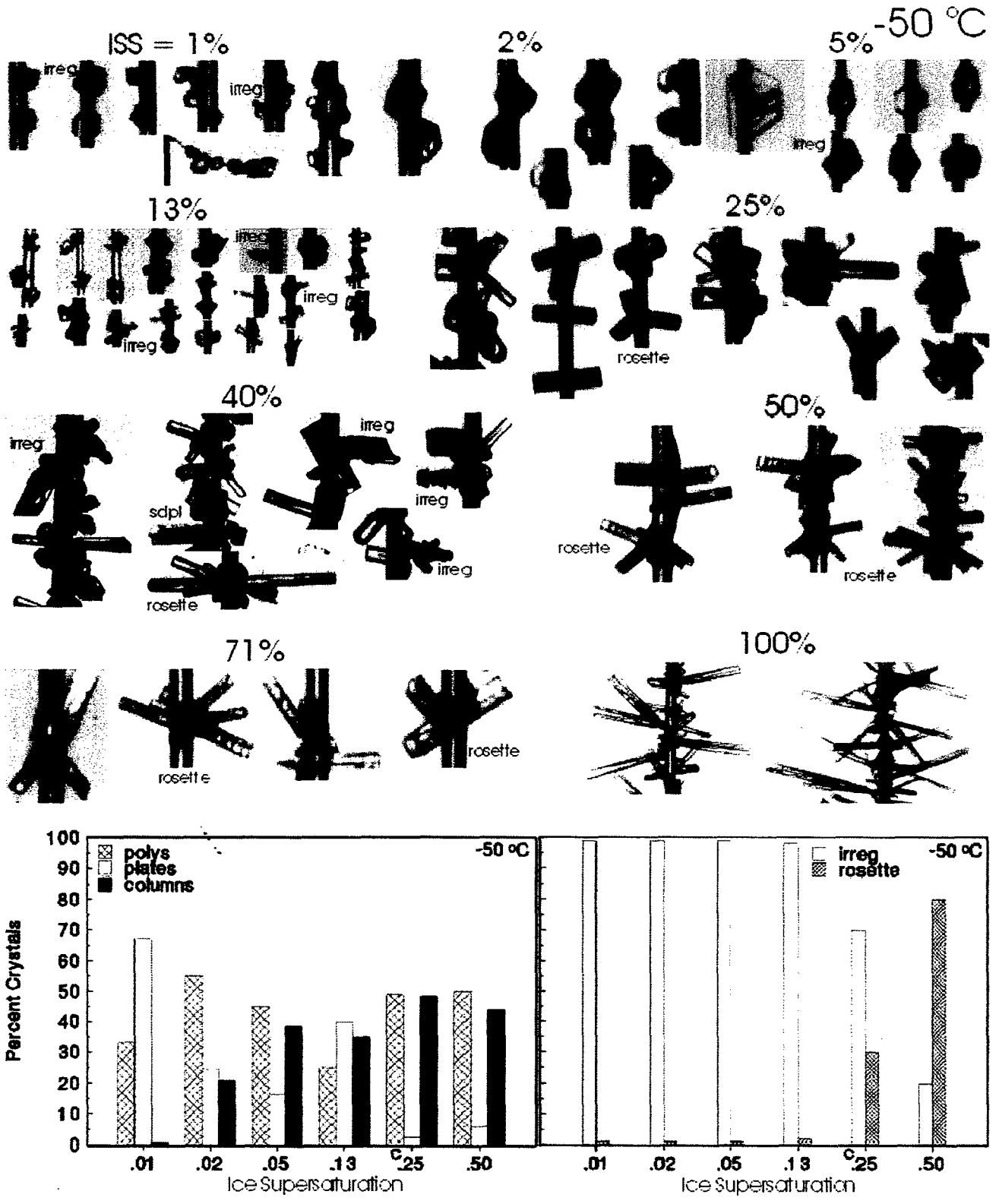
-50 °C
ISS = 1%
2%
5%
13%
25%
40%
50%
71%
100%
irreg
sdpl
rosette
polys
plates
columns
-50 °C
irreg
rosette
-50 °C
Percent Crystals
100
90
80
70
60
50
40
30
20
10
0
.01
.02
.05
.13
.25
.50
Ice Supersaturation
.01
.02
.05
.13
.25
.50
Ice Supersaturation

Figure 7

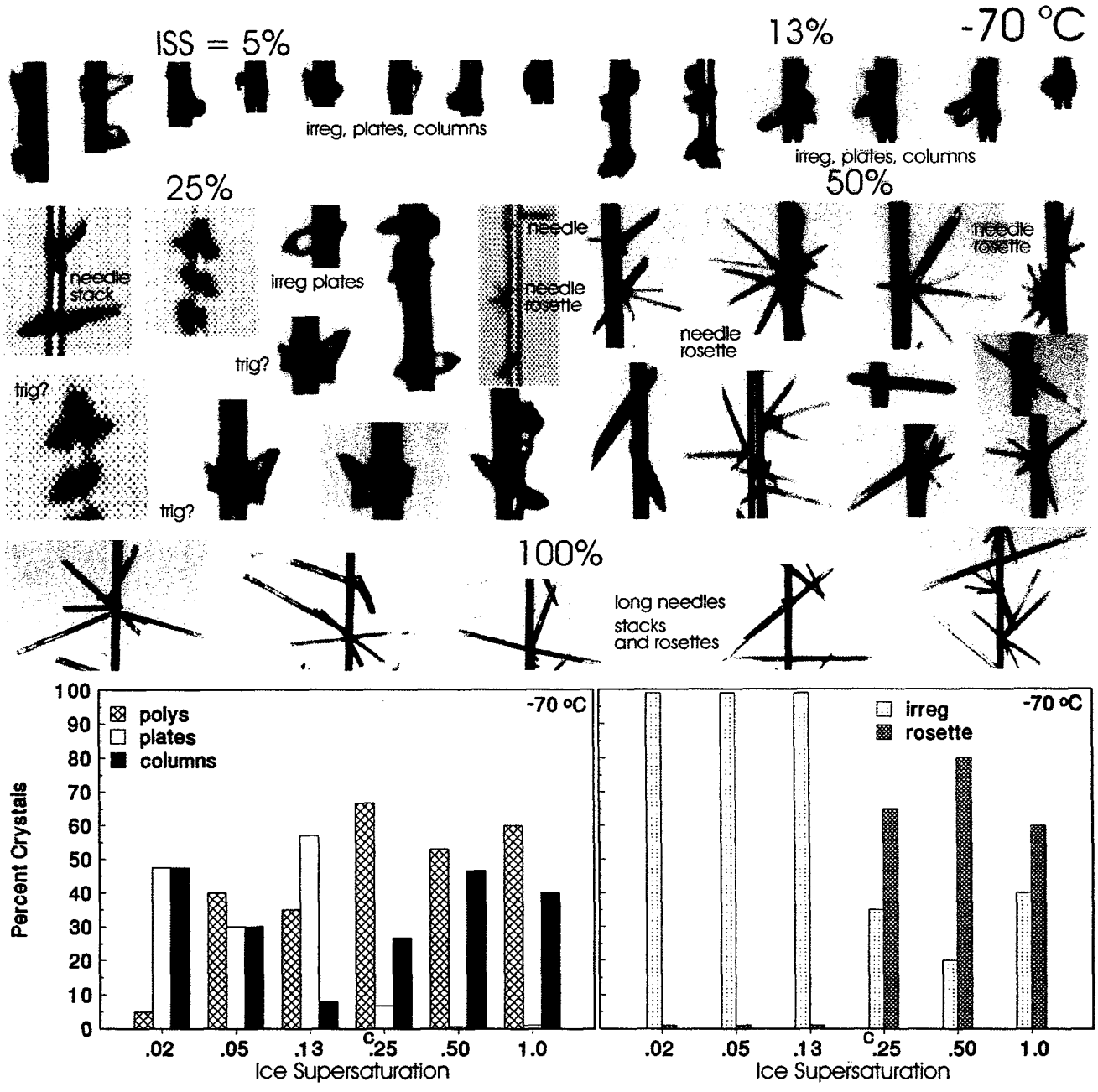
ISS = 5%
irreg, plates, columns
13%
-70 °C
irreg, plates, columns
25%
50%
needle stack
irreg plates
trig?
needle
needle rosette
needle rosette
trig?
trig?
100%
long needles
stacks
and rosettes
Percent Crystals
polys
plates
columns
-70 °C
irreg
rosette
-70 °C
.02
.05
.13
.25
.50
1.0
Ice Supersaturation
.02
.05
.13
.25
.50
1.0
Ice Supersaturation

Figure 8

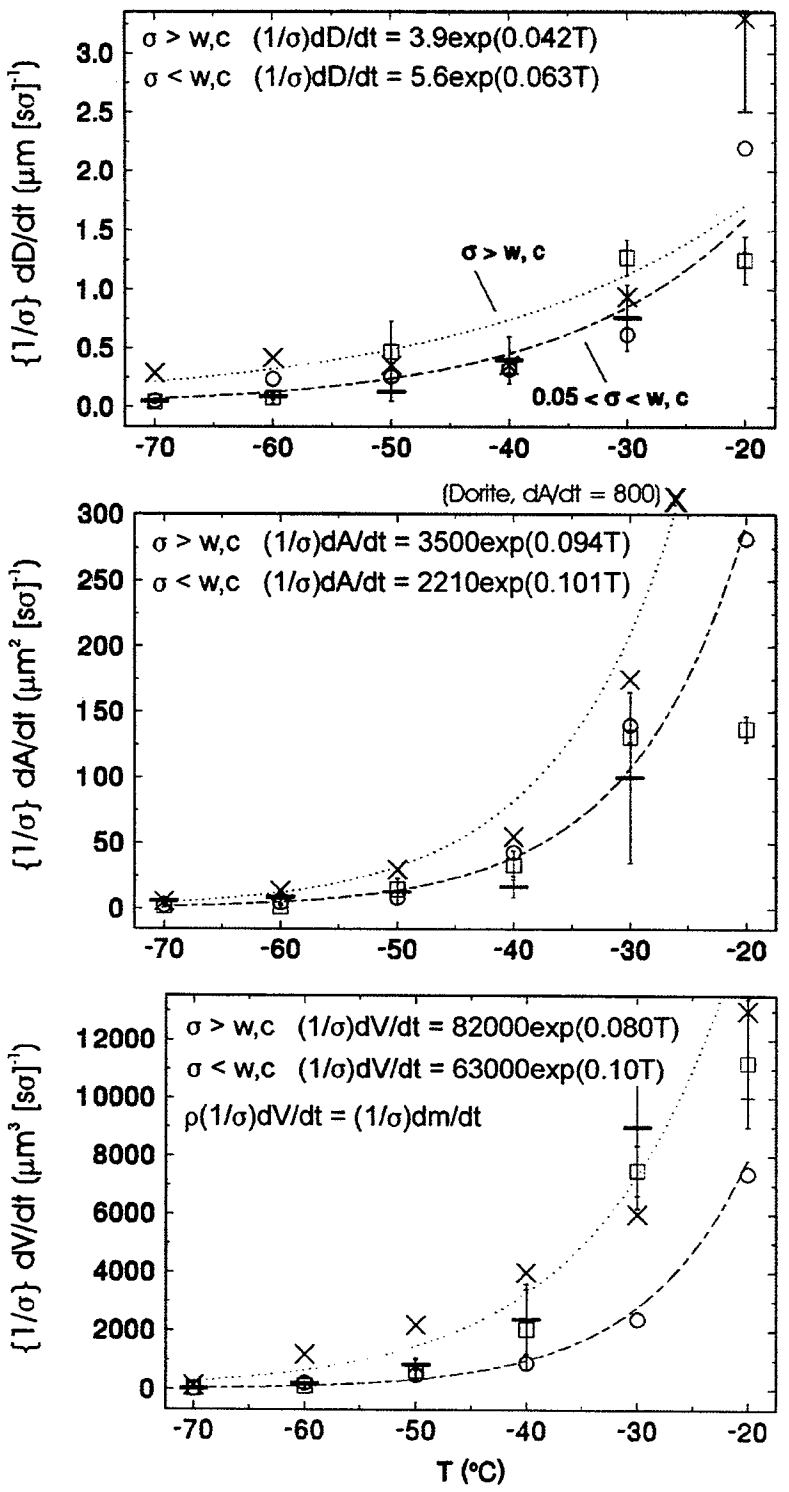

Figure 9. Derived growth rate data for dimension, area and volume related to temperature and normalized to supersaturation.

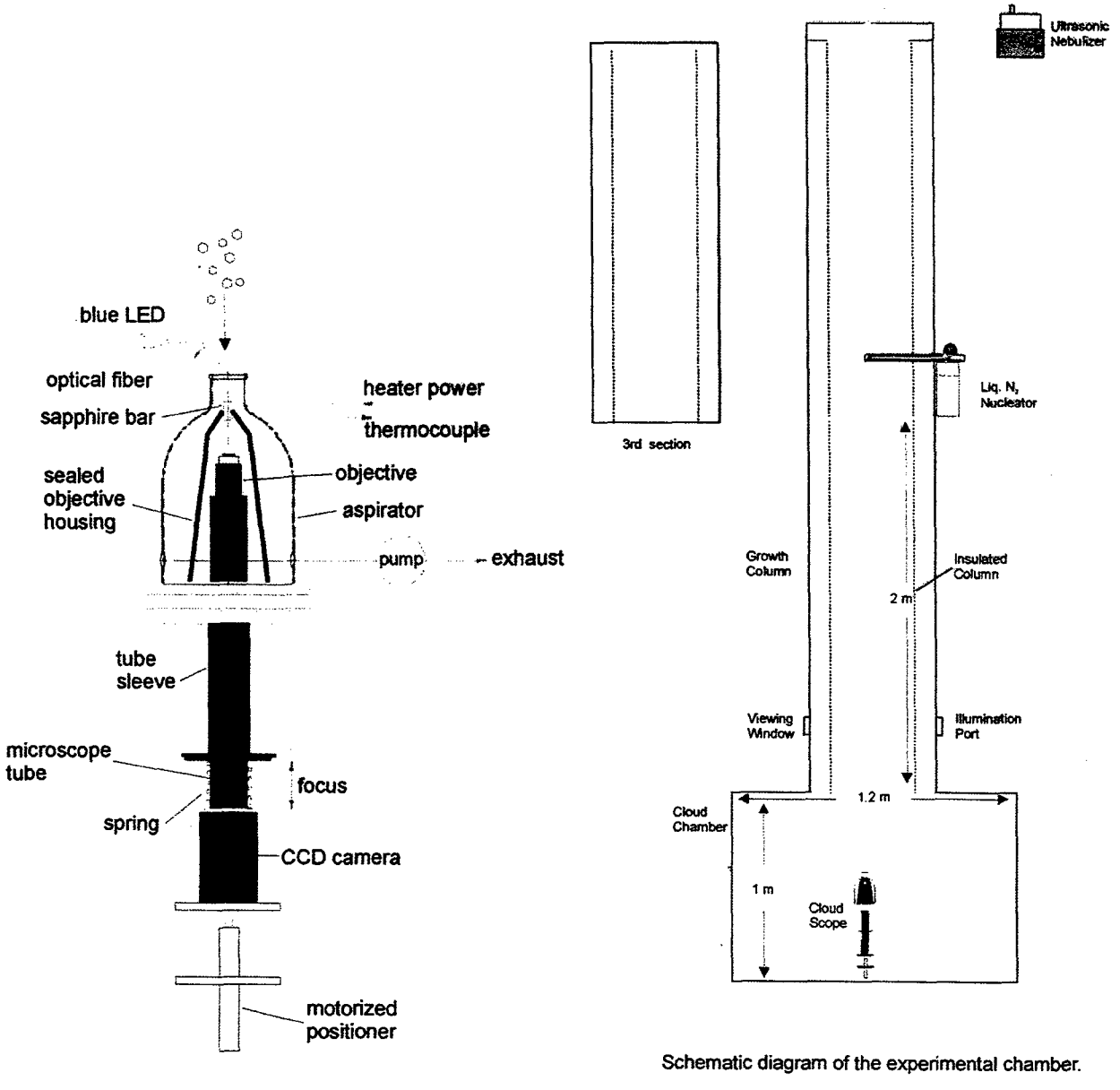

Schematic diagram of the experimental chamber.

Figure 10. Schematic of high resolution cloudscope and fall column for growing crystals at controlled temperature and near water saturation.

Figs. 11, 12. Crystals collected by the cloudscope at the base of the fall column at -20 and -40C and simultaneously passed through the optical phase measuring system described by Barkey et al (this conference).

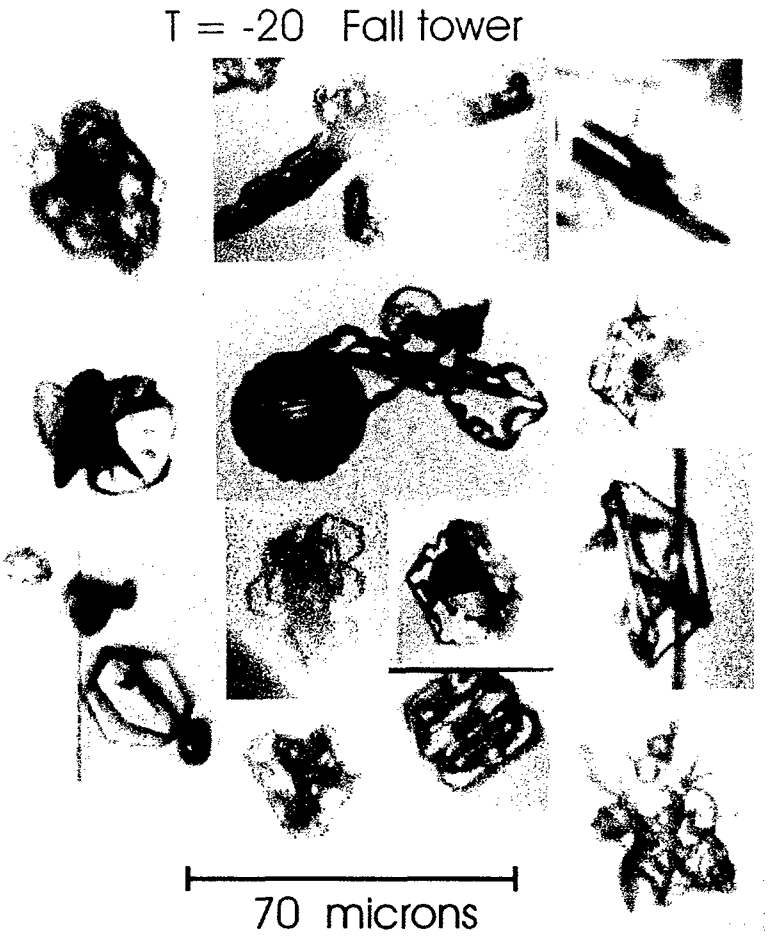

Figure 11

Figure 12

Figs. 13, 14. Schematics of arrangements of cloudscope for the balloon cirrus experiment.

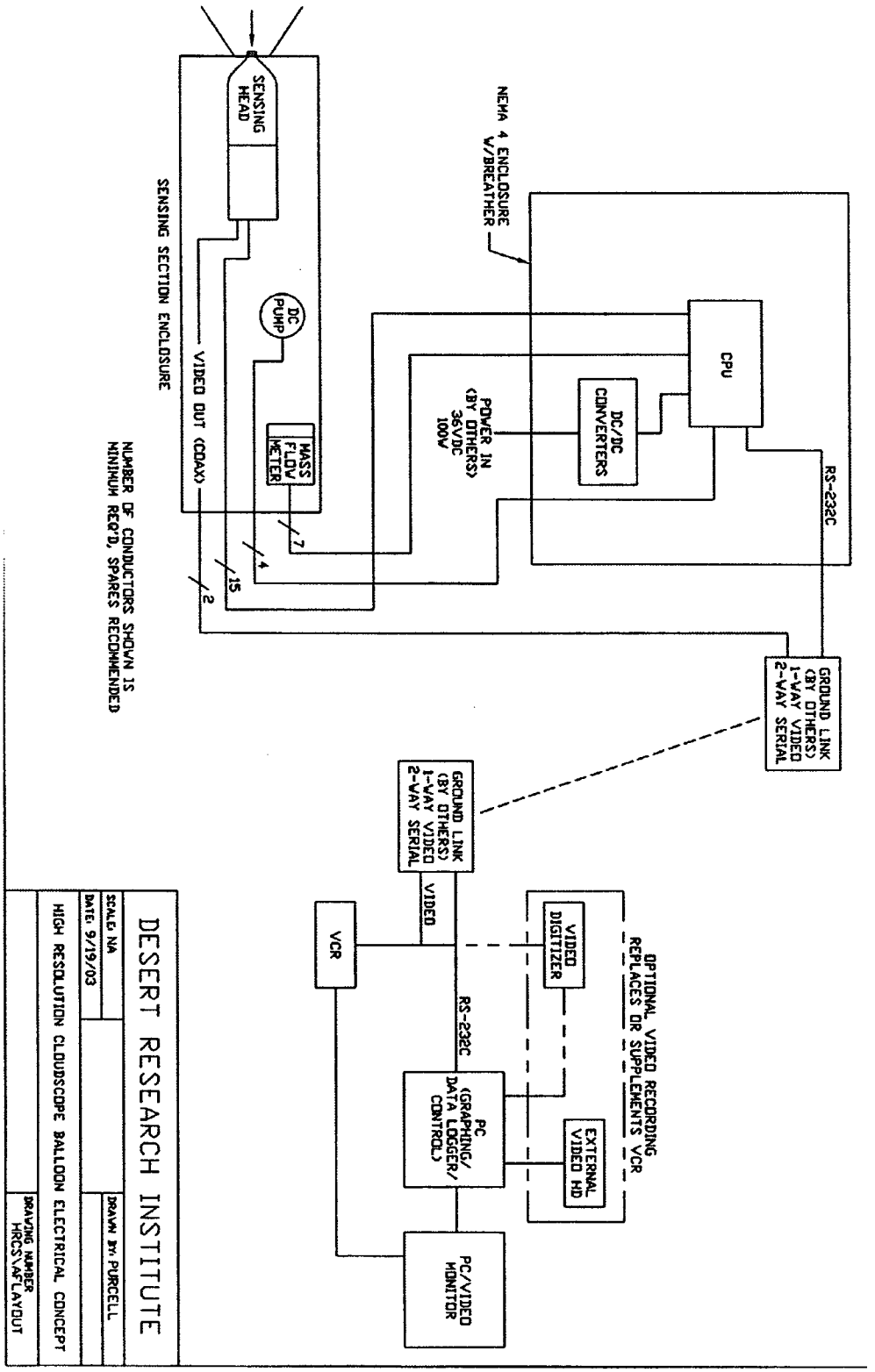

Figure 13

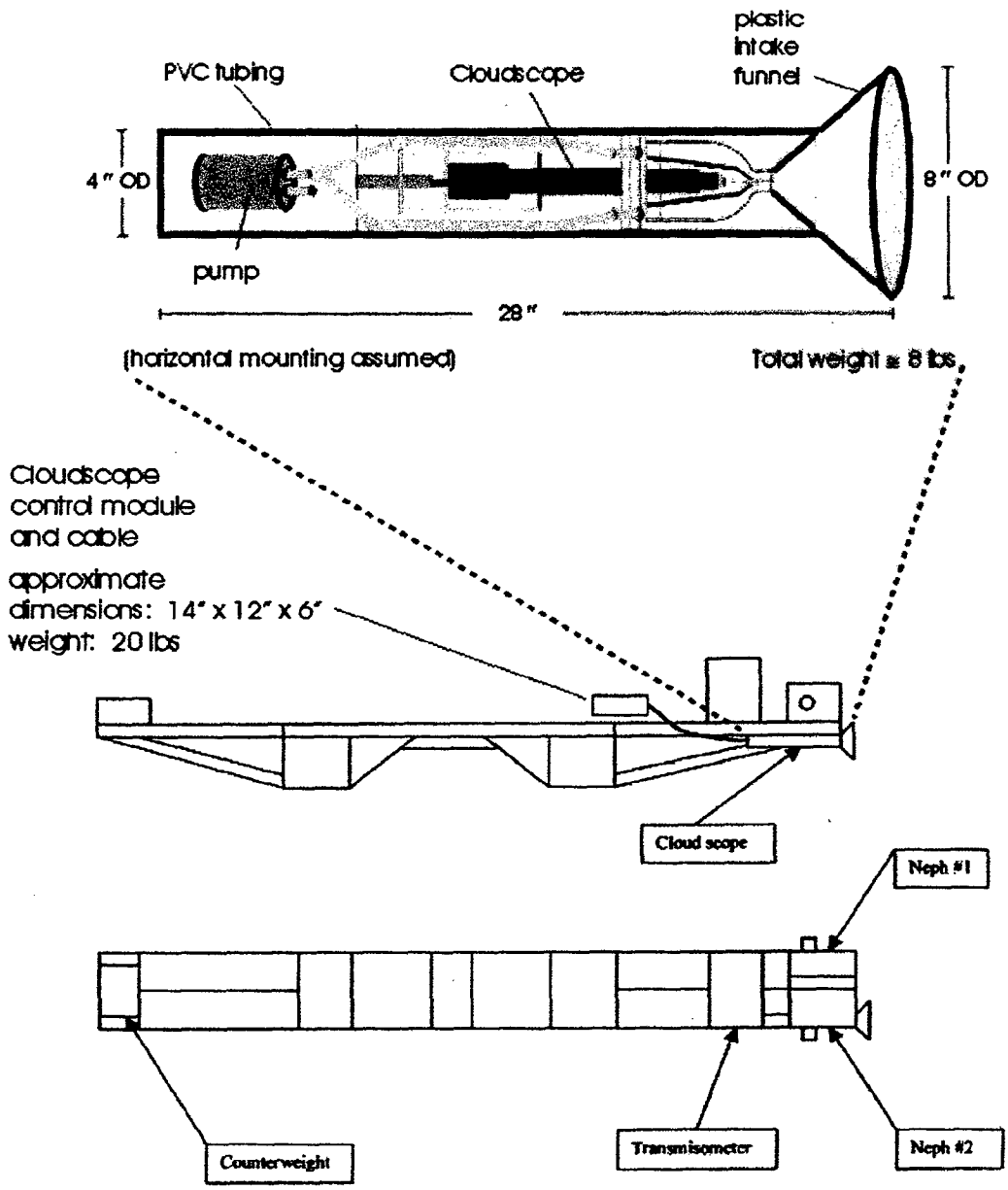
plastic
intake
funnel
PVC tubing
Cloudscope
4" OD
8" OD
pump
28"
(horizontal mounting assumed)
Total weight ≈ 8 lbs
Cloudscope
control module
and cable
approximate
dimensions: 14" x 12" x 6"
weight: 20 lbs
Cloud scope
Neph #1
Counterweight
Transmisometer
Neph #2

Figure 14

APPENDIX B

Cirrus Characterization for Laser Propagation and Global Modeling

Dr. John Hallett; Matthew Bailey
Division of Atmospheric Sciences, Desert Research Institute

With an understanding that absorption and scattering from high intensity laser beams by ice clouds is linked to the ice particle mass (for absorption), its area (for scatter) and its shape (for particle density), considerations are herein given to utilize existing laboratory studies and also previous field studies to provide insight into cirrus cloud characteristics and their variability at high levels beneath the low temperature tropical tropopause. Several studies are synthesized to provide insight into likely cirrus scenarios. The findings of this investigation were presented at the AFSOSR conference May, 2005.)

Ice, Liquid Water Content, and Particle Density Measurement in Cirrus

John Hallett, Brett Garner, Rick Purcell,
Morien Roberts, German Vidaurre, Dan Wermers
Desert Research Institute

Hallett, J., R. Purcell, M. Roberts, G. Vidaurre, and D. Wermers, 2005: Measurement for Characterization of Mixed Phase Clouds. Paper presented at the *43rd AIAA Aerospace Science Meeting*, Reno, NV, 10-13 January 2005. Paper No. 862.

DRI
Desert Research Institute

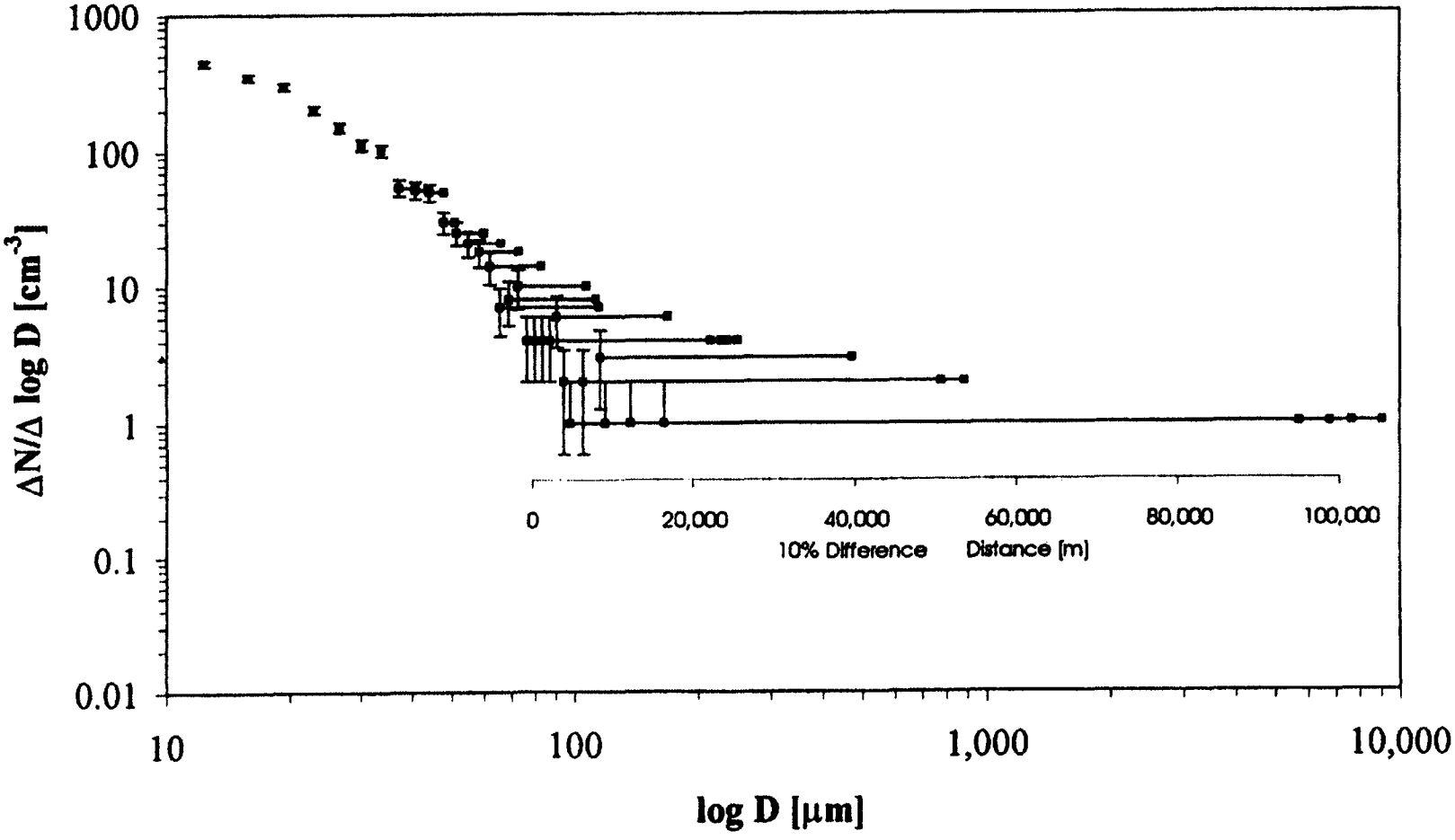
1000
100
10
1
0.1
0.01
ΔN/Δ log D [cm-3]
10
100
1,000
10,000
log D [μm]
0
20,000
40,000
60,000
80,000
100,000
10% Difference
Distance [m]

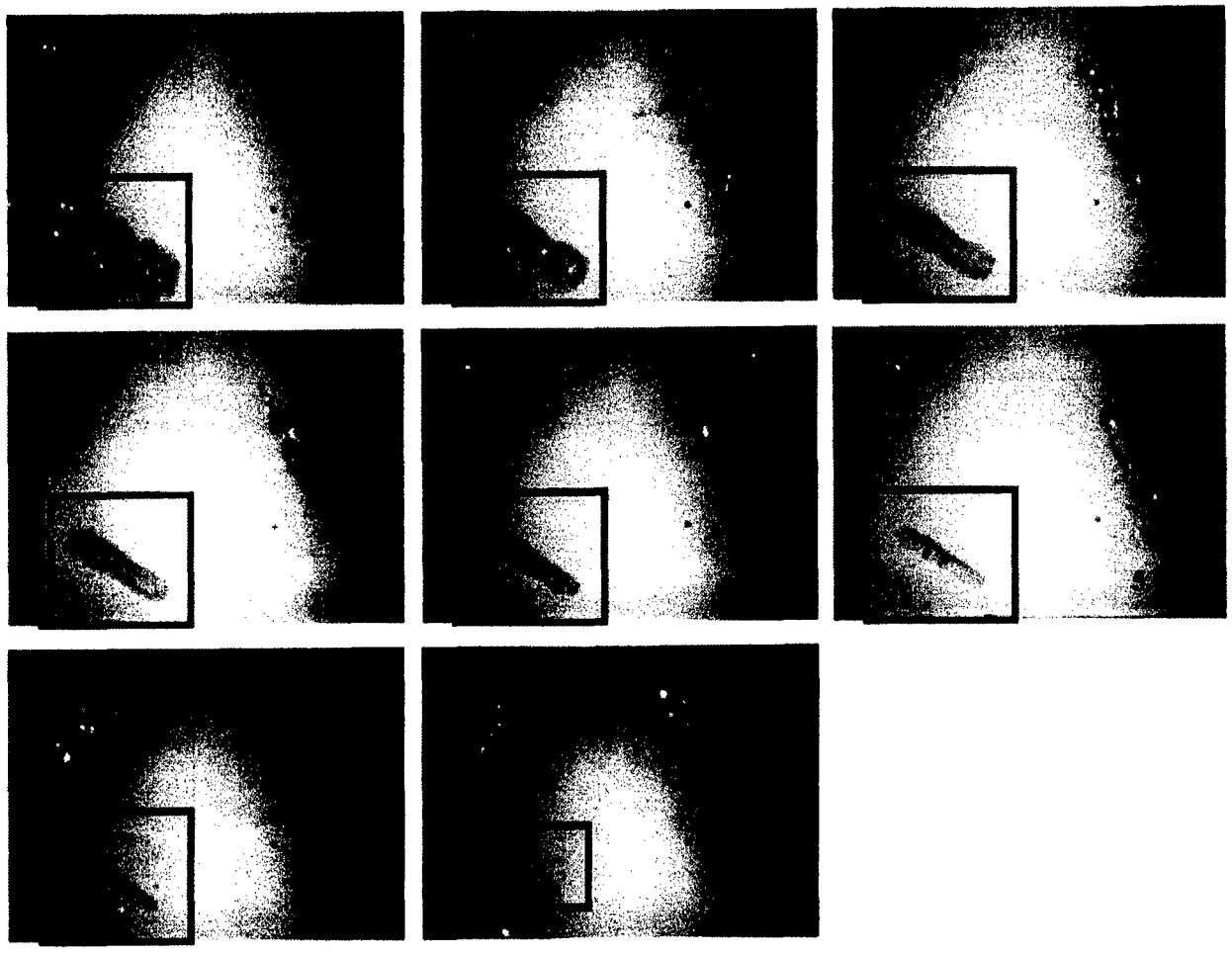

A rimed column. As it sublimated the rime is removed revealing the column.

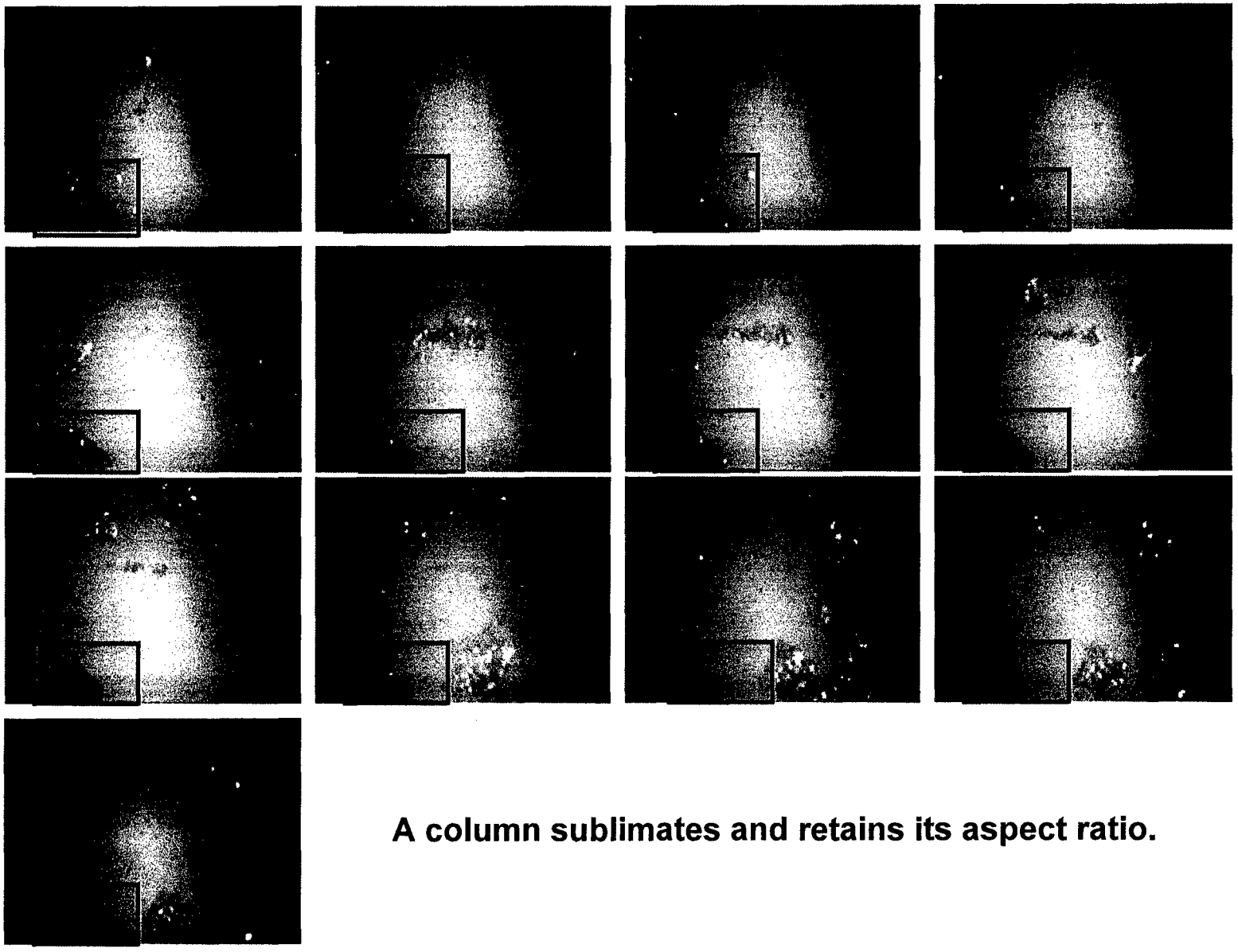

A column sublimates and retains its aspect ratio.

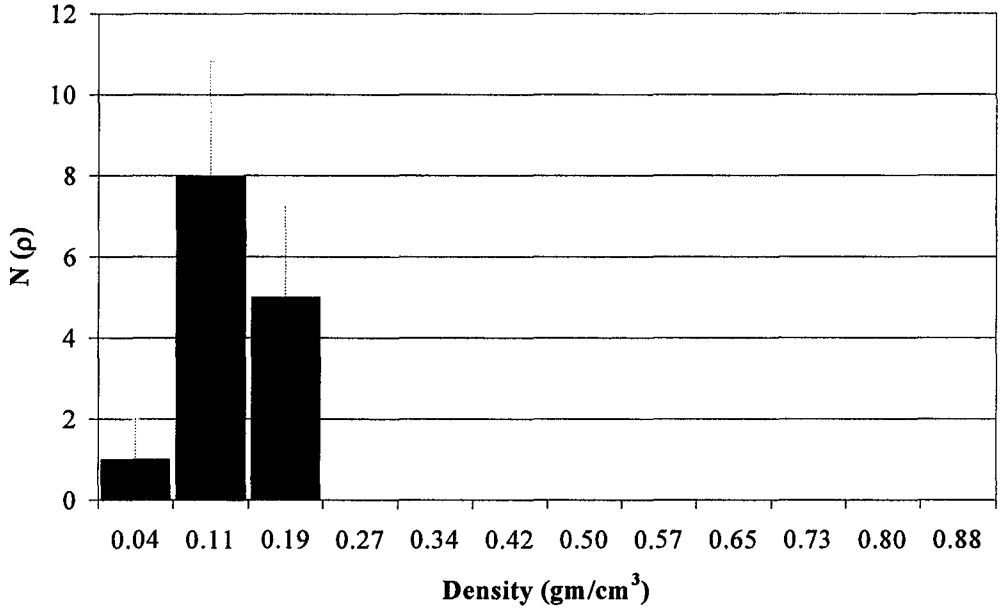

The KWAJEX density distribution for the time segment 4:20:09, tape 990730_DC8_SFCS2.

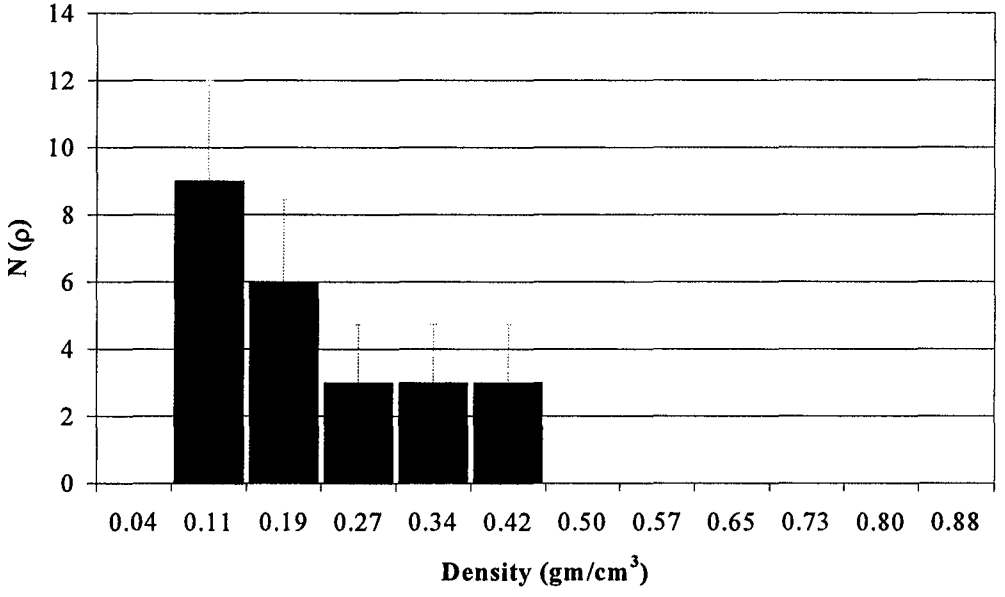

The KWAJEX density distribution for the time segment 5:07:40, tape 990730_DC8_SFCS2.

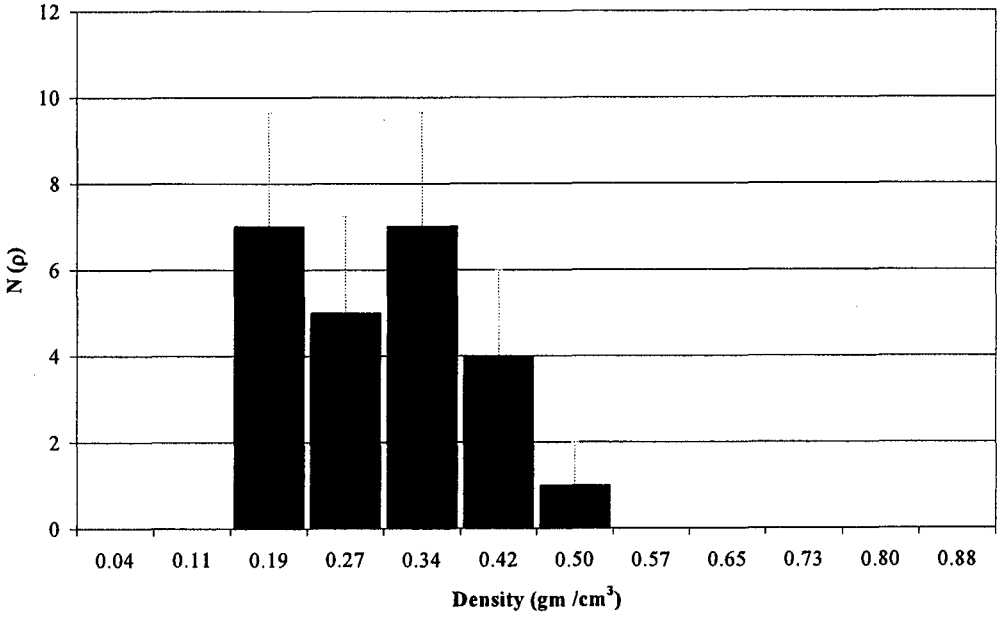

The CAMEX density distribution for flight 98 04 14 Tape #3, time segment 10:59:52.

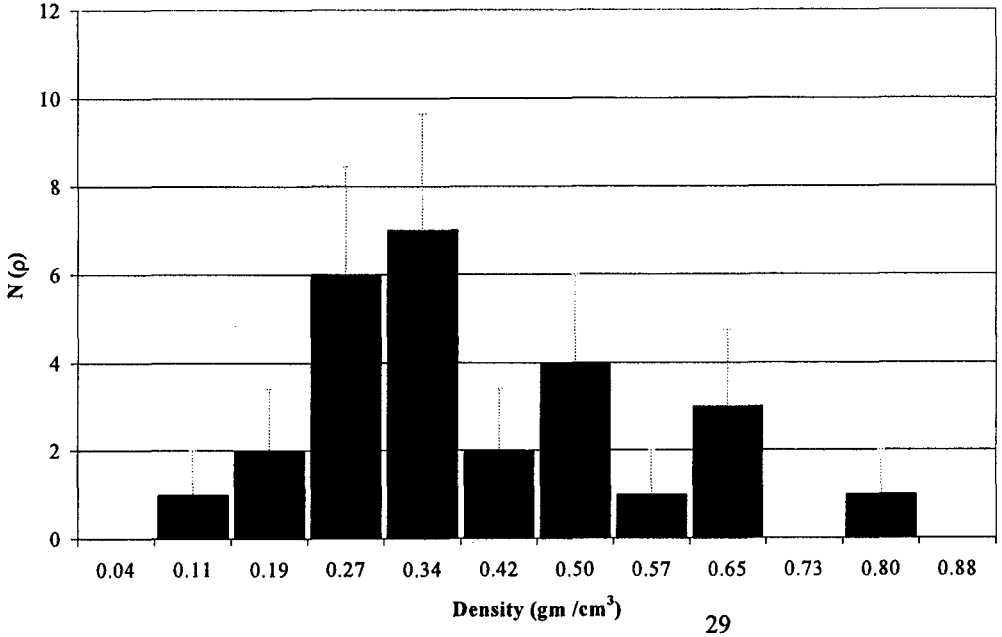

A composite distribution of time segments 10:59:51 to 11:00:00.

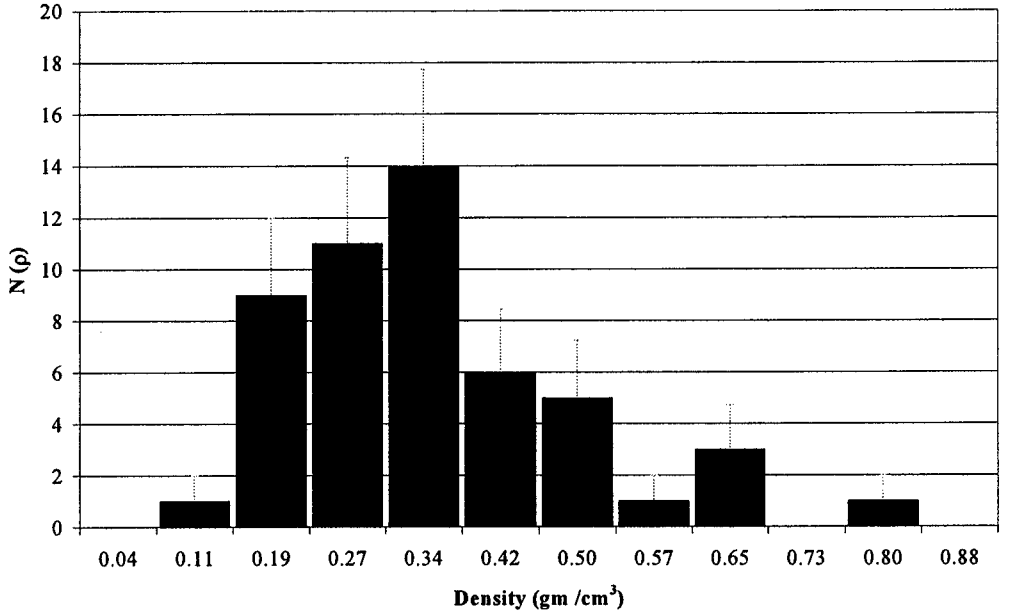

A composite distribution of time segments 10:59:51 to 11:00:00.

a)

b)

c)

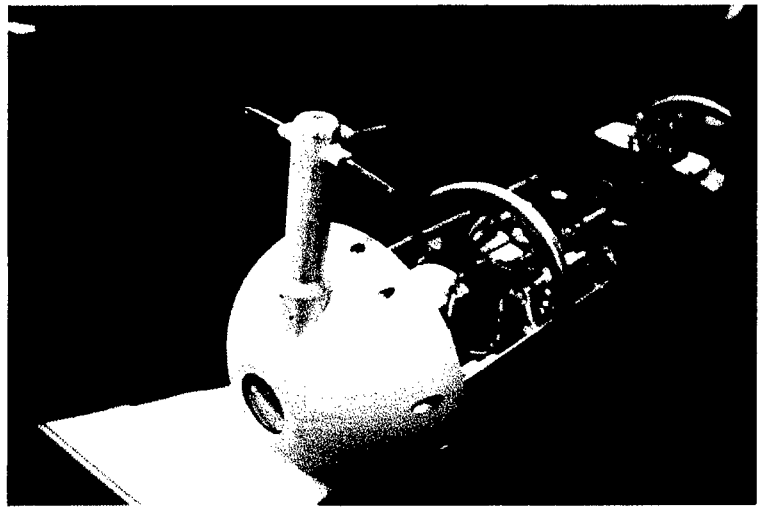

a) Small, and b) Large T probes mounted on NCAR C130. c) Shows detail of internal construction for the pod mount, with optical window for particle impaction and video recording. Both probes are oriented to be transverse to the flow and normal to the line of the re-entrant sensor.

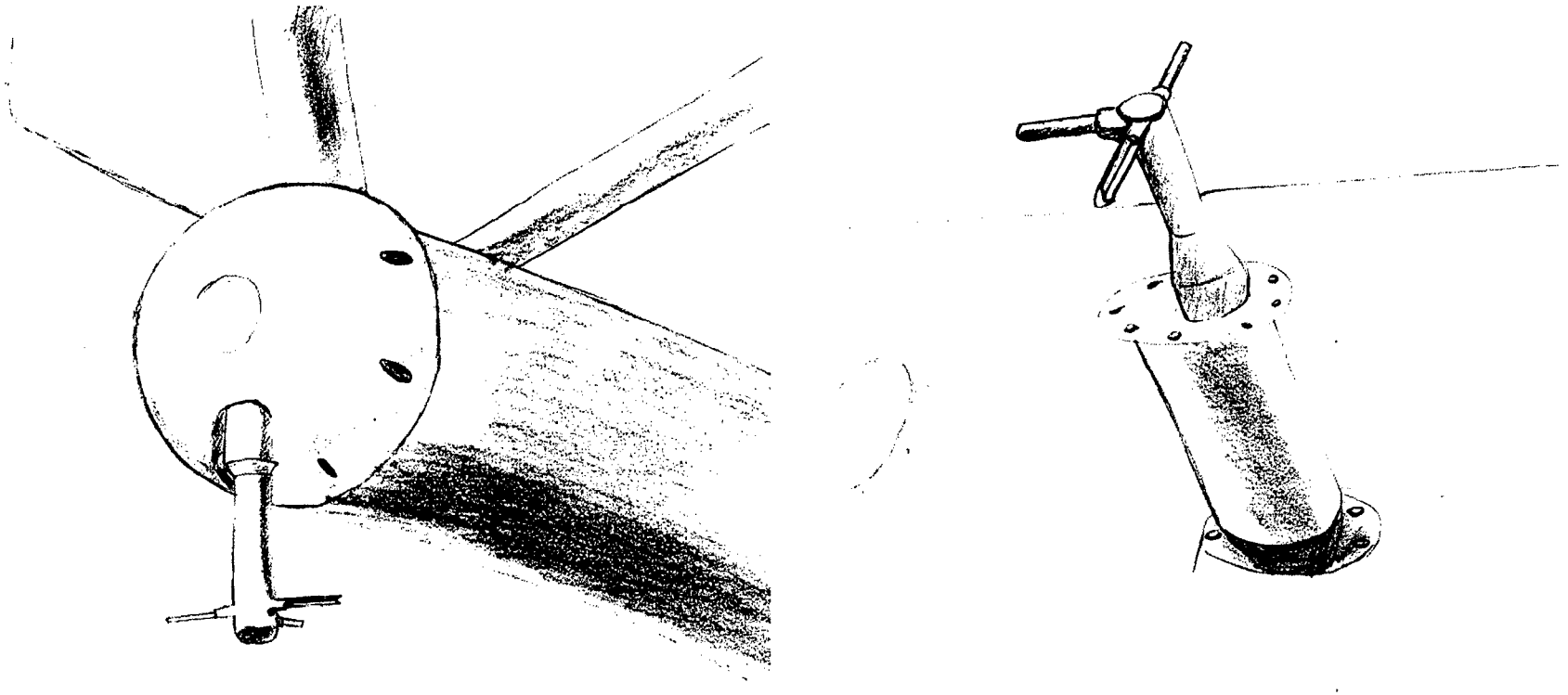

Sketches of C-130 mounting of small T probe on wing tip and large T probe on fuselage showing horizontal and vertical mounting orientations. Any difference in orientation with respect to the local airflow and associated lateral flow parallel to the sensors may result in different impaction efficiencies and splash loss.

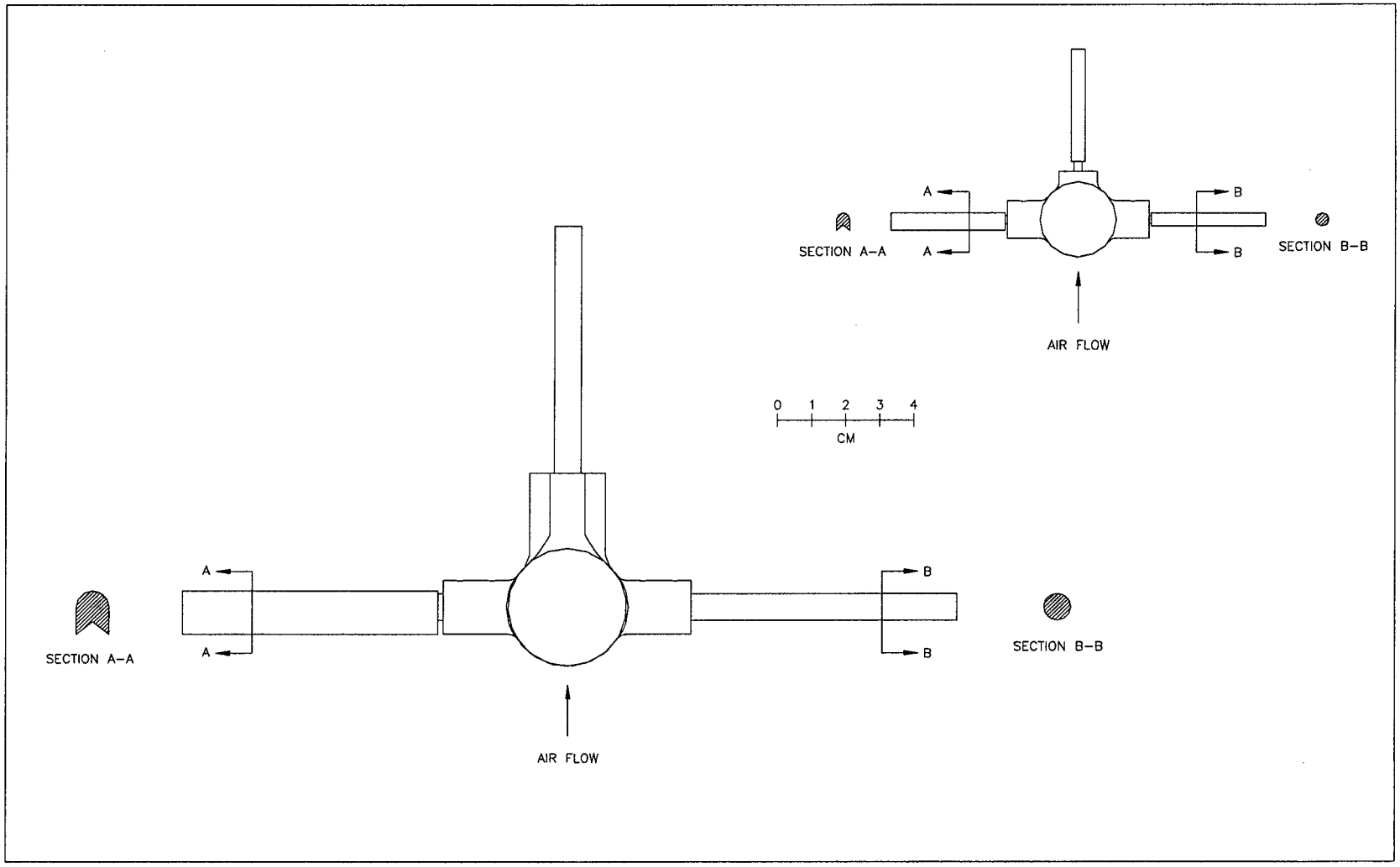

T probe showing air flow and sensor shapes for two similar shaped probes, large T, small T, having different impaction efficiency for different size. Each assembly has individual sensors with identical impaction efficiency for same size, shape and density particles.

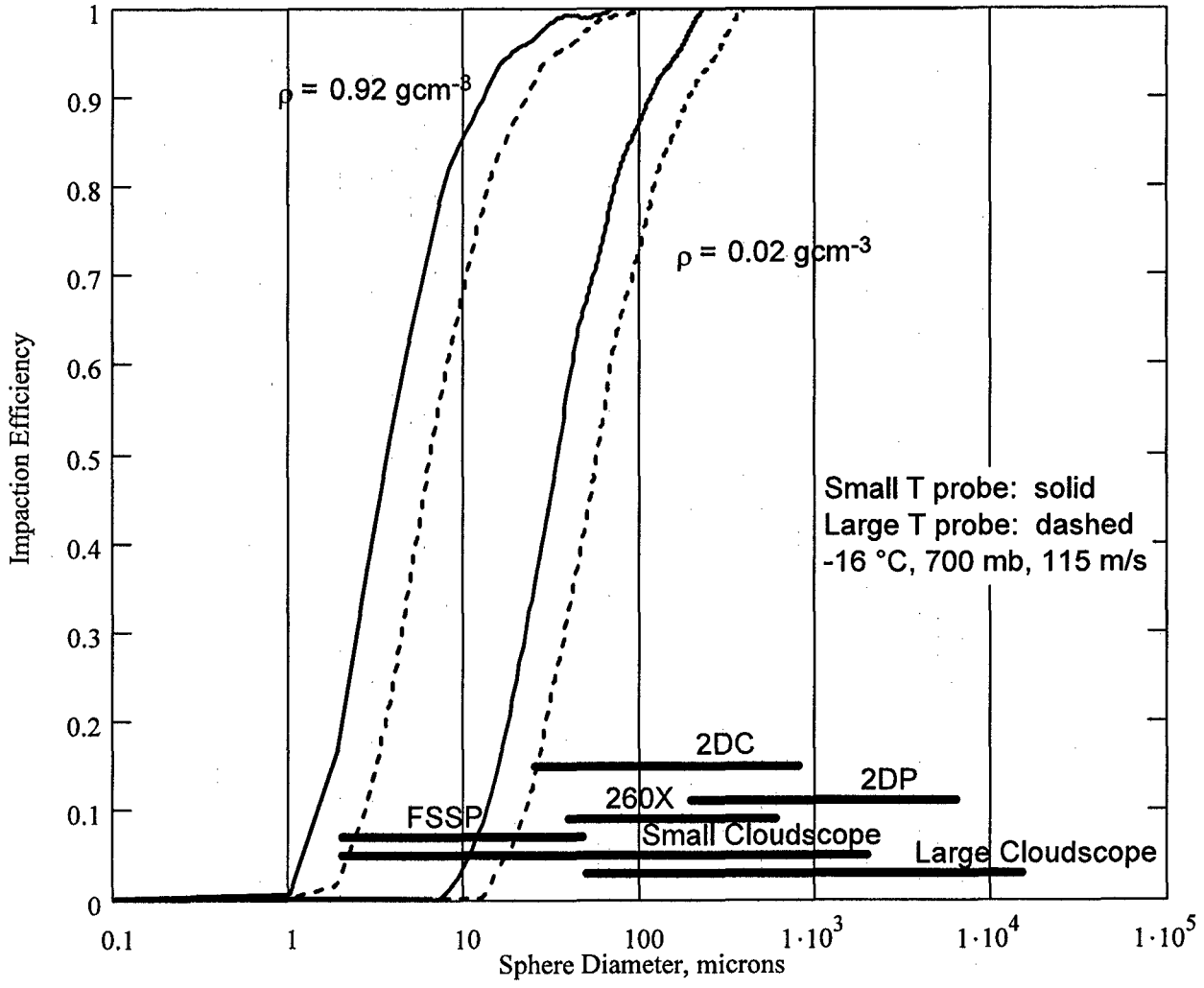

Impaction efficiency of spherical particles of different density for large and small T probes. Ranges of instruments for ancillary measurements are shown.

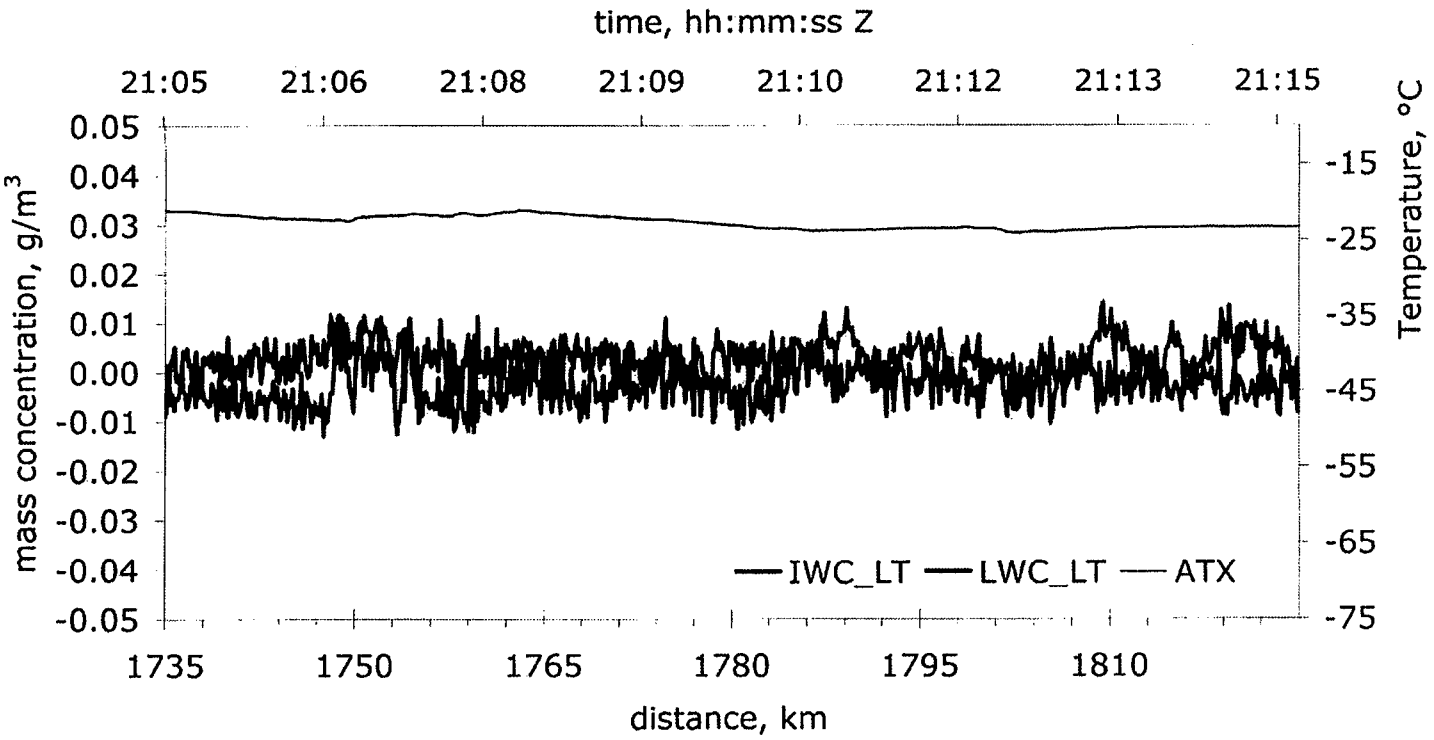

AIRS II 109rf02 Thu$_z$, Nov 6 2003

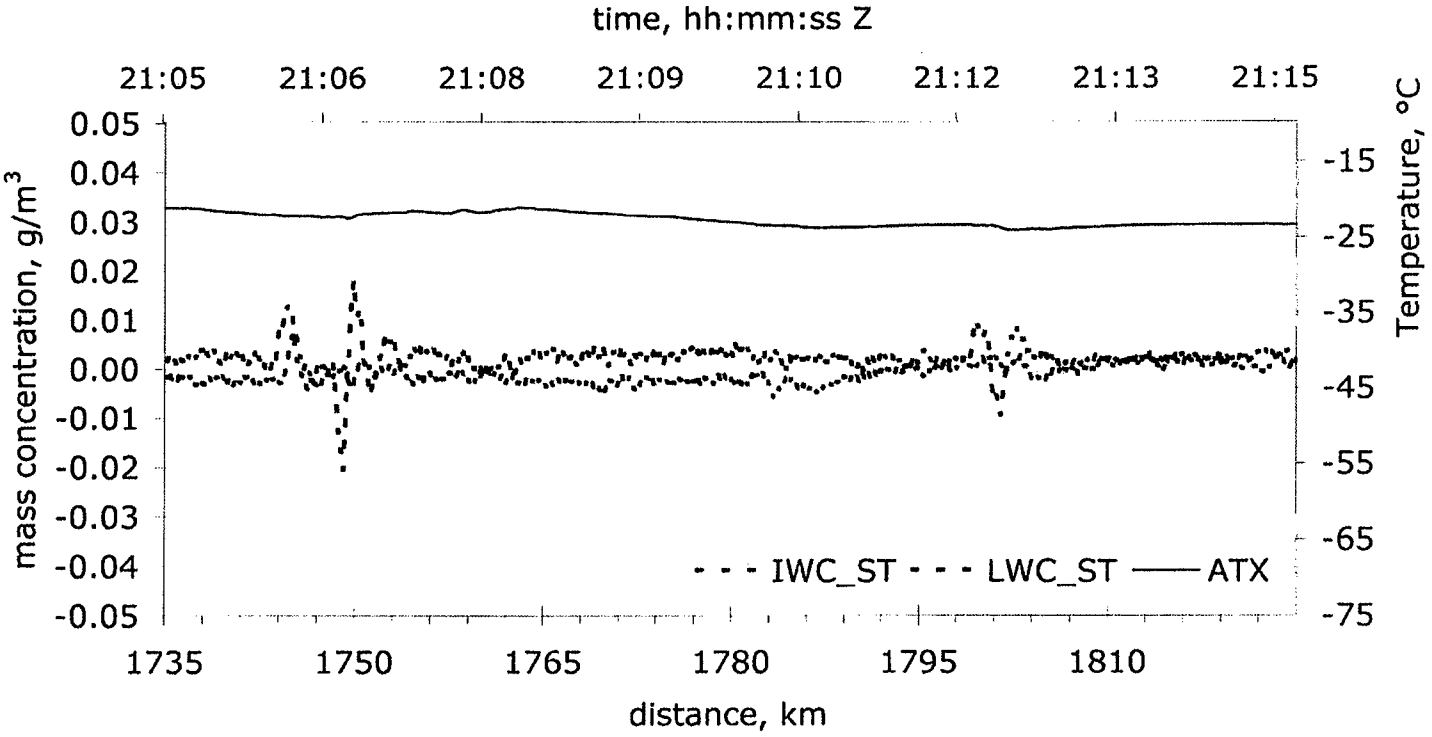

AIRS II 109rf02 Thu$_z$, Nov 6 2003

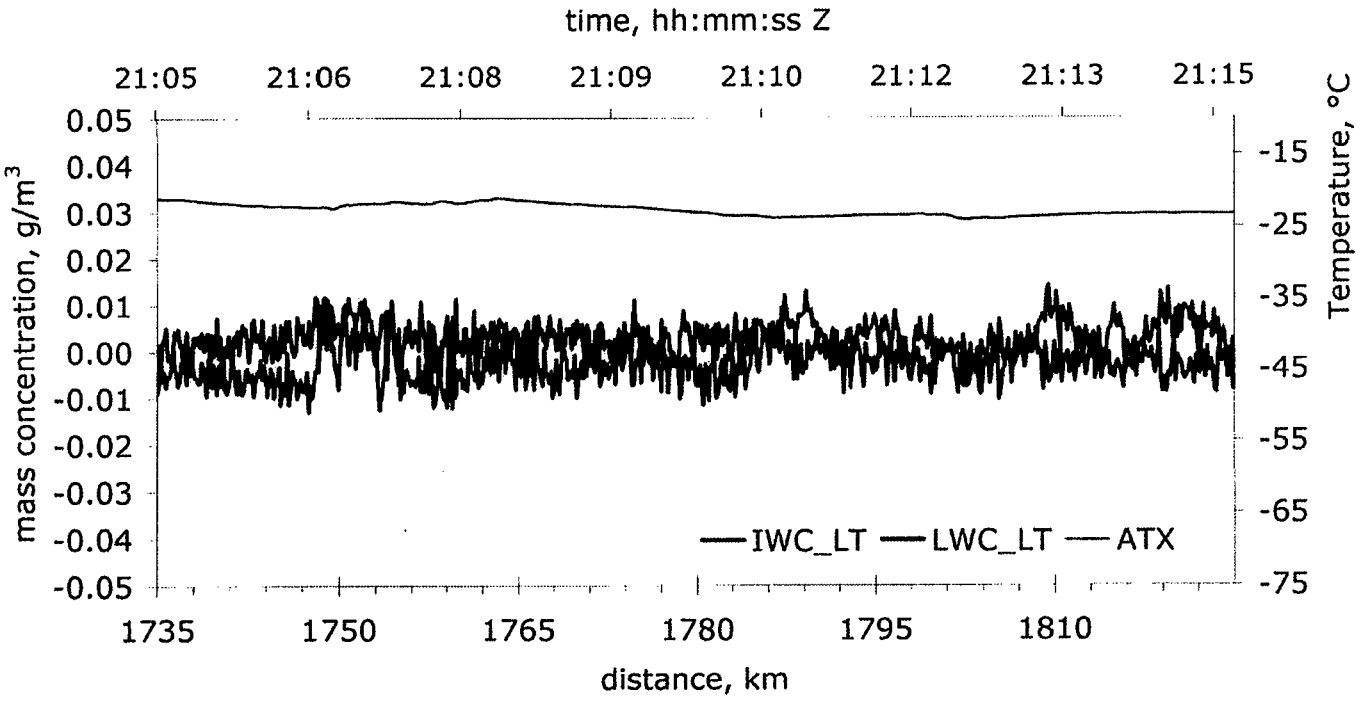

AIRS II 109rf02 Thu$_Z$, Nov 6 2003

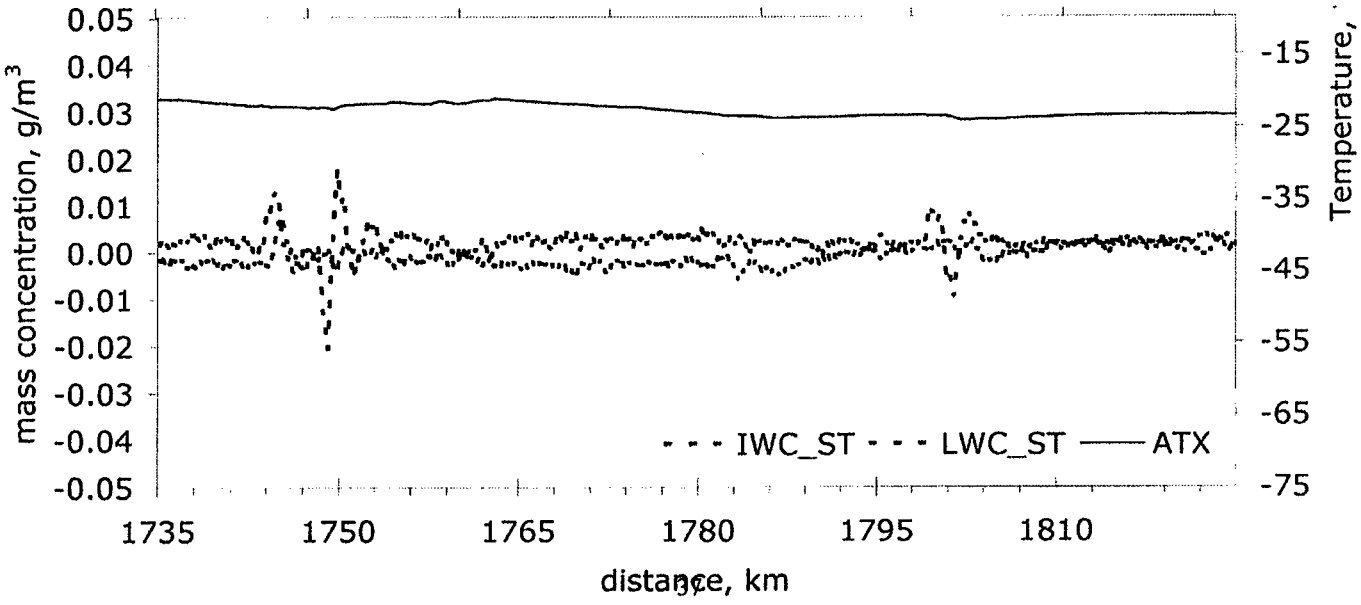

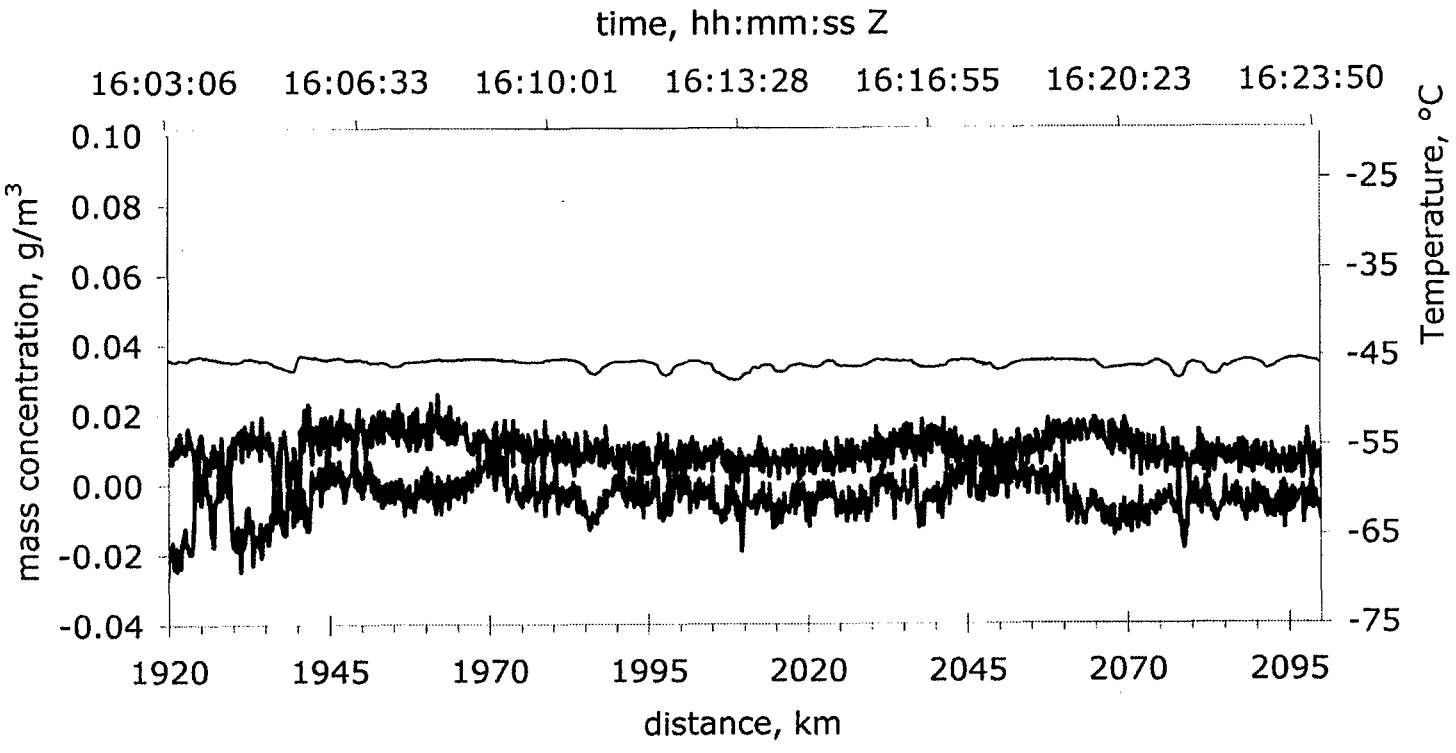

AIRS II 109rf06 Fri$_Z$, Nov 14 2003

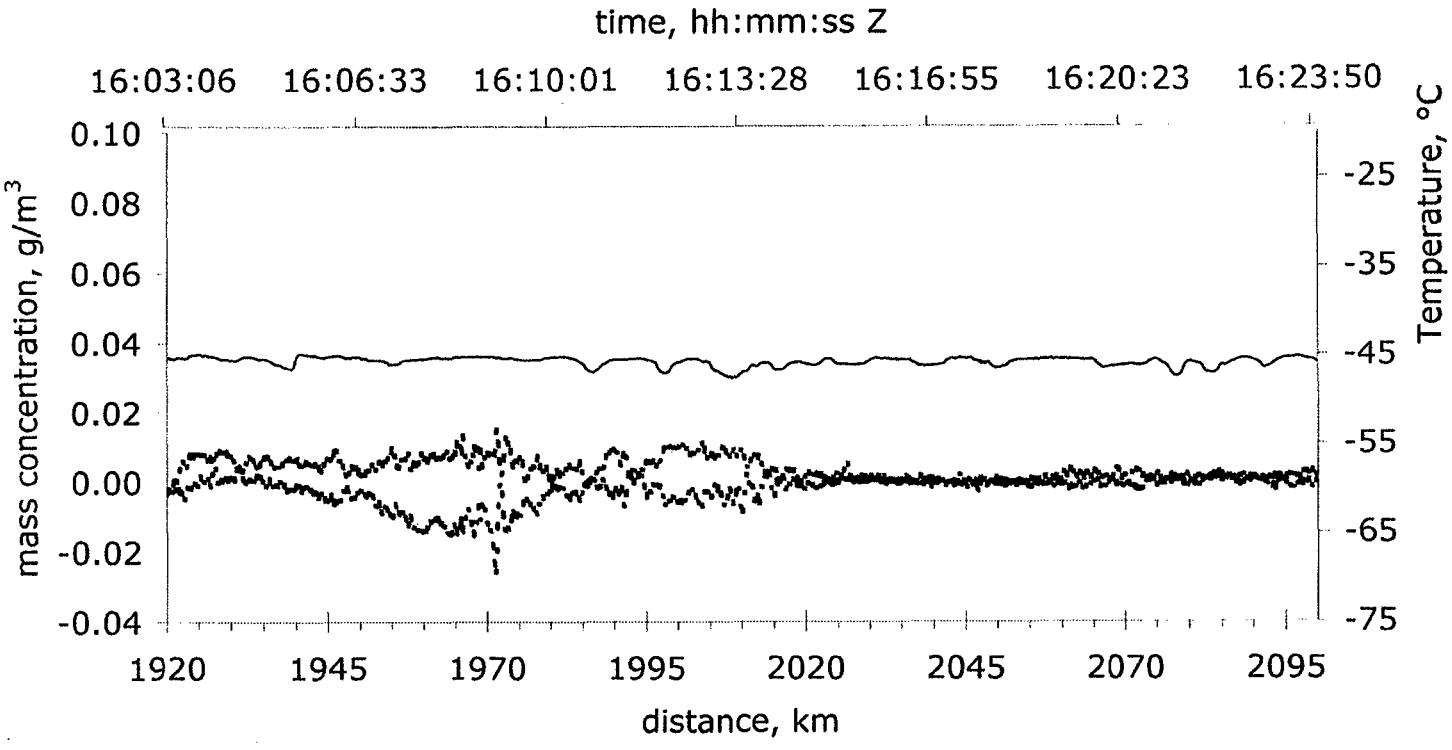

AIRS II 109rf06 Fri$_z$, Nov 14 2003

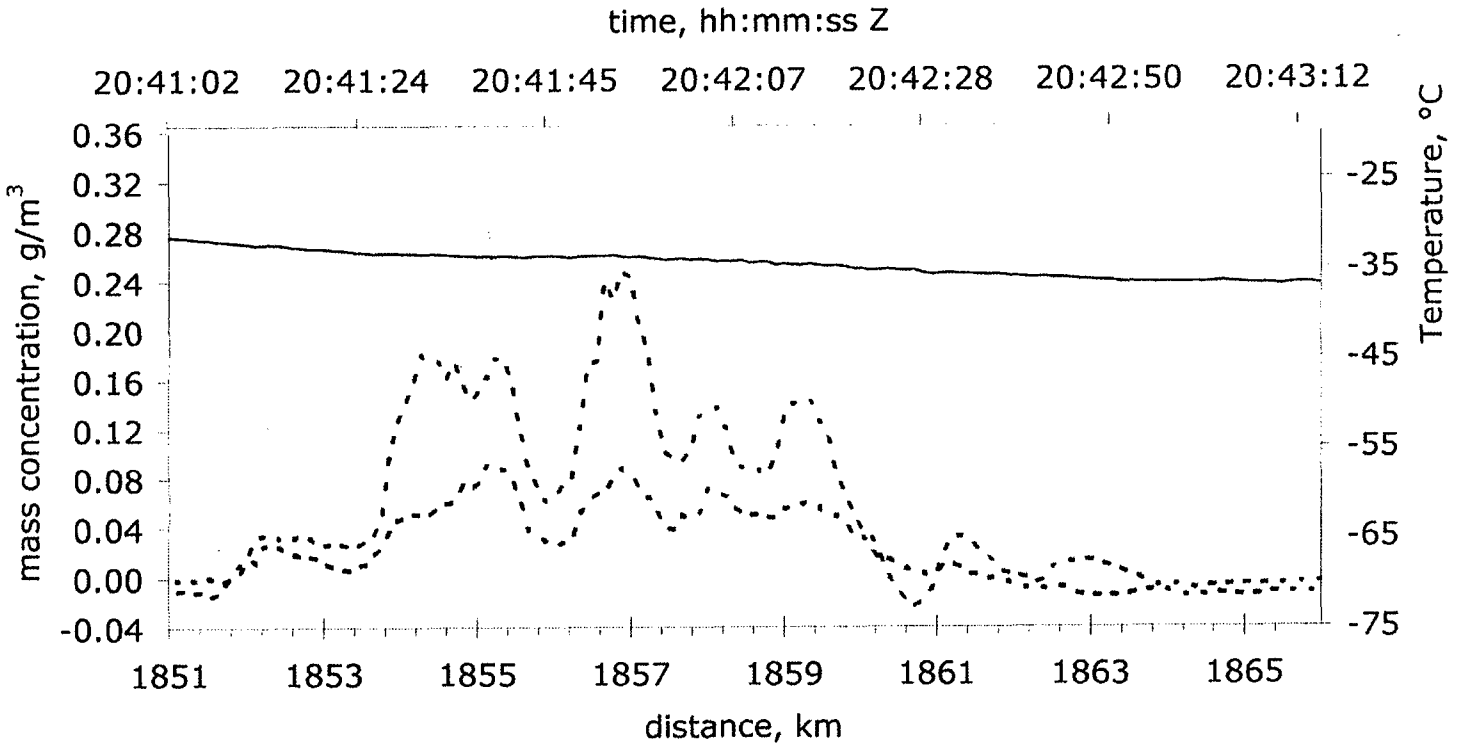

AIRS II 109rf12 Mon_Z, Dec 1 2003

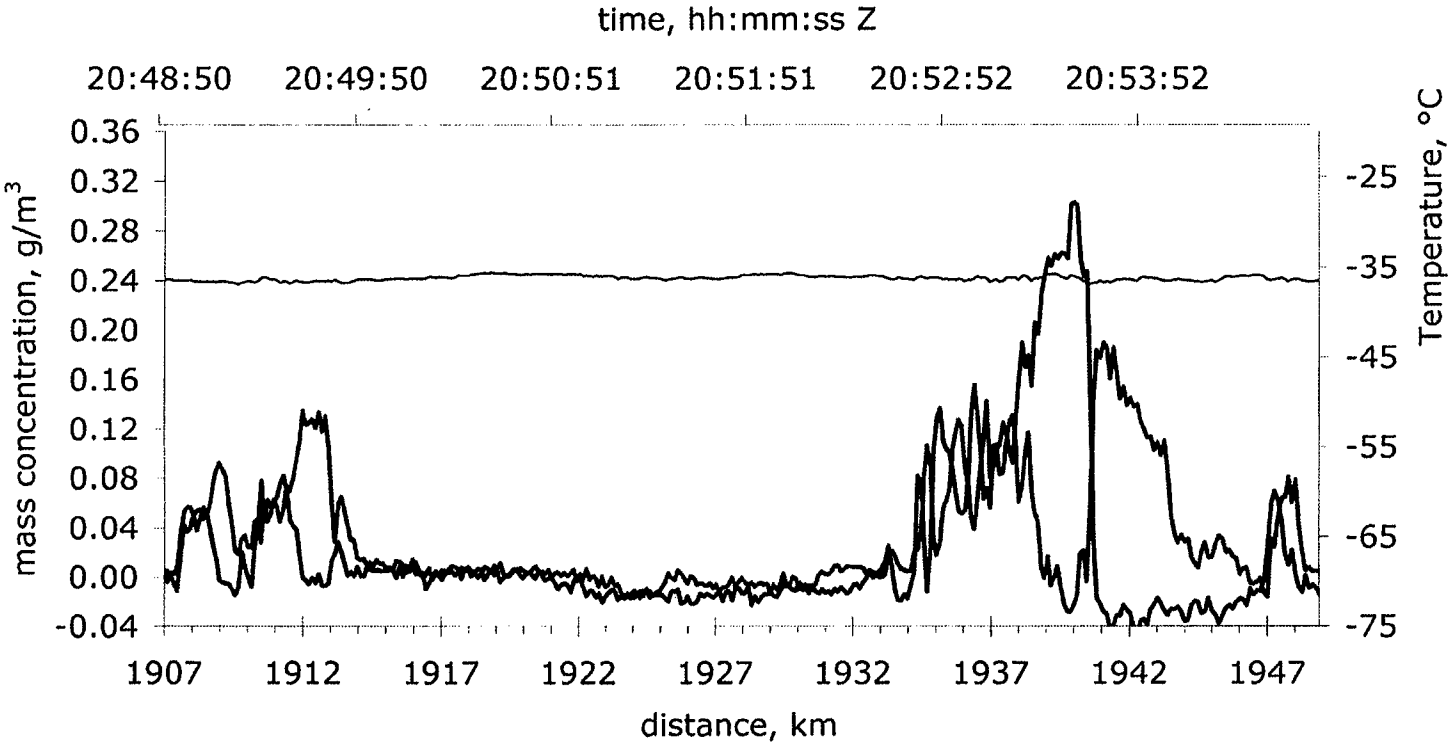

AIRS II 109rf12 Mon_Z, Dec 1 2003

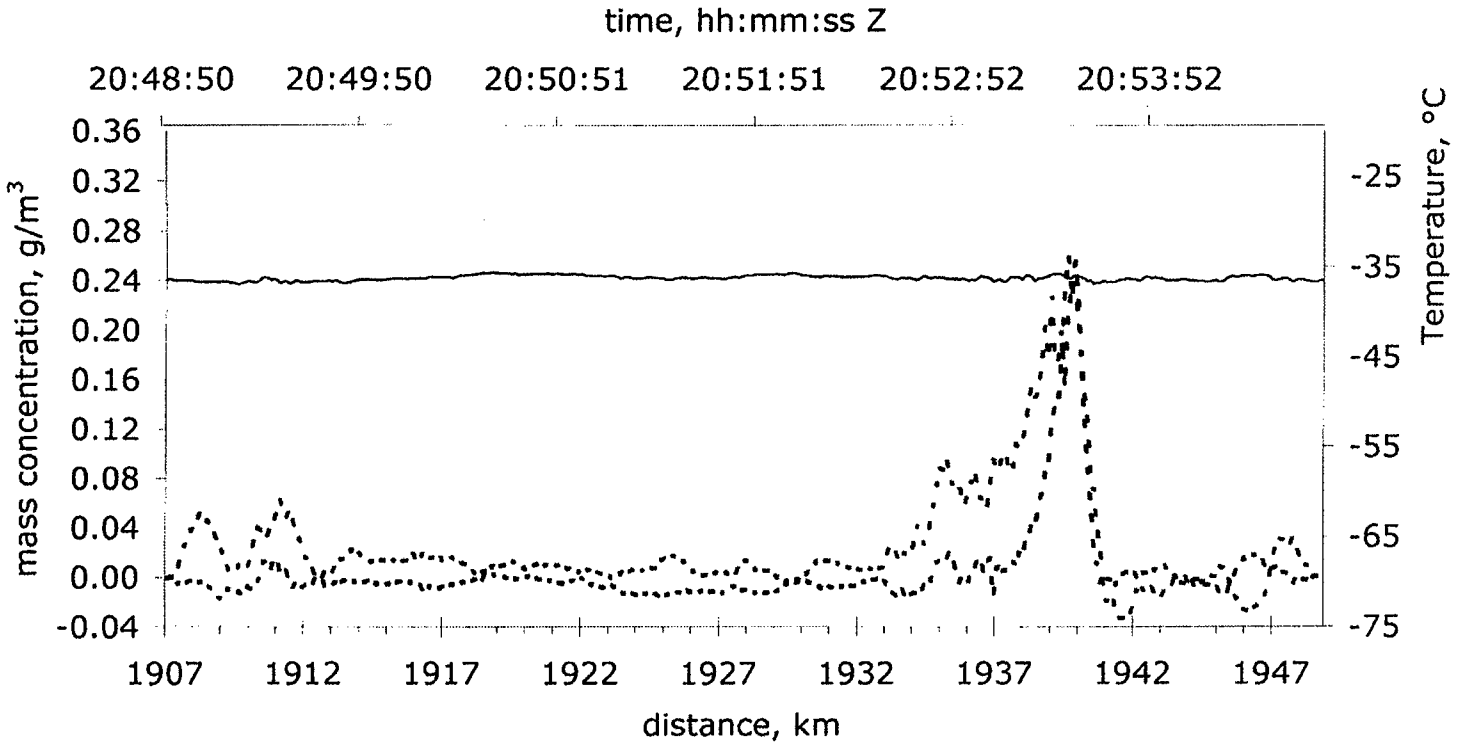

AIRS II 109rf12 Mon_Z, Dec 1 2003

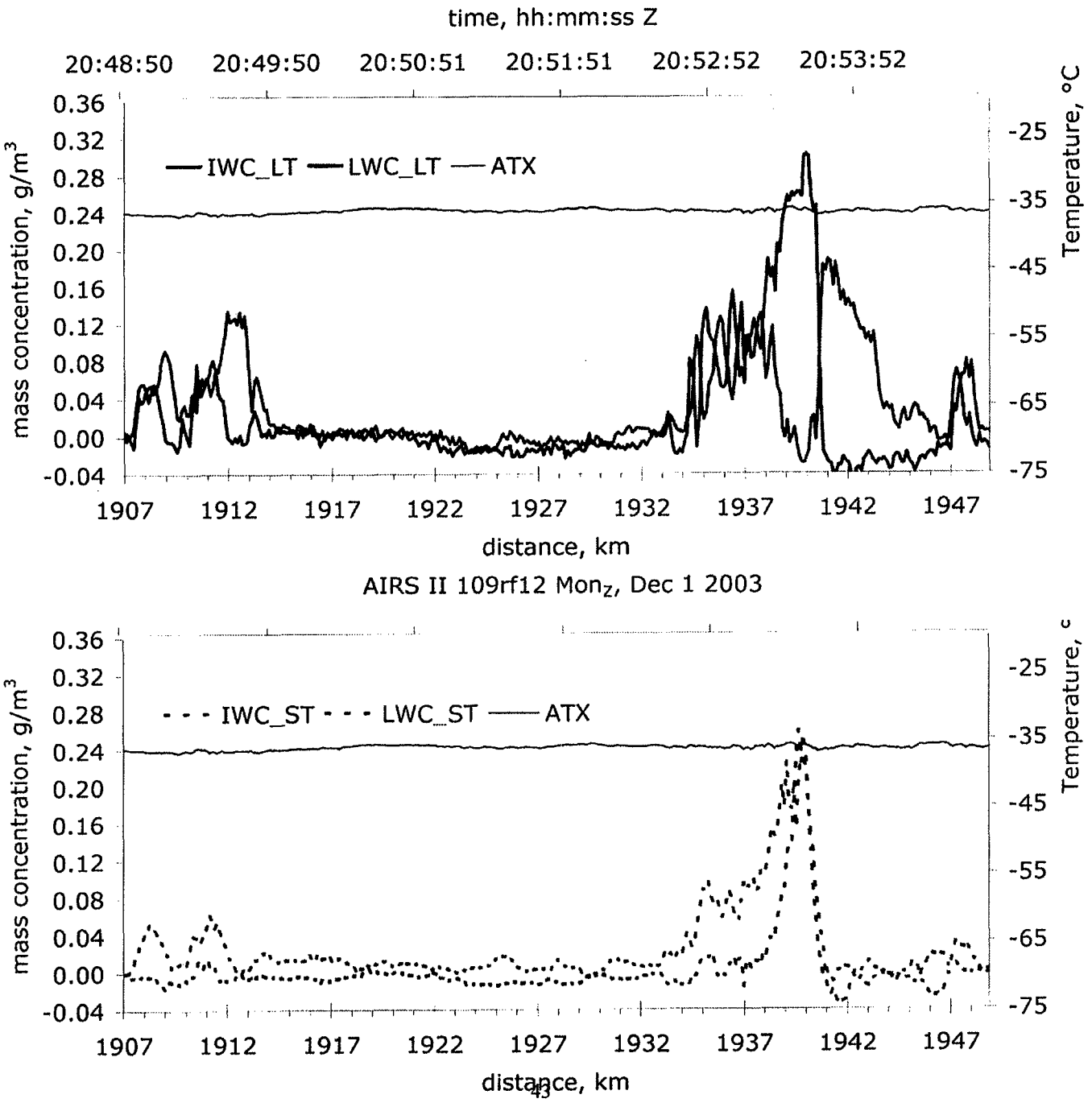
time, hh:mm:ss Z
20:48:50
20:49:50
20:50:51
20:51:51
20:52:52
20:53:52
mass concentration, g/m3
Temperature, °C
IWC_LT
LWC_LT
ATX
0.36
0.32
0.28
0.24
0.20
0.16
0.12
0.08
0.04
0.00
-0.04
-25
-35
-45
-55
-65
-75
1907
1912
1917
1922
1927
1932
1937
1942
1947
distance, km
AIRS II 109rf12 MonZ, Dec 1 2003
mass concentration, g/m3
Temperature, c
IWC_ST
LWC_ST
ATX
0.36
0.32
0.28
0.24
0.20
0.16
0.12
0.08
0.04
0.00
-0.04
-25
-35
-45
-55
-65
-75
1907
1912
1917
1922
1927
1932
1937
1942
1947
distance, km

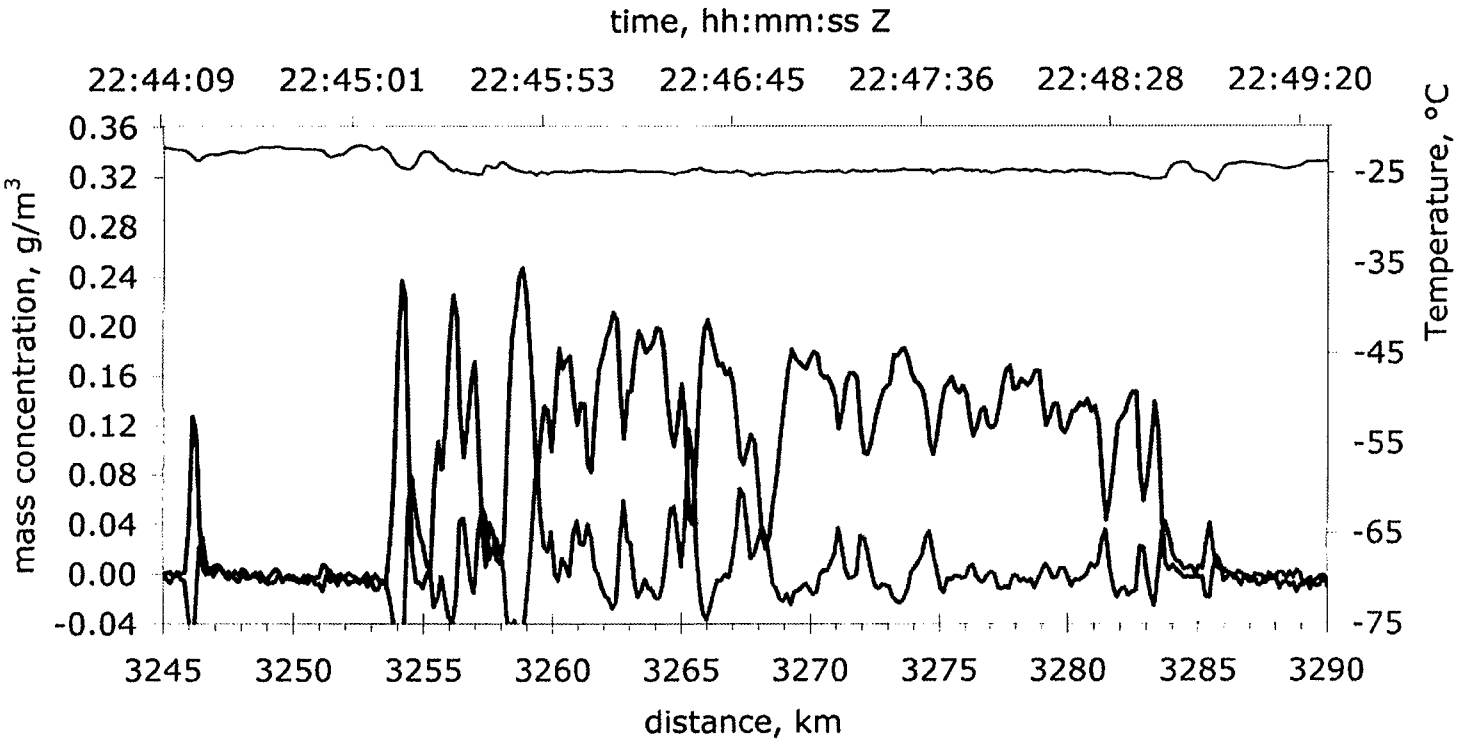

AIRS II 109rf09 Wed$_z$, Nov 19 2003

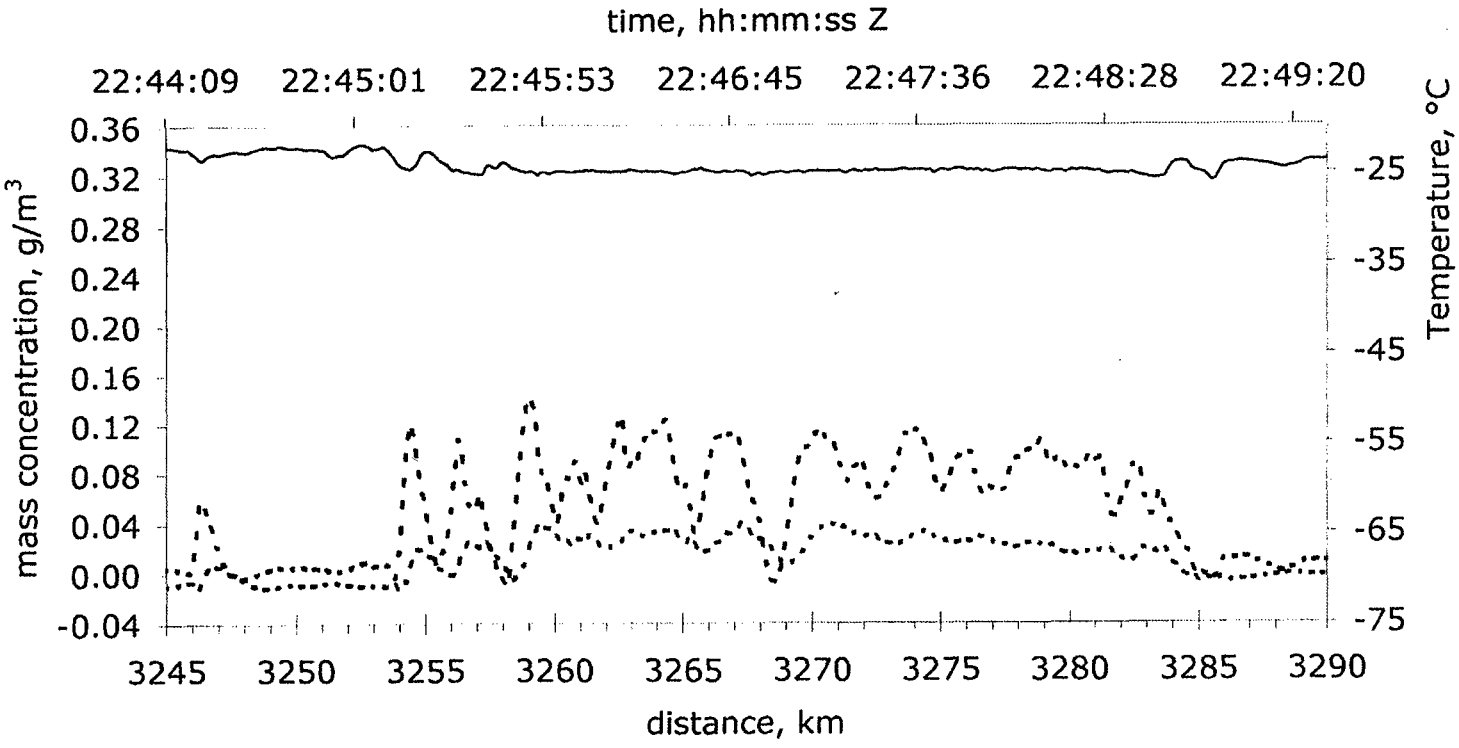

AIRS II 109rf09 Wed$_Z$, Nov 19 2003

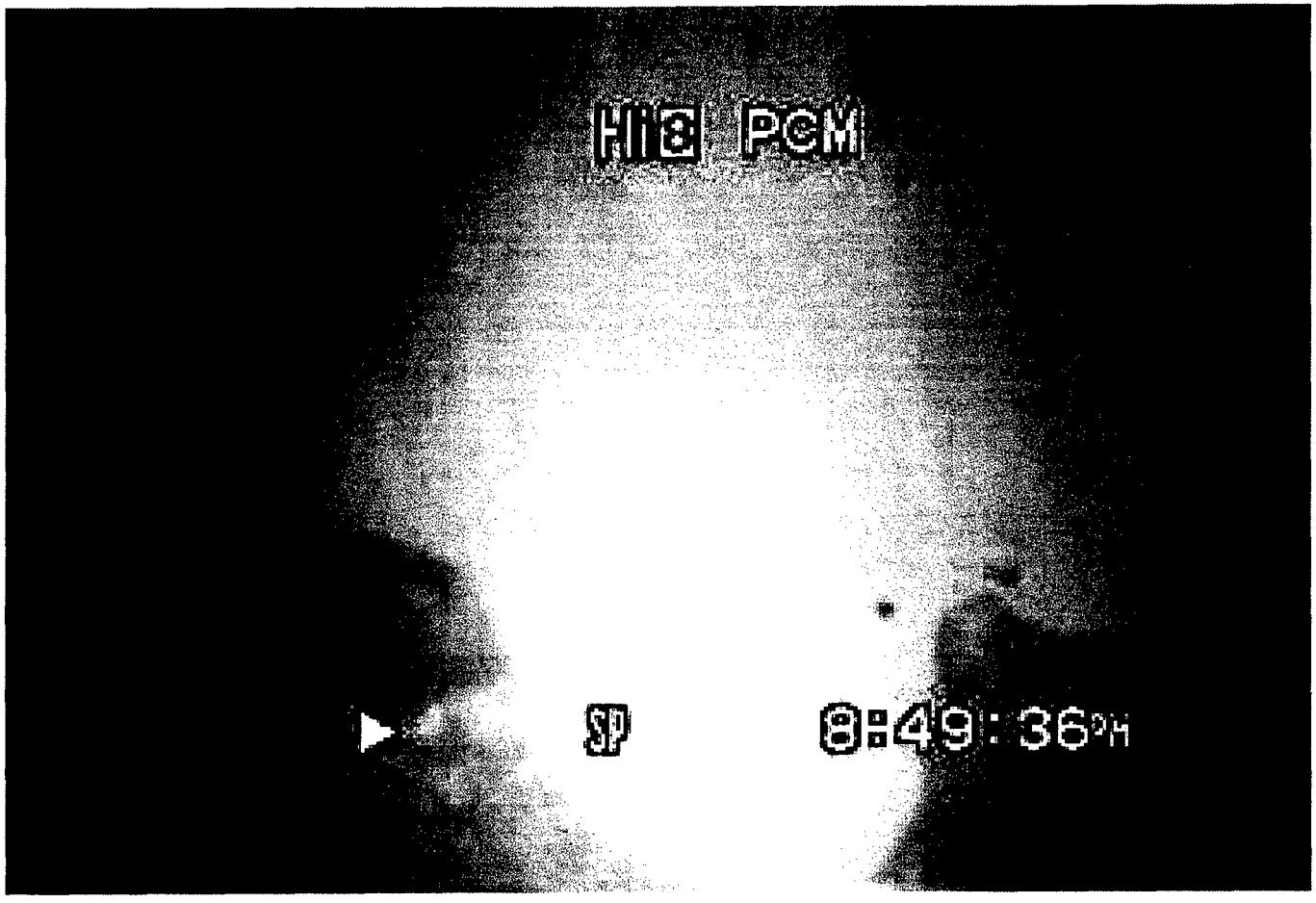

AIRSII 109rf12 Mon_Z, Dec 01 2003

14 sec

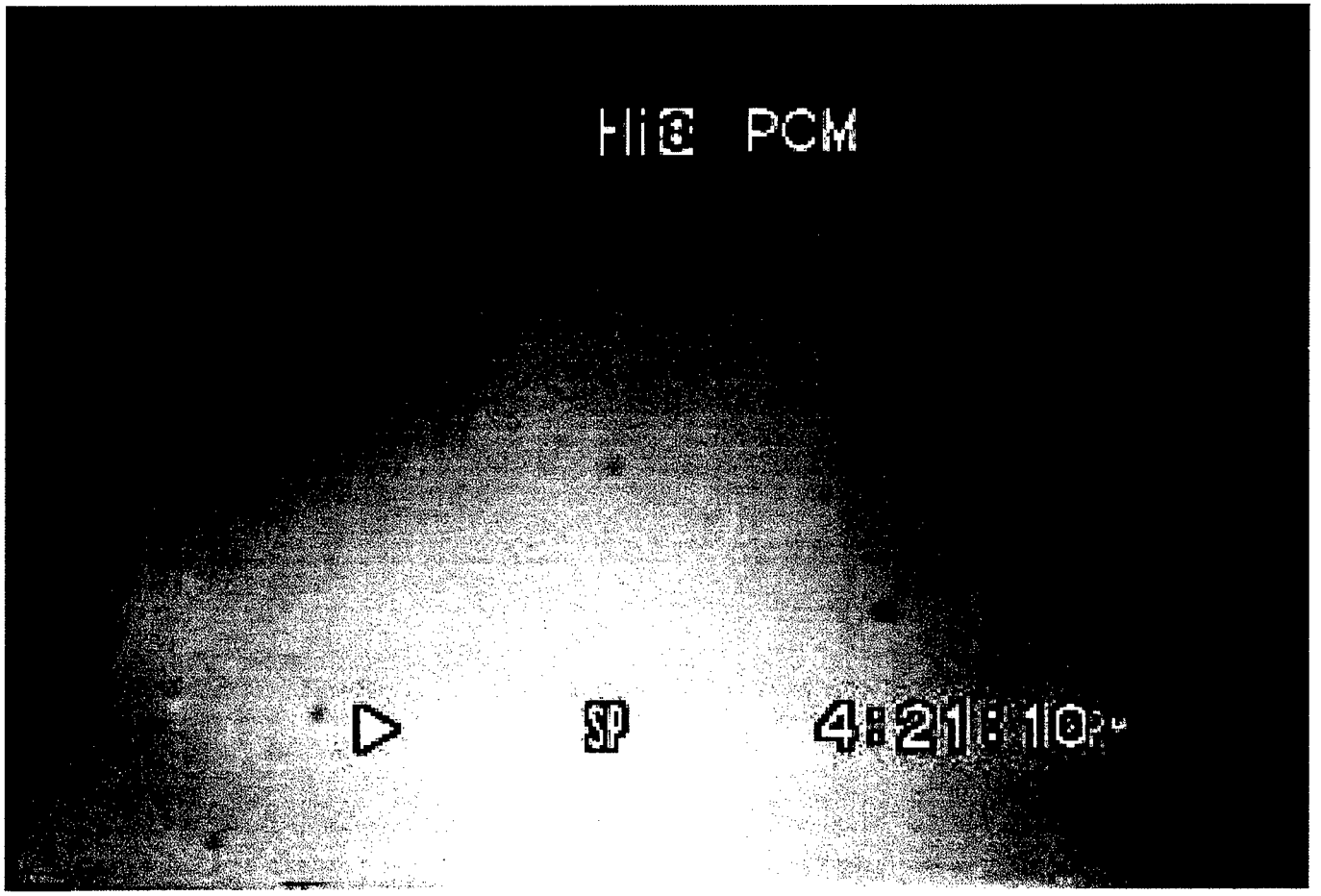

AIRSII 109rf06 Fri$_Z$, Nov 14 2003

17 sec

Conclusions

- All ice particle spectra must be specified in terms of low concentration – large size cutoff and related to a flight path long enough for statistical significance.
- Peripheral habit gives growth supersaturation for known temperature, to be related to conditions above. Temperature may be measured above aircraft by radiometer.
- Rounded large crystals indicate regions of ice subsaturation (< 85%) and scale of optical turbulence.
- In situ measurements of T probe give ice water content and liquid water content to provide a calibration of means and variance capable of extrapolation to other temperatures.
- In situ measurement of range of particle densities from 0.02 to 09g m^{-3}.
- Predict conditions along lidar path from polarization/intensity from local in situ measurements.
- Laboratory derived variances of habit together with measured density to predict path variances of properties IWC/LWC.

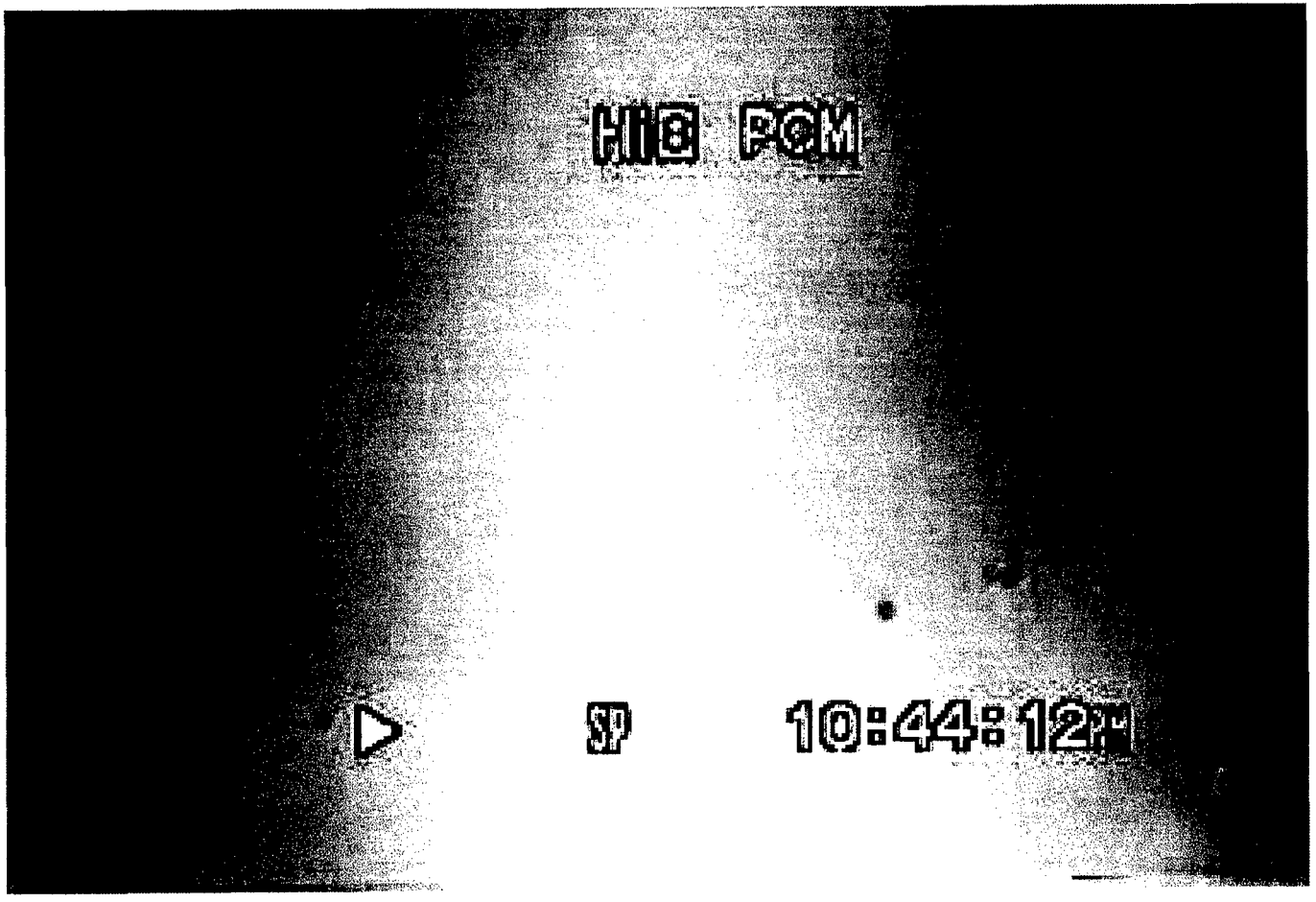

AIRSII 109rf09 Wed$_Z$, Nov 19 2003

26 sec

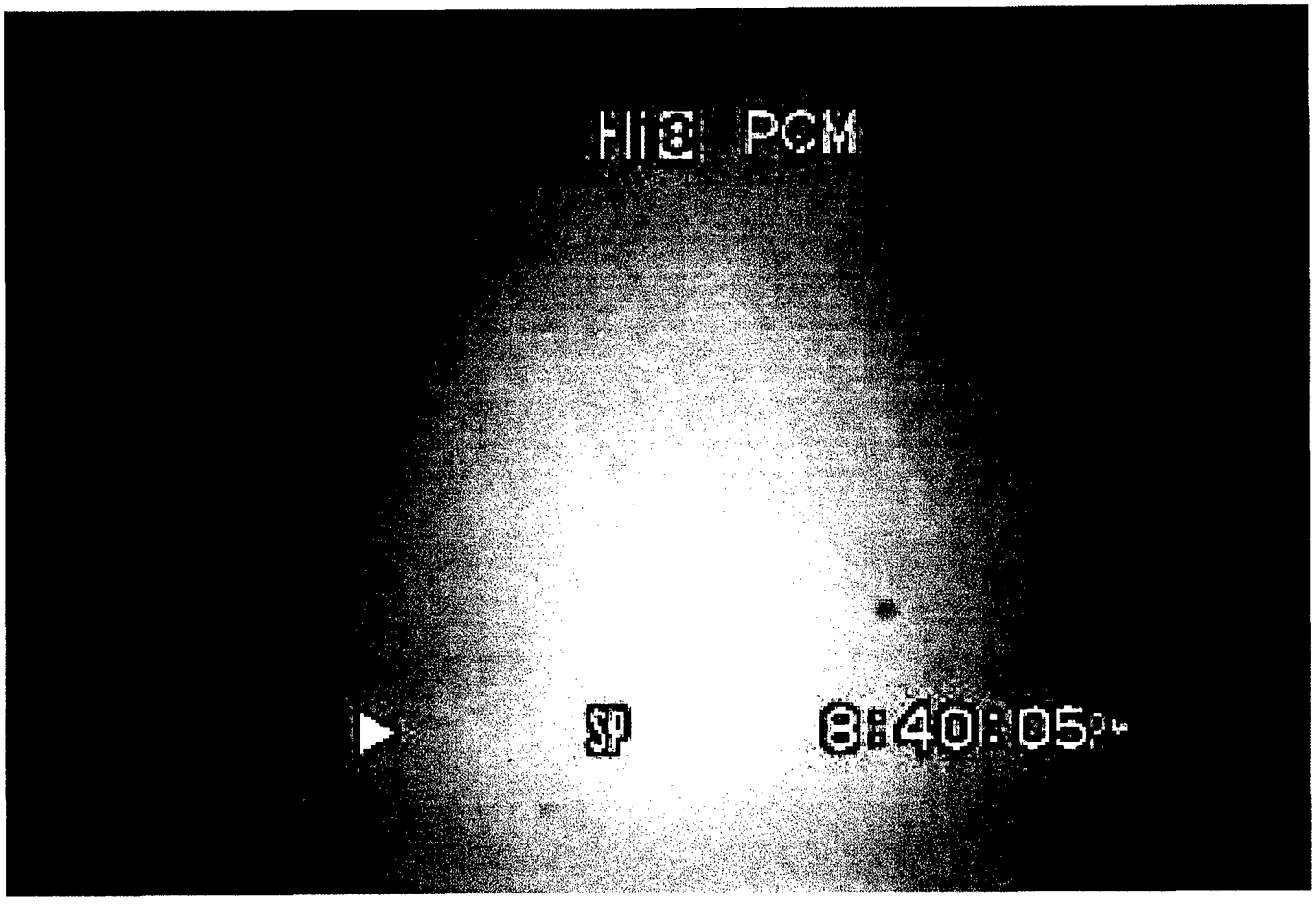

AIRSII 109rf12 Mon_Z, Dec 1 2003

56 sec

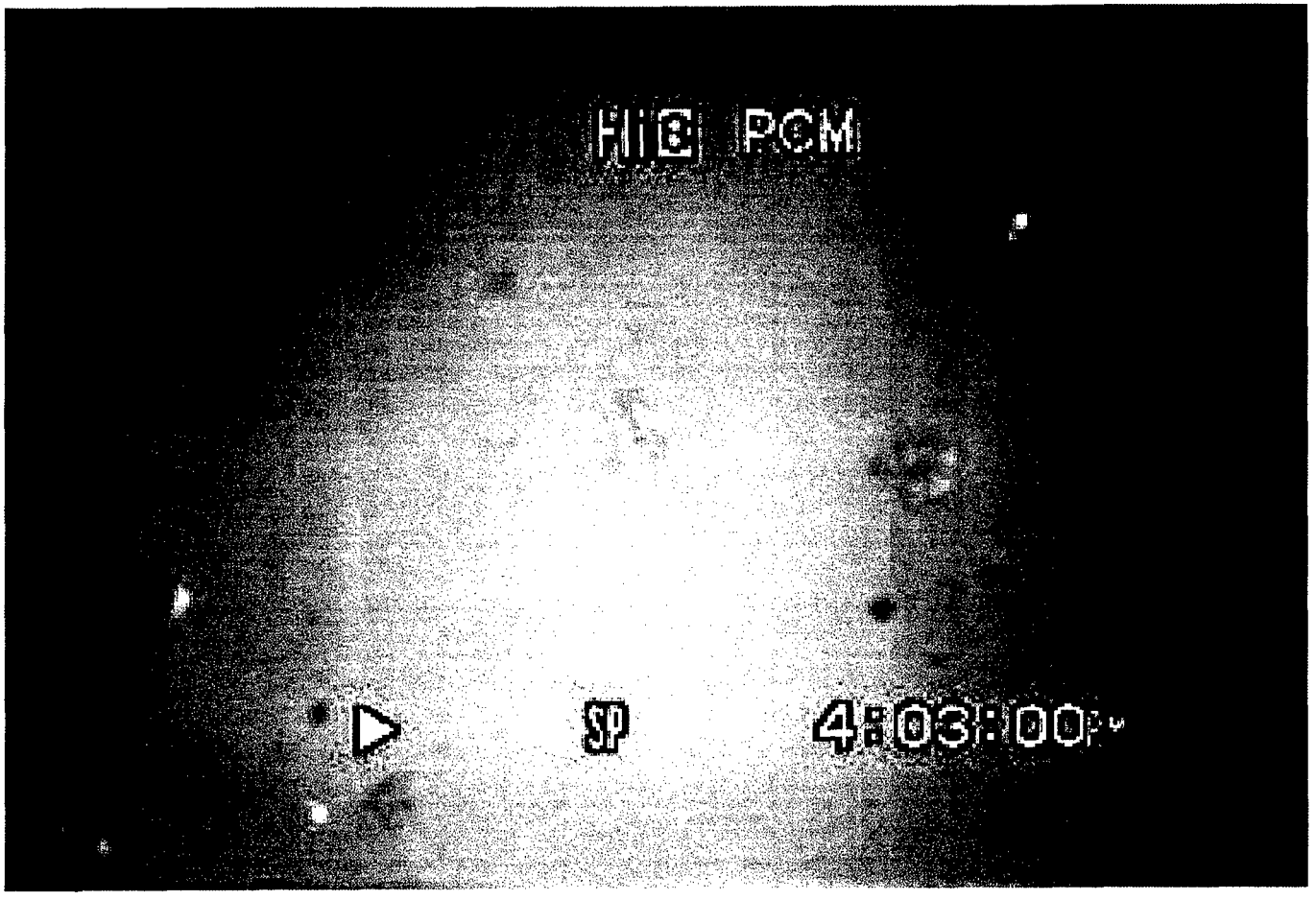

AIRSII 109rf06 Fri_Z, Nov 14 2003

2 min 20 sec

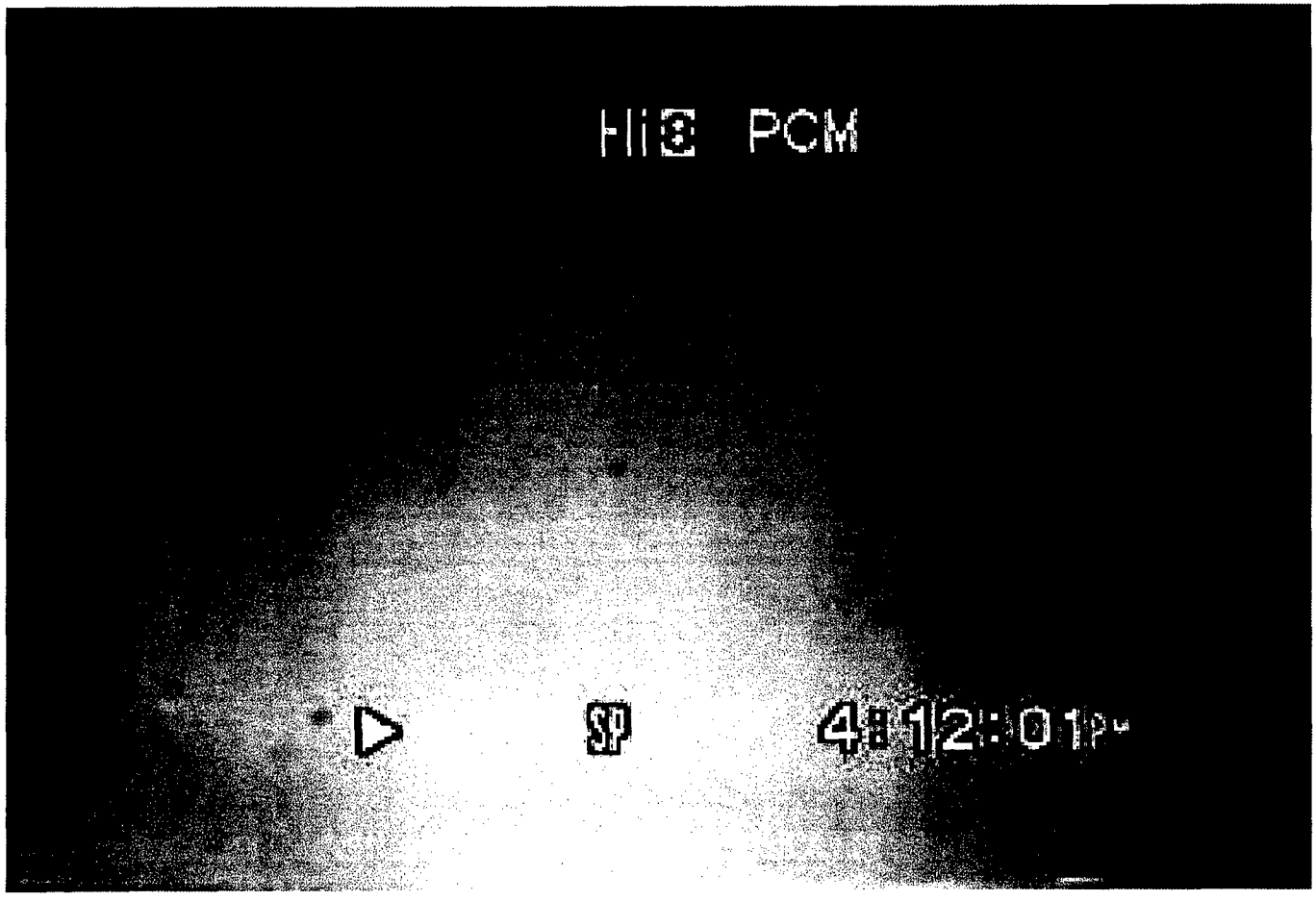

AIRSII 109rf06 Fri_Z, Nov 14 2003

14 sec

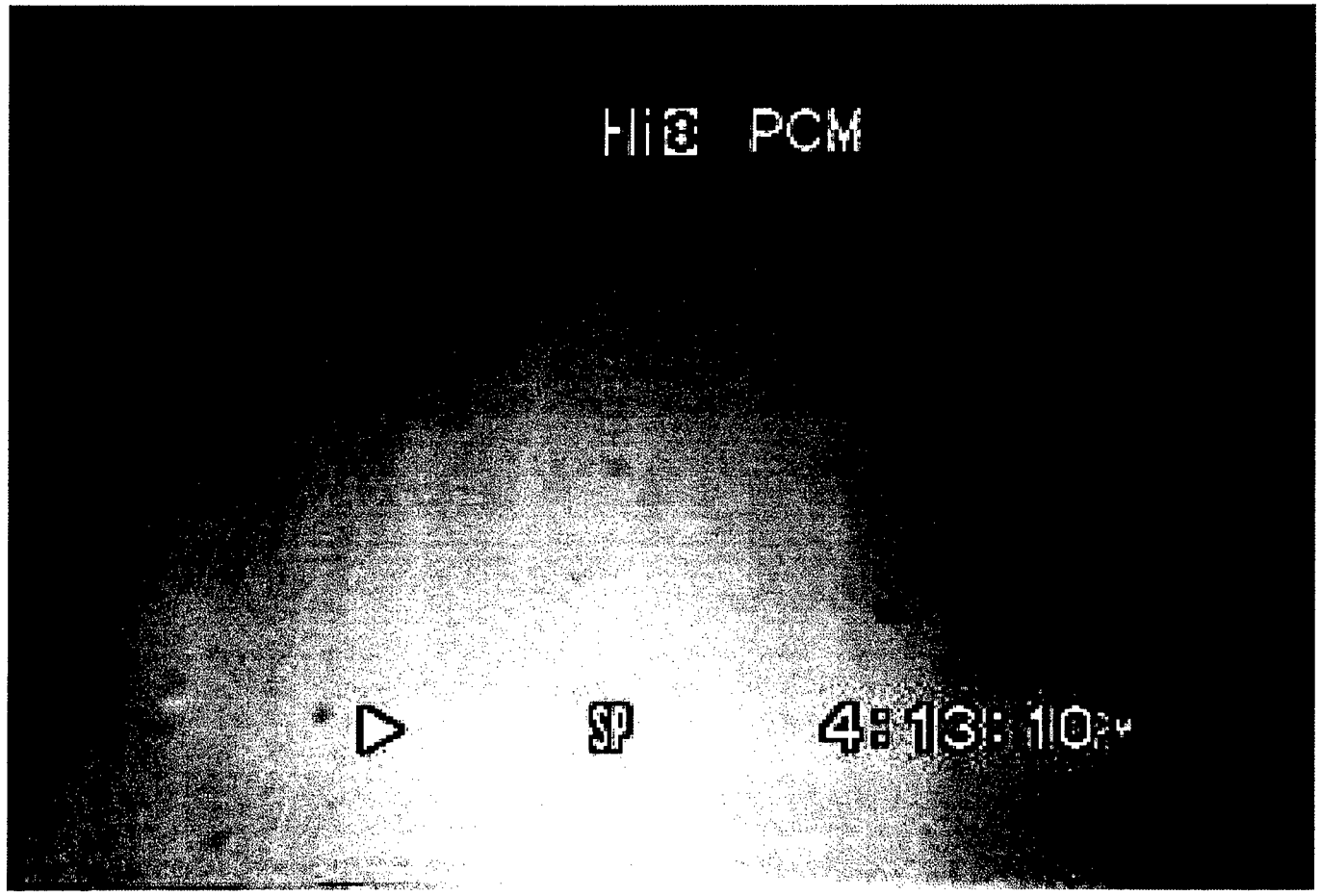

AIRSII 109rf06 Fri_Z, Nov 14 2003

19 sec

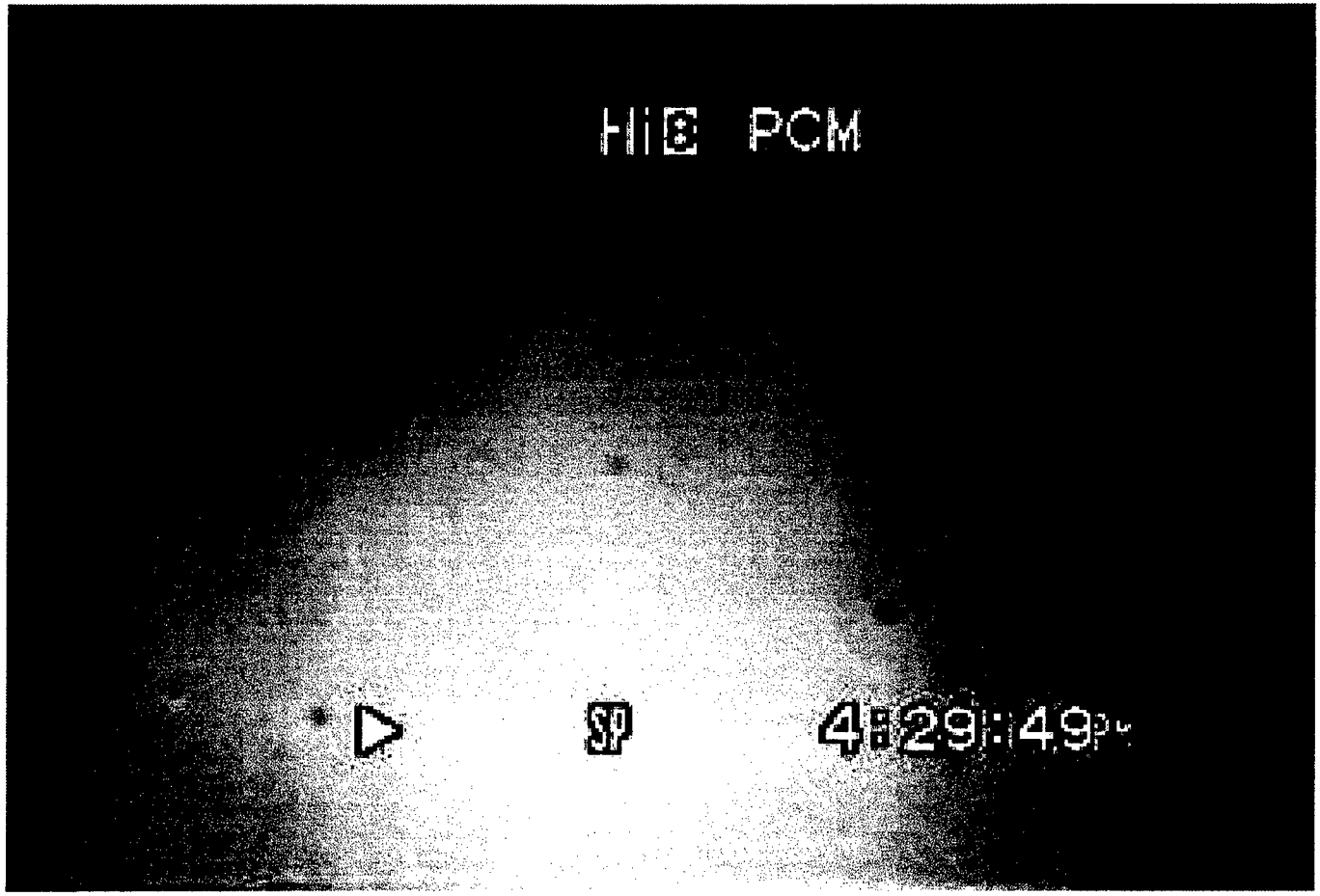

AIRSII 109rf06 Fri_Z, Nov 14 2003

2 min 46 sec

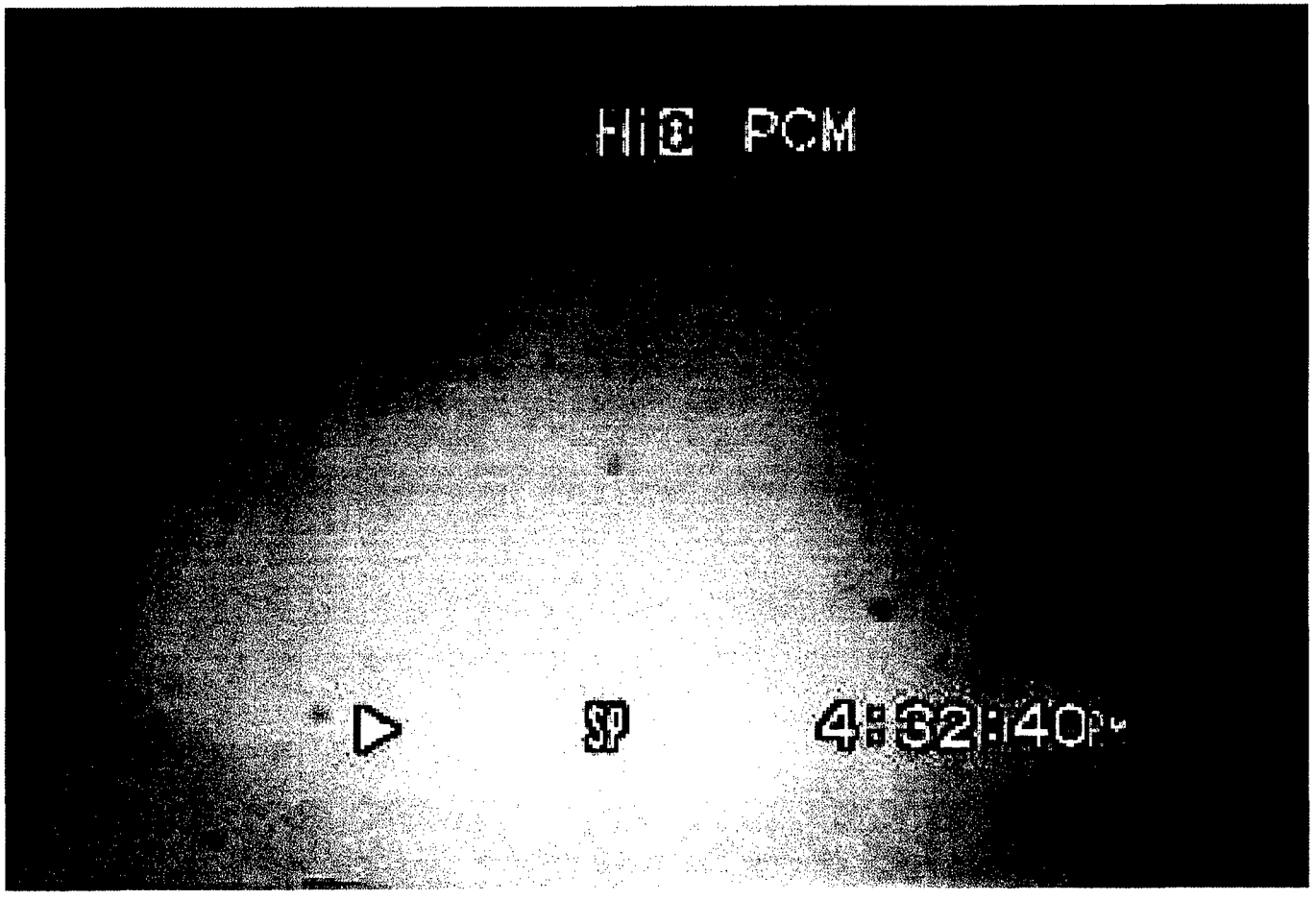

AIRSII 109rf06 Fri$_Z$, Nov 14 2003

4 min 09 sec

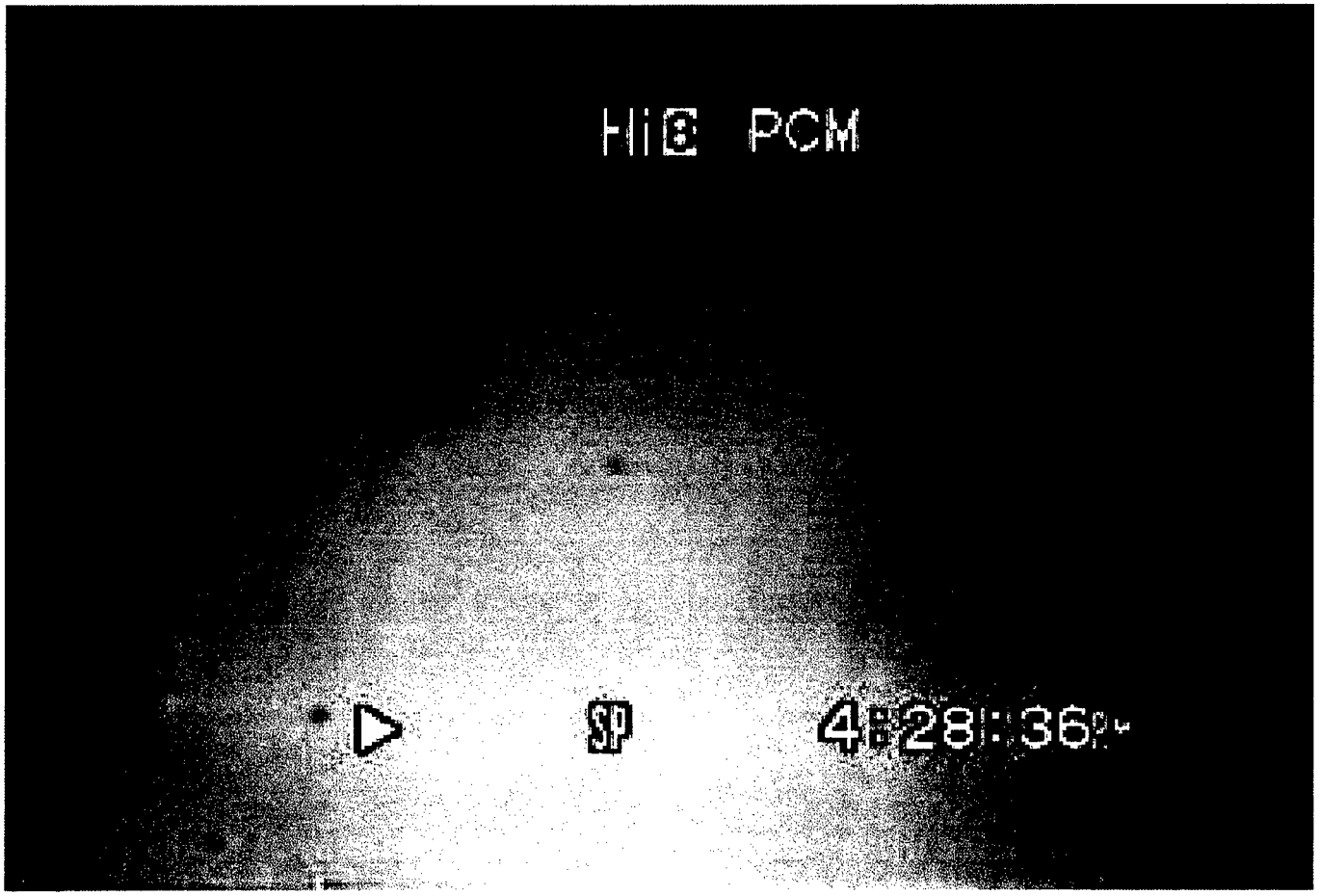

AIRSII 109rf06 Fri$_Z$, Nov 14 2003

33 sec

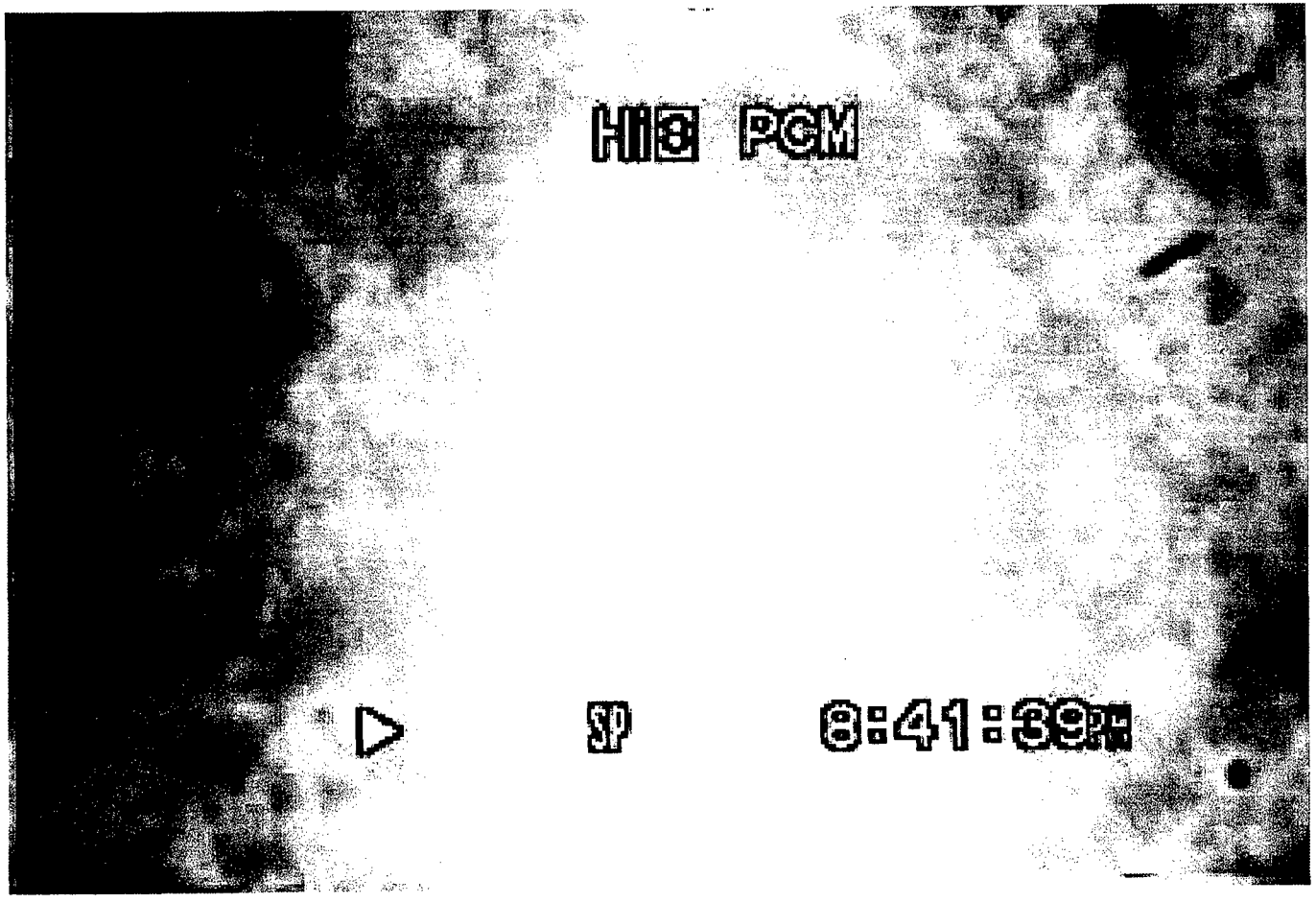

AIRSII 109rf12 Mon_Z, Dec 1 2003

47 sec

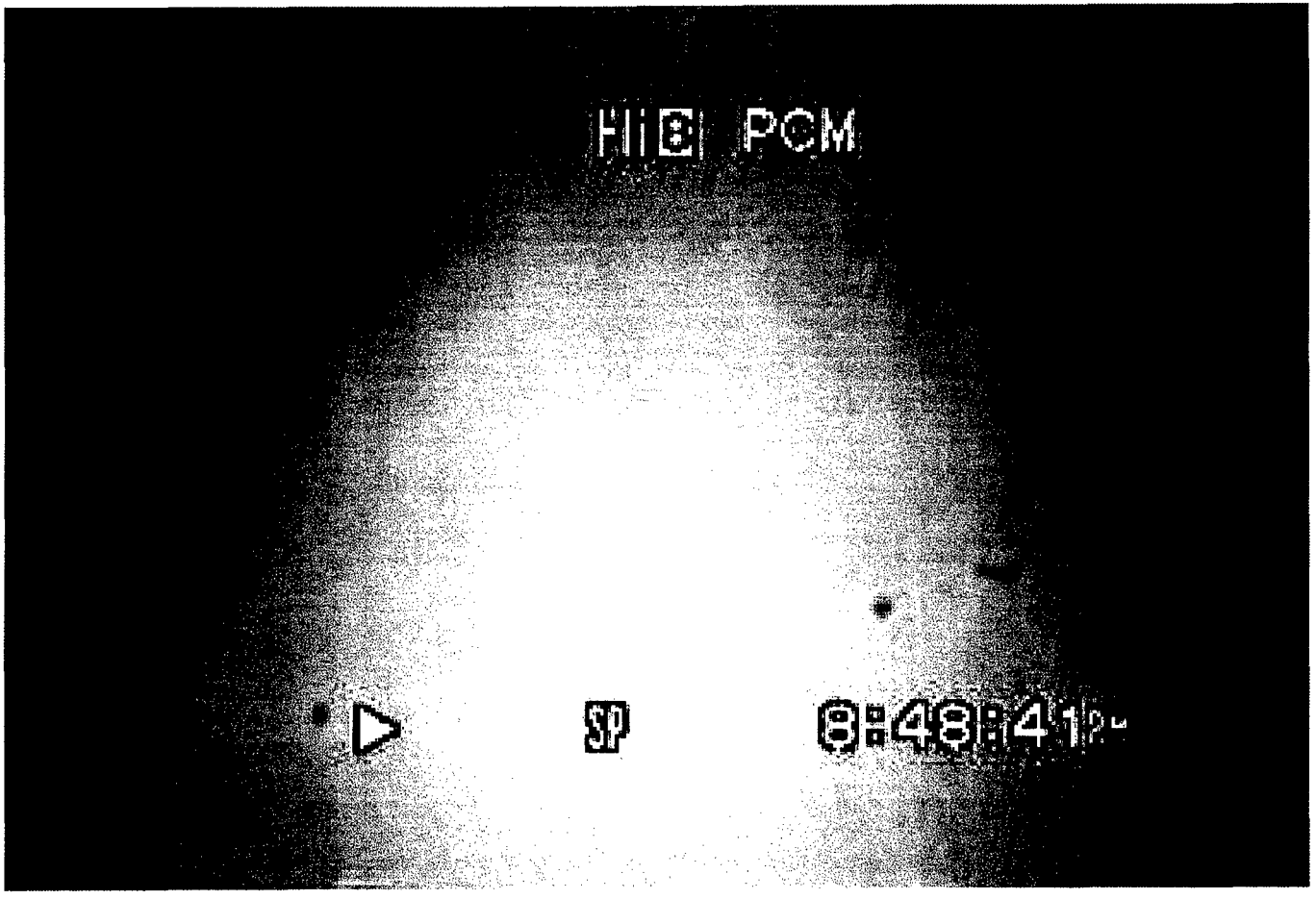

AIRSII 109rf12 Mon_Z, Dec 1 2003

1 min 11 sec

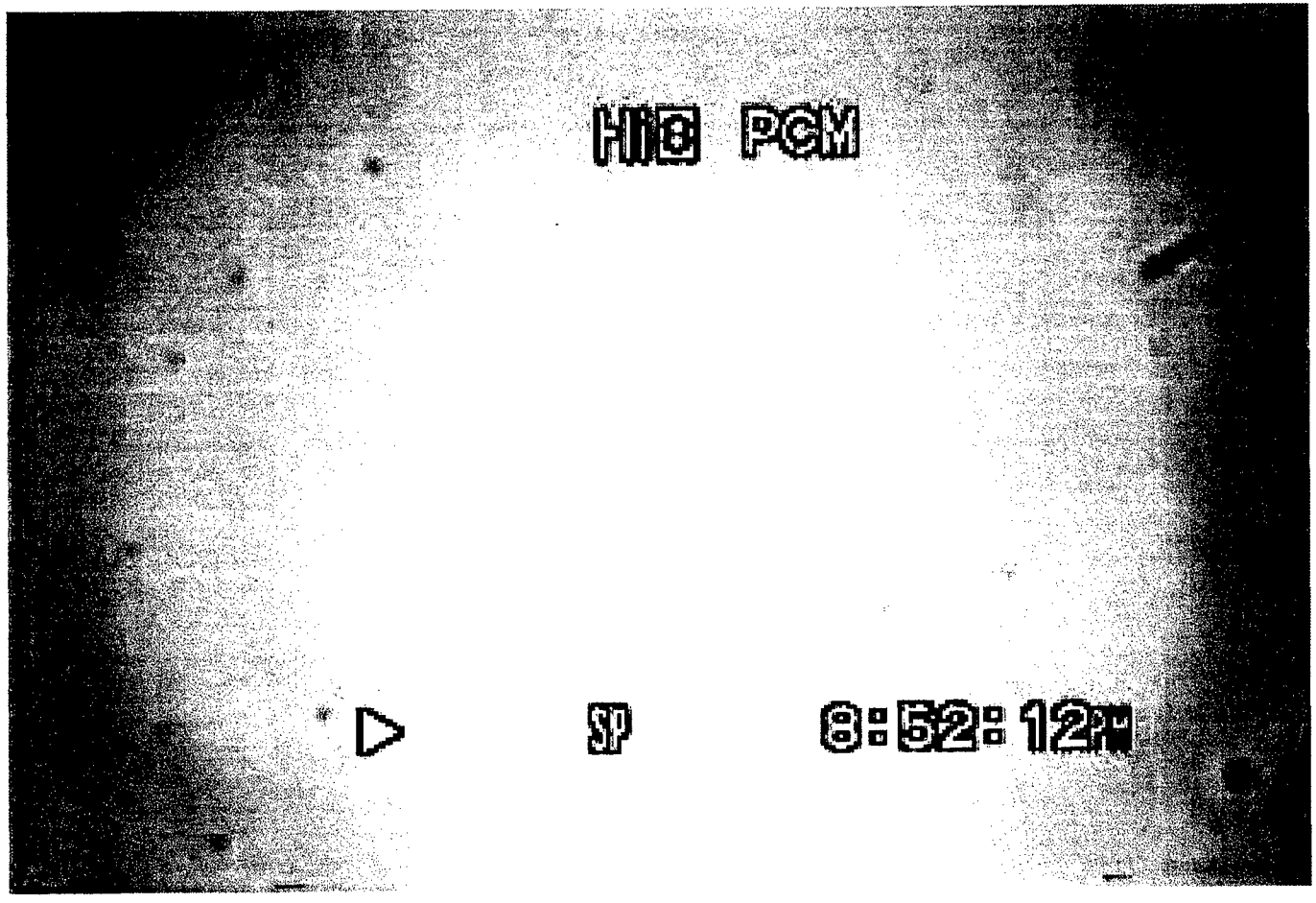

AIRSII 109rf12 Mon_Z, Dec 1 2003

1 min 04 sec

APPENDIX C

Cirrus Characterization for Laser Propagation and Global Modeling

Dr. John Hallett; Matthew Bailey
Division of Atmospheric Sciences, Desert Research Institute

The characterization of cirrus in terms of its optical properties requires information not only on the temperature and temperature range of its origin and growth but also on the circumstances of its origin and its demise through evaporation. The rationale for this approach was described in the 2003 annual report, where laboratory experiments showed both habit and growth rates dependent not only on temperature and supersaturation but also on the conditions of nucleation and the nuclei responsible. A prototype of the high resolution cloudscope, also described in that report, showed how the crystals could be captured by in situ penetration as from a balloon borne platform to provide data for such an analysis. The capture of both large aerosol particles as well as the crystals themselves, together with the ability to evaporate the collected particles is demonstrated to be not only important for the frontal and Cb cirrus but also for the subvisual cirrus occurring in the colder temperatures and higher levels in regions towards the tropics. Thus the range of cirrus up to some 60,000 ft, temperature -65C would be capable of interpretation in terms of the physical processes and laboratory simulations thereof already obtained.

In October of 2003 the cloudscope and other instruments were deployed at Holloman AFB on a platform designed for ascent into cirrus layers in the neighborhood of 40,000 ft. This was at the lower operational level and the balloon system was adjusted accordingly for a controlled flight. Figures 1 a,b show a test Balloon release. Fig 1 c shows the general terrain, with low level orographic clouds over high ground to the east. Instrument controls available in flight were ventilation velocity of a pump for particle concentration and focus to be adjusted in real time as changing temperatures resulted to changing optical paths requiring refocusing to maintain definition. Fig 2 shows the loaded gondola; Fig 3 shows the system ready for launch. High resolution was readily obtained from the camera system remote transmission in this ground based test. Also there was a Vaisala radiosonde to provide readout of temperature, relative humidity and GPS position. These instruments were collocated with the UCLA lightweight polar nephelomete Fig 4. Fig 5 is a schematic of the cloudscope, Fig 6 shows the pump system and the cloudscope with the faring removed. All instruments were thoroughly tested and found to be ready for launch as circumstances permitted.

Launch without Payload – No Cirrus

a

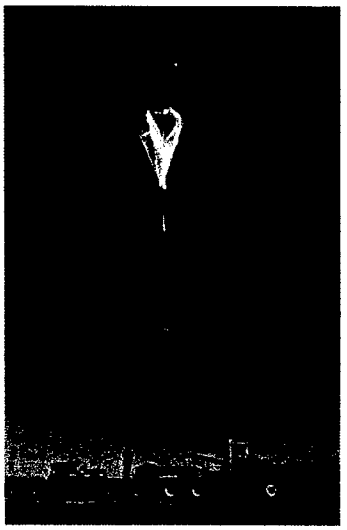

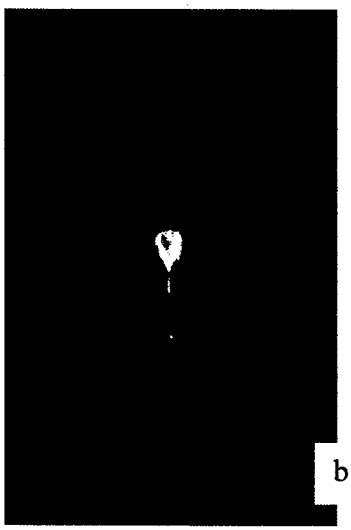

b

c

Figure 1 a,b. Launch test with simulated payload, no cirrus, Holloman AFB. Figure 1 c. Terrain over which the balloon passes with westerly wind, showing only low level orographic cloud.

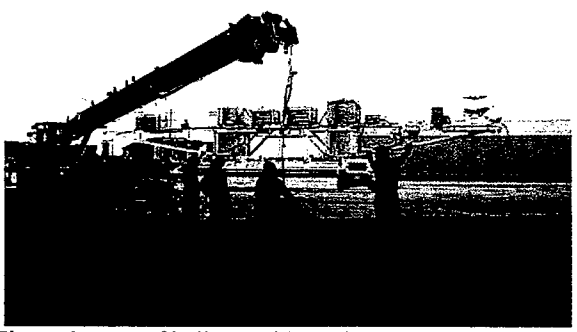

Figure 2. Test of balloon with payload, ready for inflation.

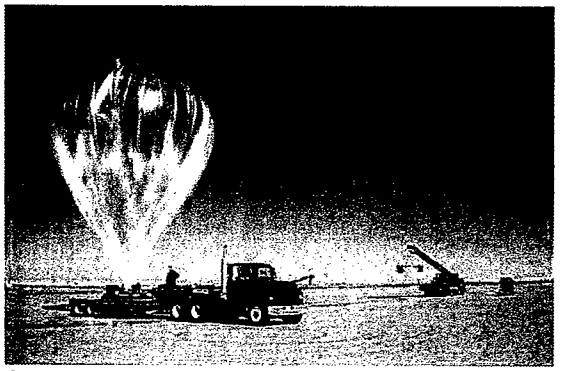

Figure 3. Launch test inflation.

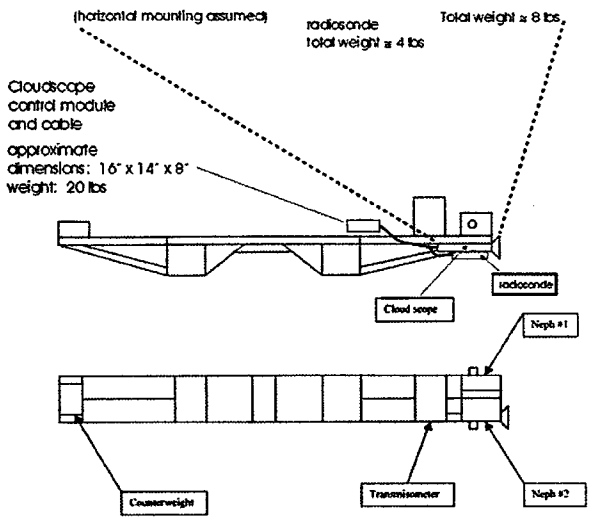

Figure 4. Layout of gondola instrumentation.

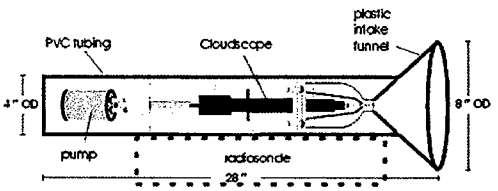

Figure 5. Schematic of cloudscope showing air sample intake faring.

Balloon Cloudscope

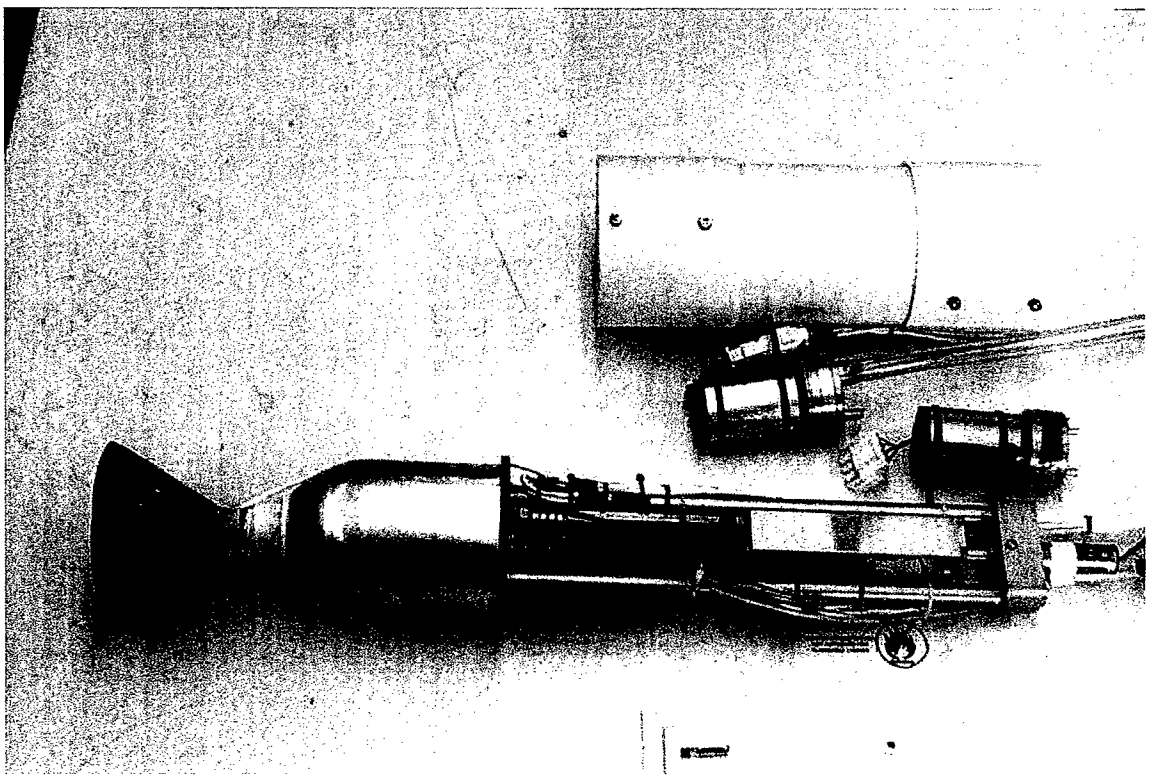

Figure 6. Detail of pump system (top) and cloudscope with faring removed (below)

APPENDIX D

The Melting Layer: A Laboratory Investigation of Ice Particle Melt and Evaporation near 0°C

R. G. ORALTAY

Environmental Engineering Department, Engineering Faculty, Marmara University, Ziverbey, Istanbul, Turkey

J. HALLETT

Desert Research Institute, Reno, Nevada

(Manuscript received 26 December 2003, in final form 25 July 2004)

ABSTRACT

Melting, freezing, and evaporation of individual and aggregates of snow crystals are simulated in the laboratory under controlled temperature, relative humidity, and air velocity. Crystals of selected habit are grown on a vertical filament and subsequently melted or evaporated in reverse flow, with the velocity adjusted for appropriate fall speed to reproduce conditions of the melting layer. Nonequilibrium conditions are simulated for larger melting ice particles surrounded by smaller drops at a temperature up to +5°C or growth of an ice crystal surrounded by freezing ice particles down to −5°C. Initial melting of well-defined faceted crystals, as individuals or in combination, occurs as a water layer >10 μm thick. For larger (>100 μm) crystals the water becomes sequestered by capillary forces as individual drops separated by water-free ice regions, often having quasiperiodic locations along needles, columns, or arms from evaporating dendrites. Drops are also located at intersections of aggregate crystals and dendrite branches, being responsible for the maximum of the radar scatter. The drops have a finite water–ice contact angle of 37°–80°, depending on ambient conditions. Capillary forces move water from high-curvature to low-curvature regions as melting continues. Toward the end of the melting process, the ice separating the drops becomes sufficiently thin to fracture under aerodynamic forces, and mixed-phase particles are shed. Otherwise ice-free drops are shed. The melting region and the mechanism for lowering the melting layer with an increasing precipitation rate are associated with smaller ice particle production capable of being lofted in weaker updrafts.

Corresponding author address: J. Hallett, 2215 Raggio Pkwy., Reno, NV 89512.
E-mail: John.Hallett@dri.edu

43rd AIAA Aerospace Science Meeting
10 – 13 January 2005, Reno, NV

Paper No. 862

Measurement for Characterization of Mixed Phase Clouds

J. Hallett*, R. Purcell†, M. Roberts‡, G. Vidaurre§, and D. Wermers**
Desert Research Institute, Reno, Nevada, 89512

Mixed phase clouds, as supercooled water droplets and ice particles, are closely associated with aircraft icing situations in as far as they are an intrinsic component of a region of the atmosphere between all supercooled water and all ice particles. Characterization of such regions requires measurements over different scales from < meters to >10km, times from a fraction of a second to minutes at aircraft speed. Techniques are described using different diameter, different geometry, constant temperature 'T' probes to measure separately ice content, liquid water content for cloud size and precipitation size particles simultaneously, with cloudscope images to provide particle density and crystalline characteristics. Results from NCAR C-130 during AIRS II demonstrate the sharpness of such interfaces as lying within instrument resolution. Questions arise on the role of such regions in aircraft icing in as far as a mixed region may build more rapidly or more slowly through different accretion geometry and accretion or erosion, involve different heat balance for melt or evaporation and provide different persistence of conditions for operational considerations. Conceptual definitions of mixed phase cloud are necessary, involving an understanding of the mechanism of formation, continuance and decay of such interfaces, as are practical definitions related to measurement capabilities of available and future instruments.

* Research Professor, Division of Atmospheric Sciences, 2215 Raggio Parkway, Reno NV 89512, AIAA Member
† Associate Research Mechanical Engineer, DRI/DAS, 2215 Raggio Parkway, Reno NV 89512
‡ Computer Engineer, DRI/DAS, 2215 Raggio Parkway, Reno NV 89512
§ Graduate Student, DRI/DAS, 2215 Raggio Parkway, Reno NV 89512
** Assistant Research Electronics Engineer, DRI/DAS 2215 Raggio Parkway, Reno NV 89512

Laboratory and In Situ Observation of Deposition Growth of Frozen Drops

ALEXEI V. KOROLEV

Sky Tech Research, Inc., Richmond Hill, Ontario, Canada

MATTHEW P. BAILEY AND JOHN HALLETT

Desert Research Institute, Reno, Nevada

GEORGE A. ISAAC

Cloud Physics Research Division, Meteorological Service of Canada, Toronto, Ontario, Canada

(Manuscript received 18 March 2003, in final form 10 November 2003)

ABSTRACT

The water vapor deposition growth of frozen drops with diameter greater than 100 μm has been studied in a thermal diffusion chamber. For varying periods of time, it was found that frozen drops experience spherical growth. The characteristic time of spherical growth depends on supersaturation, temperature, and drop size, and it varies from minutes to tens of minutes. The average rate of frozen drop growth agrees well with that predicted by the Maxwellian growth equation for ice spheres. Observations in natural clouds conducted with a cloud particle imager probe has yielded evidence that frozen drops may retain spheroidal shapes for at least 15–20 min under conditions close to saturation over water. These observations are in agreement with the laboratory experiments. The observation of frozen drops in natural clouds may be correlated to freezing drizzle generated by overlying cloud layers that may lead to hazardous in-flight icing.

Corresponding author address: Alexei V. Korolev, Sky Tech Research, Inc., 28 Don Head Village Blvd., Richmond Hill, ON L4C 7M6, Canada.
E-mail: alexei.korolev@rogers.com

Growth Rates and Habits of Ice Crystals between −20° and −70°C

MATTHEW BAILEY AND JOHN HALLETT

Desert Research Institute, Reno, Nevada

(Manuscript received 15 October 2002, in final form 2 October 2003)

ABSTRACT

A laboratory study of ice crystal growth characteristics at temperatures between −20° and −70°C has been performed at ice supersaturations and pressures comparable with those in the atmosphere using a horizontal static diffusion chamber. Maximum dimension, projected area, and volume growth rates, in addition to habit frequency, have been measured for individual habit types as functions of temperature, ice supersaturation, and air pressure. It was found that from −20° to −40°C and at ice supersaturations in excess of 2%, the most frequent habits observed were platelike polycrystals and plates, the complexity of forms increasing with increasing supersaturation. Columns appear with low frequency in this temperature range for all supersaturations. At low ice supersaturation (1%–2%), the habit consists of thick plates, compact polycrystals, and occasional short columns and is the region with the highest frequency of pristine crystals capable of producing halos.

Just colder than −40°C, there is a marked shift to columnar behavior except at low to moderate ice supersaturation (<10%) where the habit is essentially the same as at warmer temperatures with a small increase in the frequency of short columns. At moderate ice supersaturation (10%–25%), long solid columns and polycrystals with columnar and platelike components are observed. Above approximately 25% ice supersaturation, bullet rosettes, long columns, and column-containing polycrystals are observed, the frequency of bullet rosettes and columns increasing with increasing ice supersaturation. At −60°C and colder, needle forms appear along with columnar forms.

These characteristics are portrayed in a habit diagram as a function of temperature and ice supersaturation and are essentially in agreement with the vast majority of atmospheric in situ observations at these temperatures, both of which depart from the previous habit diagrams at temperatures colder than −20°C compiled by Kobayashi, Magono and Lee, and Hallett and Mason.

Habit growth rates and habit frequencies have been measured at 10° temperature increments. Exponential fits of these results yield functions that can be used to estimate growth rates and habit distributions at intermediate temperatures for ice supersaturations as low as 1% up to the maximum values, which might be encountered in the atmosphere due to ventilation effects, approximately up to 50% above water saturation between −25° and −40°C and extrapolated water saturation colder than −40°C. Within each habit and under identical growth conditions, observed extremes in growth rates for individual crystals in comparison with average values show variances of ±50%, reflecting a variance in aspect ratio that suggests a critical role of crystalline defects in growth characteristics. These results indicate an even more complex behavior of ice crystal habit than that observed between 0° and −20°C, a behavior that depends not only on temperature and ice supersaturation, but also on vapor diffusivity, related to air pressure, and the initial nucleation process.

Corresponding author address: Dr. Matthew Bailey, Desert Research Institute, 2215 Raggio Parkway, Reno, NV 89512-1095.
E-mail: bailey@dri.edu

JOURNAL OF GEOPHYSICAL RESEARCH, VOL. 108, NO. D7, 4225, doi:10.1029/2001JD001140, 2003

Horizontal structure of the electric field in the stratiform region of an Oklahoma mesoscale convective system

Qixu Mo[1] and Andrew G. Detwiler
Institute of Atmospheric Sciences, South Dakota School of Mines and Technology, Rapid City, South Dakota, USA

John Hallett
Atmospheric Sciences Division, Desert Research Institute, Reno, Nevada, USA

Robert Black
Hurricane Research Division, National Oceanic and Atmospheric Administration, Miami, Florida, USA

Received 17 July 2001; revised 1 April 2002; accepted 6 December 2002; published 15 April 2003.

[1] This analysis combines vertical electric field components E_z observed by two research aircraft flying horizontally at two levels, with vertical soundings of thermodynamic parameters and E_z made by five balloons, to produce a quasi-three-dimensional view of the space charge distribution in the trailing stratiform cloud region behind a mesoscale convective system (MCS) that developed in central Oklahoma late in the afternoon of 2 June 1991. The balloons were launched serially at one-hour intervals from two sites separated by 80 km along a north-south line as the MCS moved eastward, yielding two east-west time-height cross-sections of the E_z structure within the quasi-steady state trailing stratiform region behind the MCS. The balloon measurements are consistent with a vertical stack of five rearward- and downward-sloping horizontal sheets of charge of alternating polarity, beginning at the bottom with a negative charge layer below the 0°C level and a positive layer near the 0°C level. This structure persisted for more than 2 hours. The two aircraft flew back and forth along a north-south line through the balloon launch sites during the balloon launch period. Aircraft measurements demonstrated that the vertical electric field (E_z) at constant altitude varied in the north-south direction. The peak magnitudes of E_z deduced from the airborne instrument systems agreed with the magnitudes deduced from the balloon measurements at the aircraft altitudes of 4.5 km and 5.8 km AGL. Rapid reversals in polarity of E_z with peak magnitude >50 kV m^{-1} observed by the aircraft at 4.5 km, just above the 0°C level, confirms the thin concentrated positive charge layer observed there by balloons and suggests that this charge layer is undulating above and below 4.5 km altitude, at least in the north-south direction. Microphysically, this layer contained large aggregates and pockets of low cloud liquid water concentration. At the 5.8 km level, the polarity of E_z was always positive but the magnitude varied from zero to 25 kV m^{-1}. Aircraft-observed E_z at both altitudes varied on horizontal scales of ~10 km or greater at both levels, suggesting that the charge density derived using the one-dimensional infinite-layer Gauss's law approximation applied to the balloon soundings of E_z is valid in this study. These observations show that layers of charge can persist for hours as they advect rearward in a storm-relative sense, possibly due to continuing in situ charge separation, and/or due to weak dispersion, slow recombination and slow settling of charge attached to low mobility low terminal velocity ice hydrometeors. *INDEX TERMS:* 3304 Meteorology and Atmospheric Dynamics: Atmospheric electricity; 3314 Meteorology and Atmospheric Dynamics: Convective processes; 3329 Meteorology and Atmospheric Dynamics: Mesoscale meteorology; *KEYWORDS:* atmospheric electricity, convective processes, lightning, precipitation, mesoscale processes

Citation: Mo, Q., A. G. Detwiler, J. Hallett, and R. Black, Horizontal structure of the electric field in the stratiform region of an Oklahoma mesoscale convective system, *J. Geophys. Res.*, *108*(D7), 4225, doi:10.1029/2001JD001140, 2003.

[1]Now at SPEC Incorporated, Boulder, Colorado, USA.

0148-0227/03/2001JD001140$09.00

GEOPHYSICAL RESEARCH LETTERS, VOL. 30, NO. 21, 2124, doi:10.1029/2003GL017864, 2003

Extra large particle images at 12 km in a hurricane eyewall: Evidence of high-altitude supercooled water?

Robert A. Black,[1] Gerald M. Heymsfield,[2] and John Hallett[3]

Received 30 May 2003; revised 15 September 2003; accepted 25 September 2003; published 14 November 2003.

[1] The conventional wisdom about hurricanes suggests that updrafts are weak and supercooled water is scarce in the eyewall, and almost non-existent at temperatures colder than about −5°C [*Black and Hallett*, 1986]. However, there is evidence that some hurricanes are different. Questions about the existence of high-altitude supercooled cloud water cannot be answered with only the instruments aboard the typical propeller-driven aircraft. During the summer of 1998, the NASA DC-8 aircraft made penetrations of the intensifying eyewall of Hurricane Bonnie at 12 km MSL, collecting the first truly high-altitude 2-D particle imagery in a hurricane. The similarity of the splash images in Hurricane Bonnie to those from raindrops obtained at higher temperatures in other hurricanes suggests that the large images obtained by the DC-8 were soft, low density graupel, rather than hard, high-density graupel particles or frozen raindrops. This implies that these particles grew to several millimeters in diameter at altitude, rather than simply advecting from lower, warmer altitudes. This growth in turn requires the presence of deeply supercooled cloud droplets. Thermal emission from supercooled water aloft increases the microwave brightness temperatures, giving a misleading impression that there is much less ice aloft than actually exists. The extra attenuation from the occasional presence of large graupel at these altitudes reduces the ability of microwave sensors to see precipitation at lower altitudes. Both of these effects impede efforts to accurately quantify condensate mass remotely from radiometric data such as that provided by the TRMM satellite. *INDEX TERMS:* 0320 Atmospheric Composition and Structure: Cloud physics and chemistry; 0305 Atmospheric Composition and Structure: Aerosols and particles (0345, 4801); 3314 Meteorology and Atmospheric Dynamics: Convective processes; 3354 Meteorology and Atmospheric Dynamics: Precipitation (1854); 3374 Meteorology and Atmospheric Dynamics: Tropical meteorology. **Citation:** Black, R. A., G. M. Heymsfield, and J. Hallett, Extra large particle images at 12 km in a hurricane eyewall: Evidence of high-altitude supercooled water?, *Geophys. Res. Lett.*, *30*(21), 2124, doi:10.1029/2003GL017864, 2003.

[2] The drops approaches −40°C. The homogeneous nucleation rate is also faster for (large) raindrops than cloud drops, leading them to freeze at warmer temperatures than −40°C. The growth rate of the ice embryos at these temperatures is also expected to be so fast that the drops that are nucleated freeze almost instantly. These results are so compelling that most researchers assume all liquid water freezes spontaneously at −40°C, indicating the need for caution in interpreting data that seem to indicate the existence of supercooled cloud at such temperatures in the absence of in-situ observations.

[3] Nevertheless, deeply supercooled cloud liquid water has occasionally been reported. Lidar measurements in cirrus clouds at temperatures colder than −20°C [*Sassen and Benson*, 2001] and aircraft penetrations at temperatures as cold as −37.5°C in midlatitude convection [*Rosenfeld and Woodley*, 2000] both indicated that supercooled cloud existed. In the case of *Rosenfeld and Woodley*, the accumulation of rime ice on the windscreen of their aircraft showed that supercooled cloud was present. Neither of these researchers mentioned observing precipitation.

[4] Tropical oceanic convection is not known for the strength of its updrafts, but exceptions occasionally occur in hurricanes. Hurricane Emily on 22 September 1987 was one such storm [*Black et al.*, 1994]. This hurricane was observed to contain updrafts with peak vertical velocities >20 m s^{-1} near the melting level continuously for several hours while it was finishing a rapid deepening cycle. Updrafts of this magnitude are required to loft substantial quantities of supercooled cloud drops, raindrops and dense graupel to high altitude. However, no direct measurements of large rimed particles were obtained to confirm that this occurs in a hurricane. This situation changed in 1998, when the NASA DC-8 aircraft made several eyewall penetrations in Hurricane Bonnie at about 12,000 m above mean sea level (MSL) on 23 August 1998. On this day, Bonnie was located east of the Bahamas at about 24.7°N, 71.7°W and was moving slowly NW at about 2 m s^{-1}.

[1]NOAA Atlantic Oceanographic and Meteorological Laboratory, Hurricane Research Division, Miami, Florida, USA.
[2]NASA Goddard Space Flight Center, Mesoscale Atmospheric Processes Branch, Greenbelt, Maryland, USA.
[3]University of Nevada, Desert Research Institute, Reno, Nevada, USA.

0094-8276/03/2003GL017864$05.00

AIAA 2002-0677

AIRCRAFT ICING IN GLACIATED AND MIXED PHASE CLOUDS

John Hallett* and George A. Isaac†
*Desert Research Institute, Reno, NV
†Cloud Physics Research Division, Meteorological Service of Canada, Downsview, ON

ABSTRACT

Ice accretion on aircraft results from supercooled cloud droplets freezing following impact on aircraft and instrument leading edges. The icing shape depends on conditions - static temperature (i.e. the droplet temperature), dynamic temperature, and aircraft and local airspeed. Deicing or anti-icing strategies, such as the use of boots and active heating, depend on knowledge of the ice build-up characteristics and estimates of the thermal and mechanical rate processes. The presence of ice particles either intimately mixed with supercooled cloud or in patches may influence the icing process. The accretion process may be examined in detail by a new aircraft mounted instrument, the DRI Cloudscope. Particles accrete on a forward facing window and are imaged from behind and the side. Ice particles impacting the window, heated just a few degrees above 0°C, melt rapidly on contact. For an unheated window, the ice particles stick near the stagnation point. The thickness of this accreted ice then increases to an equilibrium value, a balance between accretion and erosion. Deicing power requirements for a thermal anti-icing system must take into account total {ice + liquid} latent heat under some conditions, as both ice and liquid water are accreted and require melting and/or evaporation.

Light-scattering properties of plate and column ice crystals generated in a laboratory cold chamber

Brian Barkey, Matt Bailey, Kuo-Nan Liou, and John Hallett

Angular scattering properties of ice crystal particles generated in a laboratory cloud chamber are measured with a lightweight polar nephelometer with a diode laser beam. This cloud chamber produces distinct plate and hollow column ice crystal types for light-scattering experiments and provides a controlled test bed for comparison with results computed from theory. Ice clouds composed predominantly of plates and hollow columns generated noticeable 22° and 46° halo patterns, which are predicted from geometric ray-tracing calculations. With the measured ice crystal shape and size distribution, the angular scattering patterns computed from geometrical optics with a significant contribution by rough surfaces closely match those observed from the nephelometer. © 2002 Optical Society of America

OCIS codes: 010.1310, 010.2940, 290.5820, 290.5850.

B. Barkey (brian_barkey@juno.com) and K. N. Liou are with the Department of Atmospheric Sciences, University of California, Los Angeles, Los Angeles, California 90095. M. Bailey and J. Hallett are with the Desert Research Institute, Atmospheric Science Center, P.O. Box 60220, Reno, Nevada 89506.

Received 6 March 2002; revised manuscript received 2 July 2002.

0003-6935/02/275792-05$15.00/0

Q. J. R. Meteorol. Soc. (2002), **128**, pp. 1461–1483

Nucleation effects on the habit of vapour grown ice crystals from −18 to −42 °C

By M. BAILEY and J. HALLETT*
Desert Research Institute, USA

(Received 28 October 2001; revised 1 February 2002)

SUMMARY

Ice crystals have been nucleated and grown by a new method where supersaturation is controlled by combining static diffusion chamber and expansion chamber techniques. Crystals were nucleated and grown on 50 μm diameter glass filaments at pressures of 500 to 300 hPa, typical of clouds with temperatures from −18 to −42 °C, respectively. Crystals were also nucleated on particles of finely powdered silver iodide and kaolinite adhering to glass filaments, in order to investigate effects on habit due to different nucleating materials. Critical supersaturations for nucleation were measured for each case and were in good agreement with previous nucleation studies. Crystals were grown at ice supersaturations which ranged from less than 1% to just above water saturation. For ice growth below a critical supersaturation, nucleation was achieved by applying a brief adiabatic expansion to the static diffusion chamber with a filament in place and the chamber evacuated to the target pressure for the temperature of interest. Nucleation occurred at a critical supersaturation, followed by growth at a lower value. A review of past laboratory experiments and recent *in situ* observations reveals good agreement between laboratory and field observations when the effects of nucleating methods and growth times are taken into account. Contrary to studies which report the habit of ice as 'prism'-like or columnar below approximately −22 °C, the habit is found to be plate-like for temperatures ranging from −18 °C to −40 °C at ice supersaturations relevant to the atmosphere. Additionally, the plate-like-habit distribution is dominated by polycrystalline forms, which is consistent with aspects of past laboratory studies and recent observations obtained with improved aircraft instrumentation. The habits and habit distributions obtained from glass and kaolinite most closely resemble those observed in the atmosphere, while the results from silver iodide show large differences. Below −40 °C, the habit becomes columnar except at low supersaturation, and is still dominated by polycrystals which appear as rosettes for ice supersaturations greater than about 20%. 'Bullet rosettes' were observed to nucleate and grow on clean glass threads below −40 °C but not on kaolinite which predominantly grew single columns and irregular polycrystals with columnar components; silver iodide produced single columns with few polycrystals. This behaviour indicates that rosettes result from ice nuclei which share few or no crystallographic similarities with ice, and is consistent with that expected from homogeneous nucleation. Critical supersaturation measurements for nucleation were extended down to −70 °C, and revealed that below −40 °C ice crystals can nucleate on glass at ice supersaturations of 25%, and at values of approximately 15% on kaolinite or silver iodide.

ELSEVIER

Atmospheric Research 62 (2002) 149–169

ATMOSPHERIC RESEARCH

www.elsevier.com/locate/atmos

The alignment of ice crystals in changing electric fields

T.C. Foster [1], J. Hallett*

Desert Research Institute, 2215 Raggio Parkway, Reno, NV 89512, USA

Received 1 August 2001; accepted 1 December 2001

Abstract

Orientation of ice crystals in the form of thin plates (diameter up to 30 μm, thickness 0.5 to a few μm) was investigated optically for crystals nucleated in a supercooled cloud in a laboratory cold chamber. Random orientation caused by Brownian rotation of small crystals (apparent as twinkling) and alignment caused by airflow resulting from fall motion of larger crystals was changed by application of an electric field either as a step or as an oscillating square wave of variable frequency of order 1–10 Hz. Video records and time exposed still photographs demonstrated crystal fall, oscillation, and orientation changes with electric field magnitude and frequency. Thin film interference colours provided crystal thickness, mass, and moment of inertia. Realignment began for electric fields greater than 0.5–1 kV/m and was complete above 10 kV/m. Measurements of degree of alignment (from random orientation to completely parallel to the electric field) and its time dependence (of order tenths of seconds) are consistent with predictions of a theoretical oscillator model based on electrical torques on ellipsoids in viscous air. In a changing electric field at low frequency, the crystal realignment varies along with the variation field and at high frequency they remain aligned along the average field. These results are applied to larger crystals as occur in the atmosphere with implication for remote sensing of ice by radar and lidar as influenced by local electric fields and with the possibility of their remote measurement by optical observation of changing crystal orientations.

Keywords: Ice crystal; Crystal orientation; Electric field; Interference colour

* Corresponding author.

E-mail addresses: tfoster@calpoly.edu (T.C. Foster), hallett@dri.edu (J. Hallett).

[1] Permanent address: California Polytechnic State University, San Luis Obispo, CA, USA.

0169-8095/02/$ - see front matter
PII: S0169-8095(02)00008-X